ABSTRACT

Title of Document:	POINTING, ACQUISITION, AND TRACKING FOR DIRECTIONAL WIRELESS COMMUNICATIONS NETWORKS
	John Robertson Rzasa, Doctor of Philosophy, 2012
Directed By:	Professor Christopher C. Davis, Department of Electrical and Computer Engineering

Directional wireless communications networks (DWNs) are expected to become a workhorse of the military, as they provide great network capacity in hostile areas where omnidirectional RF systems can put their users in harm's way. These networks will also be able to adapt to new missions, change topologies, use different communications technologies, yet still reliably serve all their terminal users. DWNs also have the potential to greatly expand the capacity of civilian and commercial wireless communication. The inherently narrow beams present in these types of systems require a means of steering them, acquiring the links, and tracking to maintain connectivity. This area of technological challenges encompasses all the issues of pointing, acquisition, and tracking (PAT).

The two main technologies for DWNs are Free-Space Optical (FSO) and millimeter wave RF (mmW). FSO offers tremendous bandwidths, long ranges, and uses existing fiber-based technologies. However, it suffers from severe turbulence effects when passing through long (>kms) atmospheric paths, and can be severely affected by obscuration. MmW systems do not suffer from atmospheric effects nearly as much, use much more sensitive coherent receivers, and have wider beam divergences allowing for easier pointing. They do, however, suffer from a lack of available small-sized power amplifiers, complicated RF infrastructure that must be steered with a platform, and the requirement that all acquisition and tracking be done with the data beam, as opposed to FSO which uses a beacon laser for acquisition and a fast steering mirror for tracking.

This thesis analyzes the many considerations required for designing and implementing a FSO PAT system, and extends this work to the rapidly expanding area of mmW DWN systems. Different types of beam acquisition methods are simulated and tested, and the tradeoffs between various design specifications are analyzed and simulated to give insight into how to best implement a transceiver platform.

An experimental test-bed of six FSO platforms is also designed and constructed to test some of these concepts, along with the implementation of a three-node bi-connected network. Finally, experiments have been conducted to assess the performance of fixed infrastructure routing hardware when operating with a physically reconfigurable RF network.

POINTING, ACQUISITION, AND TRACKING FOR DIRECTIONAL WIRELESS
COMMUNICATIONS NETWORKS

By

John Robertson Rzasa

Dissertation submitted to the Faculty of the Graduate School of the

University of Maryland, College Park, in partial fulfillment

of the requirements for the degree of

Doctor of Philosophy

2012

Advisory Committee:

Professor Christopher C. Davis, Chair

Professor Gilmer L. Blankenship

Professor Thomas E. Murphy

Professor Julius Goldhar

Professor Douglas Currie, Dean's Representative

Dedication

To my parents and brother, to whom I owe all.

Acknowledgements

This thesis is the culmination of over ten years worth of effort, starting from when I was an undergraduate lab technician working in Dr. Davis's antenna lab, through my master's degree, working as a faculty research associate and finally to my Ph.D work. Dr. Davis's mentorship has helped me throughout, and I am forever indebted to him for his guidance and patience.

I also thank the members of my thesis committee for their guidance on my work as well as their feedback.

I must sincerely thank John "J" Pyle of the IREAP machine shop for teaching me how to be a machinist for the last 10 years. Without his help, none of what I built in this thesis would exist.

I must also thank the many people who have been part of our group during my time here and have helped me run tests, proofread papers, and bounces ideas off of: Mohammed Eslami, Shawn Ho, Ehren Hwang, Navik Agrawal, Sugi Trisno, Yu-Ju Hung, Jaime Llorca, Peter Pham, Quirino Balzano, Dave Coleman, and anyone I might have forgotten.

I also would like to thank the sponsors of some of the work seen here, namely LGS, TRX Systems, ARA, and KeyW Corporation for their generous support.

Last, but not least, I thank my family with all my heart for supporting me all these years and putting up with me!

Table of Contents

List of Tables

List of Figures

List of Abbreviations

AHRS – Attitude Heading Reference System

BER – Bit Error Rate

CPAT –Coarse Angle Pointing, Acquisition and Tracking

DTCN–Designated Topology Control Node

DWN–Directional Wireless Network

EDFA–Erbium Doped Fiber Amplifier

FFOV–Full Field of View

FPA– Focal Plane Array

FPAT–Fine Angle Pointing, Acquisition and Tracking

FSM–Fast Steering Mirror

IM/DD–Intensity Modulation with Direct Detection

INU–Inertial Navigation Unit

MmW–Millimeter Wave

PAT– Pointing, Acquisition and Tracking

PID–Proportional, Integral, Derivative

PPR–Pulses Per Revolution

RSS–Received Signal Strength

RTK–Real-Time Kinematic

TDOA–Time Delay of Arrival

UART–Universal Asynchronous Receiver/Transmitter

List of Publications

[1] Eslami, M., Rzasa J., Davis, C., "A stereo PTZ tracking and surveillance system with two dynamic cameras operating in a master-slave relationship," Proc. SPIE, 8517, 2012

[2] Eslami, M., Wu, C., Rzasa, J., Davis, C., "Using a plenoptic camera to measure distortions in wavefronts affected by atmospheric turbulence, " Proc. SPIE, 8517, 2012

[3] Rzasa, J., Milner, S., Davis, C., "Design and Implementation of Pan-Tilt FSO Transceiver Gimbals for Real-Time Compensation of Platform Disturbances Using a Secondary Control Network," Proc. SPIE, 8162, 2011

[4] Franco, J. C., Rzasa, J., Milner, S. D., Davis, C. C., "Transmission of high definition imagery using hybrid FSO/RF links for real-time surveillance, event detection, and follow-up," Proc. SPIE, 6709, 2007.

[5] Ho, T., Rzasa, J., Milner, S., Davis, C., "Robust optical alignment systems using geometrical invariants," Proc. SPIE, 6709, 2007

[6] Balzano, Q., Rzasa J., Davis., C., et al., "High Capacity Tactical Networks with Reconfigurable, Steerable, Narrow-Beam Agile Point-to-Point RF Links," Proc., IEEE Milcom, 2007

[7] Davis, C., Beard, B., Rzasa, J., et al., "International intercomparison of specific absorption rates in a flat absorbing phantom in the near-field of dipole antennas," IEEE Trans. on Electromagnetic Compatibility, Vol. 38 No. 3, 2006

Chapter 1: Introduction

1.1 Motivation

Over the last decade, the world's demand for bandwidth has been rapidly increasing. This demand spans both the commercial, industrial and military markets. The use of fiber-optic and copper fixed infrastructures has provided a worldwide network with low latency, reasonable redundancy, and high reliability. However, the communications landscape of the military and aerospace industries is much more complex. In these areas, communications nodes may be moving about at high speeds, high altitudes, and in ground systems, over variable terrain. Even in light of all these challenges, users still require reliable, high bandwidth data communications. To go beyond the familiar realm of omnidirectional RF communications systems, requires new technology, such as directional wireless, which can provide greater bandwidth but with the concomitant challenge of pointing, acquisition, and tracking (PAT). When wireless transmissions become more directional, the focused energy allows for greater data rates over potentially longer distances, but over a smaller angular range. This naturally leads to the requirement of being able to point the electromagnetic waves at the desired location. We can see examples of this every day in the sectored antennas dotting many tall buildings, which provide us with cell phone service. Even though their 90-120° beam widths are still quite wide, using multiples of these allows for much greater coverage and capacity than a single omnidirectional antenna.

When the data capacity of a system continues to increase, the carrier frequency

must also increase at some point. This inherently leads to narrower beams because of the

relationship between wavelength, antenna aperture size, and beam divergence for RF

transmitters: $\theta = \dfrac{1.22\lambda}{D}$, where D is the antenna diameter in the case of a dish antenna.

For example, a 5.8GHZ directional RF antenna has a beam width of 12°. A 24 GHz

system has a beam width of 3° and an 80GHz system has a beam width of 0.87° (all three

using a 0.3m diameter antenna). This directionality gets even more extreme in the area of

free-space optical communications (FSO) where beam widths can approach 10μrad at

1550nm for long distance links. All these issues are compounded when the transceivers

are on the move, be it on land, sea or air. The ability to find, acquire, and maintain a link

in these situations requires close attention to PAT. Regardless of what type of transceiver

is involved (RF or FSO), the basic concept of what is required to achieve PAT is the

same, though the accuracy required and acquisition/tracking methods will vary.

Before a directional link can be formed, the two ends must be aware of each

other's positions in space in a common coordinate system. There are a variety of methods

for determining this, the most popular being optical beacons or by GPS. In recent years,

GPS has taken over in almost all systems because of its relatively small positioning error

and wide availability. After the positions of the two transceivers have been determined,

they must then be pointed at each other. In all situations besides phased-arrays (which

due to their astronomical cost are left to the realm of large military systems), the

transceivers are rotated using a mechanical positioning platform, commonly known as a

gimbal. For some directional RF transceivers, the pointing precision of a gimbal is

enough to point and track while continuing to receive adequate signal. However, in the

case of FSO where the beam divergences are orders of magnitude less than in RF

systems, some additional pointing mechanism must be used to bring the beams

completely into alignment. In the RF domain this is usually achieved with spiral scanning

or raster scanning of the primary beam. In FSO, the primary method is with the use of a

fast scanning mirror (FSM). Once a link has been established, the PAT system must then

track the transceivers and adjust their positions accordingly to maintain connectivity even

as the platforms themselves are moving. Looking at figure 1.1 below, we can see the

information required to point two links at each other.
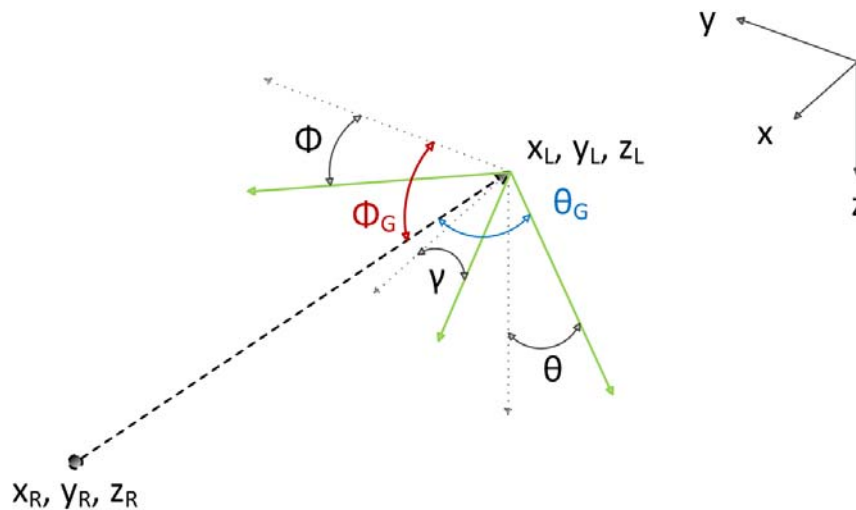
Figure 1.1: Pointing between two locations in space

For two points in space, in order to find the azimuth and elevation angles that two

transceivers must rotate to in order to point at each other, their positions and orientations

in space must be known. The position information can readily be found using GPS, and

its error is fairly manageable for long range links. The orientation information can be

somewhat more problematic. The two orientation angles that are determined with respect to earth's gravity (pitch and roll) can be measured with great precision using an inclinometer (in a static situation). The last angle (yaw) is much harder to find since it has no absolute reference. Integration of a gyroscope's velocities over time can give decent results, but it can develop large angular drifts. Digital compasses are also a possibility, however they are very imprecise (>0.5° error), not very consistent, and can be effected by the presence of nearby metals and magnetics (such as are found in motors). The yaw angle can also be determined from looking at GPS coordinates over time and finding the platform's heading, but this is limited by the GPS accuracy and output rate, and requires that each data point have sufficient separation from the last. In recent years a new device has entered the market, called the attitude heading reference system (AHRS). These modules integrate gyroscopes, accelerometers, magnetometers, temperature and pressure sensors, and GPS in order to give a full position and orientation solution for a mobile platform, while using the other sensors to provide error correction to the gyroscopes. It is worth noting that in dynamic situations inclinometers cannot be used because of their degradation in the presence of acceleration. In these instances, all the orientation angles are found by integrating the outputs of gyroscopes over time, and doing extensive filtering to provide accurate signals.

1.2 Challenges in the Implementation of DWNs

While the information given above may make the PAT problem for directional wireless seem fairly straightforward, there are actually several issues that have delayed its implementation in large scale networks.

Until recently perhaps the biggest factor affecting the implementation of DWNs has been need. While bandwidth needs have been increasing steadily, omnidirectional and coarse-directional RF systems have been sufficient so far in providing adequate bandwidth to military and aerospace systems. However, in recent years things have progressed to the point that the only option to feasibly expand bandwidth in the operational theatre is with directional RF using frequencies beyond 60GHz and FSO. This need has spurred a greatly renewed interest in both transceiver technology and its usually overlooked companion, PAT.

Even given somewhat variable interest, research in DWN has progressed steadily in the last decade, with several fielded systems in both RF and FSO demonstrating high quality results in terms of tracking, data rates, and reliability. However, to date there has been no unclassified implementation of a multi-node DWN in either >24GHz RF or FSO. This is not without reason, as the complexity of such a system is much greater than that of a single link. The cost for many of these systems is also prohibitive enough to prevent large numbers of them being made. Is it worth noting that even though FSO can provide much higher data rates than RF, its performance in atmospheric turbulence severely limits its range anywhere in earth's atmosphere without the use of very sophisticated and expensive adaptive optics systems, and even they are not yet mature enough to provide

the kind of reliability needed in airborne and military communications systems.

1.3 The Last Mile Problem

Bringing high data communications to the end user can be generally referred to as the "last mile problem." In terrestrial networks this is the situation where the "last mile" between a network and end user is the limiting factor in providing available data rates. For example, there might be gigabit fiber going to a switch in a residential neighborhood, but the link from that switch to each house is twisted-pair copper cable being used for DSL. In mobile tactical networks the idea is the same, in that the limiting factor is usually the data rate of the link between the end user and the next part of the chain. If everyone uses a radio that must connect with any other radio over a long distance, data rate is sacrificed for range, and bandwidth congestion will also come into play. But if some type of higher data rate relay can be placed in-between, the overall capacity to the end user can be increased. Figure 2 below illustrates the concept of a DWN as a backbone for many end users. There have been increasing requests to the engineering community for reliable high capacity DWN backbones to service the military's ever increasing network requirements. This can be seen in the various projects with this goal in mind [1-6]. While most do not envisage providing backbone level connectivity to the end user, all desire to reduce the range and sharing requirements of each end user to maximize their data capacity at their location, wherever it may be.
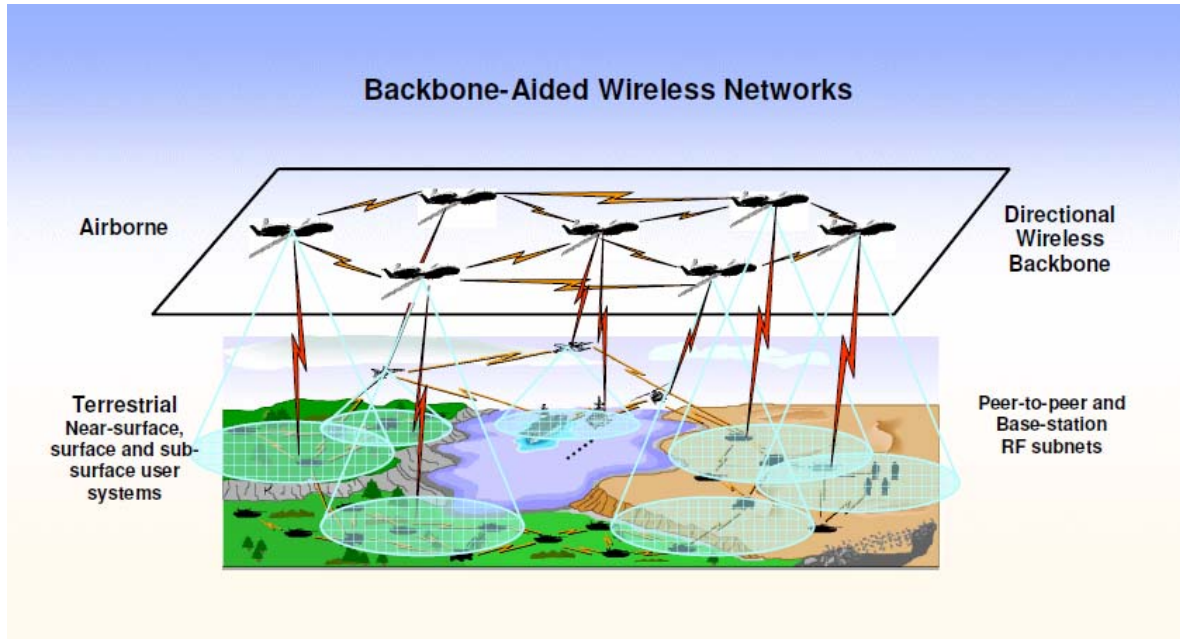
Figure 1.2: The DWN backbone serving many terminal users [7]

1.4 Advantages/Disadvantages of FSO/RF DWNs

While this dissertation will focus primarily on the PAT aspect of DWN systems, it is worth reviewing the various advantages and disadvantages of FSO and RF based platforms. These issues will later help decide on the performance specifications required for the platform, its controller, and the various sensors employed.

	FSO DWN	RF DWN (at 80GHz)
Beam Divergence (typ)	<1mrad	>10mrad
Receiver Sensitivity	-55dBm	-135dBm
Range	100km	50km
Multiplexing for Full Duplex	no	TDMA, FDMA
Turbulence effects	>0.44 dB/km	0.01 dB/km
Demonstrated Data Rate	5 Gb/s	1.25 Gb/s

Table 1.1: Comparison of FSO and RF DWN Specifications

1.5 Prior Work and Current Research Goals for DWNs

Work in DWNs has been an active research topic for many organizations in the last 20 years with the advent of directional RF systems as well as high data rate FSO technology. The transceivers themselves as well as their interactions with the atmosphere have received particular attention, and much work still continues in these areas. This includes turbulence modeling [8, 9], turbulence measurements [10], adaptive optics [11], and fast beam steering [12]. Only in the last ten years has work begun to move from single links and their operations in the atmosphere to actual mobile links and the beginnings of networks of links.

Today's cellular phone network provides reasonable data capacities to large numbers of users in a given area using omnidirectional RF signals running from 920 MHz to 2.4 GHz. These frequencies allow for enough data to be transferred, but also enough range that unreasonable transmit powers are not needed. Coupled with the high

sensitivity of coherent RF receivers, cellular communications is a relatively robust and reliable communication system. However, the data rates achievable are quite limited and not nearly enough to be used in a backhaul situation, though its use in omnidirectional systems is popular. Moving to higher frequencies (5.8 GHz, for example), the data capacity goes up, but its range in an omnidirectional system goes down. In order to still get the same range, the beam's power must be focused in the direction of interest, which sacrifices coverage for distance. It is at this frequency (which happens to be an ISM band) that directional wireless communications systems begin to appear.

Moving up to higher frequencies, the ISM band at 24 GHz can provide single channel data rates at over 100Mb/s full duplex at ranges of several miles [13]. While popular 5-10 years ago, this band has been overtaken by the two most popular bands now, 60 and 80 GHz. 60 GHz is well known because the radio technology used inside it is fairly mature and low cost. Units with gigabit capacities are widely available [14] and easy to install. However, 60 GHz lines up with an absorption band of oxygen, so these systems attenuate quickly in the atmosphere and can only be used for a few miles. In a way it provides security similar to FSO, since if the narrow beam dies off after passing the receiver, there is less chance someone will be able to intercept it.

The current state of the art in RF DWNs is in the 75-85 GHz E-Band. Not suffering from the attenuation effects of lower frequencies, it offers very high data rate communications at significant ranges. Several commercial systems are available at shorter ranges and there are multiple large government programs tasked with developing the radio hardware needed to deploy these systems at ranges over 10 km [4,5].

Depending on the antenna size used, these systems can operate with beam divergences close to 10mrad, so the PAT control becomes more stringent than for lower frequency systems. However, because many of these systems are eventually designed to go on aircraft where space and size are restricted, the smaller dishes that are used give wider beams (>20mrad). Because of the weather reliability issues of FSO and perceived robustness of RF systems, it is expected that E-Band will be the dominant transmission medium in many future DWNs.

The higher frequencies found in FSO systems give substantially higher data rates than RF, however this benefit comes at several costs. First is that the beam is much narrower, so PAT requirements are much tighter. Second is that optical communications in general is IM/DD, so the advantages of coherent detection are lost, making the optical receivers much less sensitive. Perhaps the biggest issue is how laser beams are affected by the atmosphere. This is typically the limiting factor in FSO. Turbulence has been studied extensively for many years, but even with all this research and fairly robust statistical and mathematical models, there are only a few usable mitigation techniques, such as adaptive optics and fast steering mirrors. Most current research in FSO is concentrated on turbulence modeling and mitigation, with PAT and network areas taking a backseat in most cases. Even though it may be years before FSO achieves the same reliability as RF in dynamic backhaul systems, the PAT and network concepts and hardware developed for FSO can readily be merged with work in the upcoming E-Band RF systems.

Even before a DWN network can be constructed and deployed, there are major

issues regarding how the network forms, morphs, reconfigures, and recovers from failure, not to mention who controls it, how it is controlled, and how often it is updated. Members of our group have completed much important research in this area over the years, including TCP/IP network modeling of DWNs [15], routing protocols [16], topology reconfiguration [17], mobility management [18], molecular models for networks [19], and a host of other issues.

Other current work in our group is investigating how DWNs can be modeled such that a link failure can be predicted with a high degree of certainty. This will allow the network as a whole to adapt its topology to minimize link breaks [20]. All of the network control processes exist only in simulation at the moment, as they are further ahead in development than the hardware they would control. These algorithms are of critical importance, though, since the positioning of DWN nodes in a large network to serve many end users in a dynamic environment is no simple task (figure 1.3), as evidenced by the dynamics of dozens, if not hundreds of terminal nodes moving according to their own plans, while the backbone above must adjust to ensure maximum connectivity for all nodes.
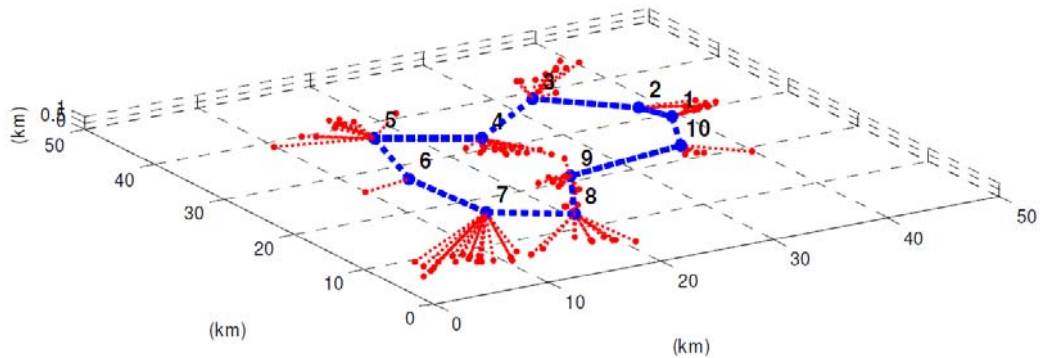
Figure 1.3: A DWN backbone adjusting to serve its terminal users [21]

As of the writing of this thesis, there are no known implementations of a multi-link DWN network anywhere in public domain. However, there have been several systems deployed that come very close, and which will mostly likely in the near future expand to multi-node networks.

Perhaps the longest running mobile DWN backbone project is at DARPA, which began as ORCLE in 2003, changed into ORCA in 2008, and then was canceled and recast with a new vendor as the appropriately named FOENEX in 2010 [1-3]. The purpose of these projects was very long range FSO links over 100's of km, in air-ground, air-air, and ground-ground configurations. They successfully demonstrated reasonably error free communications at 5 Gb/s, but with the use of sophisticated adaptive optics to mitigate turbulence effects. The ultimate goal of the project is a reconfigurable FSO backbone in the sky that also serves terminal users on the ground. Similar projects involving air-ground FSO links have been demonstrated at other institutions, and work is still ongoing

in these groups to get the BER to fixed-link numbers (10^{-9}) [22-24].

Another sophisticated project in the public domain is the FALCON program at ITT in Ohio. Their system uses modified L-3 MX12 Skyballs fitted with custom designed 2.5 Gb/s optical transceivers from JHU/APL to achieve reliable data transfer between moving air to ground and air to air links [24]. They demonstrated geopointing, beaconing lasers for alignment, fast beam steering, platform stabilization, and gigabit+ data rates over ranges of up to 100 km. All of the systems above use large and prohibitively expensive custom systems to achieve their goals, so it will be some time before they become cost effective enough to be deployed on a wide scale.

In the E-band RF regime, fielded airborne systems are scant at best, mainly because the miniaturized RF technology needed for them is still in its nascent phase. The MMIC chips that operate in this frequency range are fairly new, and the RF plumbing required to enable full duplex communications is still an active research topic [4,5]. Fixed-link systems are available in the commercial domain, although they are much larger than could be mounted on aircraft, especially UAVs [25,26]. There are several government sponsored projects addressing these dynamic platform and transceiver issues and others including antenna design, power amplifier design, gimbal design, and network control [4,5]. A project recently completed in our group delivered the first known gimbalized E-band antenna to the Air Force [5]. Due to the fact that the beam divergences are much wider than FSO, the E-band transceiver's signal can act as its own beacon and fast tracker, so only one mechanical system is required. While there is not much published research available at the moment, the rapid and heavy development push

in E-band is expected to lead to many research and development programs that will field airborne networks in the next five years.

1.6 Other Uses for Cooperative Positioning Platforms

A final note worth mentioning about the work presented in this thesis is that the hardware and software presented could be useful in areas outside of directional wireless communications. One area where others in our group have had great focus [27-30], not to mention groups all over the world, is that of autonomous surveillance. We are all familiar with the hordes of security cameras everywhere monitoring us, but almost all of them either have a person looking at them only on occasion, or not at all when they are recording to a DVR. Designing cameras and software to automatically detect certain events and alert users is a very active research field, in both person and traffic monitoring. Some of the gimbals described in this thesis are being used for long range traffic surveillance, and others have this capability built in for future use. The algorithms used to point two transceivers at each other can also be used to point cameras at targets, acquire them, and track them precisely. The concept of a secondary control network for DWN PAT acquisition and reconfiguration that is presented here can also be used to link a network of steerable and fixed cameras together, allowing them to hand off targets from one camera to another, thus giving rise to the ability for persistent autonomous surveillance.

1.7 Dissertation Contributions

This thesis advances the field of pointing, acquisition, and tracking (PAT) for autonomous directional wireless communication links and networks in four primary areas. For the first time it makes a direct comparison of the subtle differences between free space optical and directional RF (primarily in E-band) communications. First of all, this thesis investigates the relationships between transceiver characteristics such as beam divergence, receive aperture size, transmit power, and other factors, coupled with the pointing errors inherent in the system to give a designer a powerful tool for evaluating a specific design. While link budget analyses for these links are quite common, this thesis presents a novel integrated software tool for evaluating these transceivers, but also including sensor and platform characteristics. With this tool, a designer can examine the tradeoffs between various variables while restricting others based on their design constraints.

The second main contribution of this thesis is an analysis and experimental verification of scanning algorithms and properties for directional wireless network (DWN) transceivers, as well a new type of acquisition method called a chirped scan. The various properties of spiral and raster scans are analyzed, as well as the difference between their application to FSO and RF transceivers. This information was then used to examine how platform design can be optimized to provide the correct level of performance for a given application. The chirped scan is a novel method of link acquisition where a relatively wide beam angle, low data rate beacon laser is modulated with the platform's GPS data so when a wide FOV receiver catches a glimpse of this

signal, it then has enough information to initiate a geo-pointing operation without the use of an omnidirectional control channel, which is either unavailable or forbidden for use. The chirped scan can also be used in fine angle acquisition for FSO or RF whereby the receiver can transmit RSS information back to the transmitter over the alignment beam in order to aid in signal optimization. This is especially useful in bistatic systems where the transmit and receive beams are not coupled on the same FSM. Although blind link acquisition with narrow beams can be a lengthy process without some adjunct pointing information, such as GPS coordinates and orientation sensors, it is the only approach that provide almost complete covertness. Any link acquisition method that uses omnidirectional RF communication between nodes is subject the node detection.

The third contribution is the design and construction of a complete three node biconnected FSO network (with six FSO transceivers), using custom platforms employing purpose-made FPGA controllers. Although this network involved only short links using low power lasers, it presented a severe proof of principle challenge, because GPS errors have a much greater impact on the angular error of initial beam pointing for short links. These embedded systems allow for platforms responsive enough to engage in fast, precise beam alignment and tracking, while also running the radio control channel, sensor fusion algorithms, and external interfacing. As far as can be determined, this is the largest DWN network demonstrated in the public domain and the only one with a fully-functional DTCN core running on a small embedded controller. Each platform contains the same board, so any unit can become the DTCN if the current one fails. These platforms form the basis of a testbed that will be used for many more PAT

experiments in the future.

The final contribution of this thesis is the design and construction of a four node RF DWN to investigate and characterize how fixed infrastructure routers behave in the presence of physically reconfigurable networks. No published work exists in this area, so this experiment was the first known test of this concept. The results confirmed that off-the-shelf routers will reconfigure themselves properly in a DWN, with only a minor delay on top of the mechanical and synchronization delay of the platforms and transceivers.

Prior to the work described in this thesis, there have been no demonstrations of directional wireless communication networks that have not involved human intervention such as preliminary pointing using telescopes and camera systems, powerful wide angle beacons, and known geographical locations of nodes.

1.8 Organization

The organization of this thesis is as follows:

Chapter 1: Introduction and Motivation

Chapter 2: Pointing, Acquisition, and Tracking for Directional Wireless

Communications Networks

Chapter 3: Cooperative Platforms for DWNs, Hardware and Software Design

Considerations

Chapter 4: Simulations and Experimental Results

Chapter 5: Conclusions

Chapter 6: Future Work

References Cited

Chapter 2: Pointing, Acquisition, and Tracking for Directional Wireless Communications Networks

2.1 Introduction

The concept of PAT for narrow beam electromagnetic waves is a well-studied, yet still active area of research. Depending on whether the beam in question is in the RF or optical domain, the approaches for PAT can be quite different, although at some level they share several essential features. Because the beam divergences of FSO transceivers are usually at least an order of magnitude less than E-Band RF units, they always have some type of secondary alignment laser, resulting in a two-layer coupled PAT system. The secondary scan is usually a tip-tilt mirror capable of ~1 kHz bandwidths, but over small angular ranges. A RF transceiver does not need a secondary alignment actuator, however it must be able to execute fast scan patterns in order to optimize its alignment, but this must be accomplished by the same mechanical platform that does the coarse pointing. FSO is also severely affected by atmospheric effects, and certain parts of the RF domain are as well. The method in which these two technologies send, collect and detect energy is quite different, even though their pointing and tracking methods are somewhat similar.

This chapter details the background for FSO communications, atmospheric effects, mmW RF communications, the sensors employed in PAT and the considerations that must be taken when using them. Methods for pointing, acquisition,

and tracking, scanning patterns for acquisition, and the differences between FSO and RF systems with respect to PAT implementation are also detailed.

2.2 Link Fundamentals

2.2.1 FSO

Any FSO link has at least one transmitter and one receiver. While there are many variations on the components used to achieve different data rates at various ranges, the simplest (and most common) arrangement can be used to examine characteristics important to PAT such as beam divergence, spot size, receive aperture size, receiver sensitivity, and transmit power.

Figure 2.1 below shows a typical FSO transmit/receive link over a distance L that will be described later in this thesis. The transmitter consists of a laser diode mounted on a translation stage sitting behind a single transmit lens. The receiver consists of a receive lens and photodiode mounted on a translation stage at the focal point of the receive lens. If we assume that the laser diode sits at the focus of the transmit lens and the photodiode at the focus of the receive lens, then we can calculate how much power arrives at the photodiode for a given transmit power.
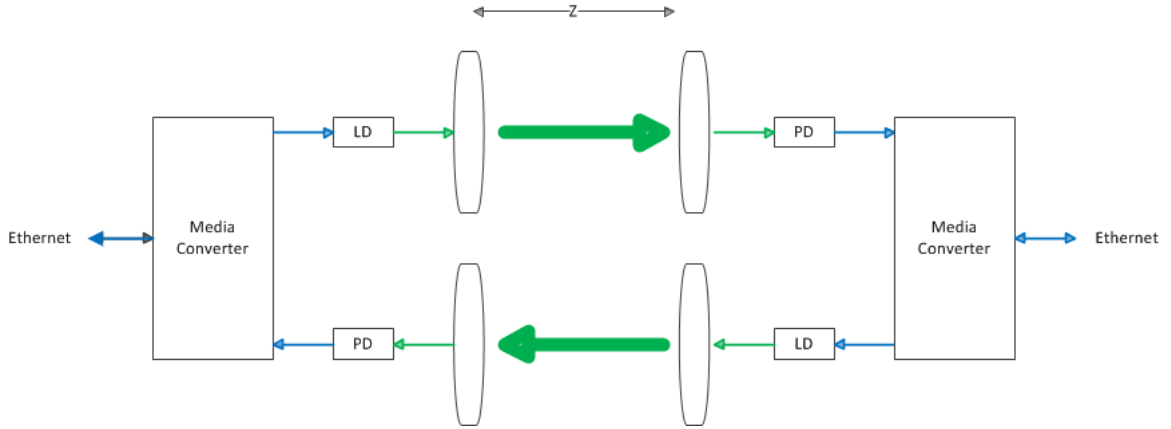
Figure 2.1: A typical FSO link. The lenses shown schematically may be separate (in a bistatic system) or shared (a monostatuc system).

The beam divergence of a transmitter is a value typically set by the designer to ensure enough power is available at the receiver without wasting extra energy, but not so narrow to make the pointing requirements impractical. The minimum spot size at the transmitter is given by:

$$w_0 = \frac{\lambda}{\theta_{beam} \cdot \pi}$$

where θ_{beam} is the beam divergence half angle at the transmitter. The spot size at the final transmitter aperture may be larger than w_0, where to avoid beam truncation the transmitter aperture diameter D should satisfy the relationship $D \geq 2.8w_0$. Without loss of generality we will assume that w_0 is at the transmitter final aperture.

Atmospheric attenuation over a distance z is accounted for by the tern $e^{-\alpha \cdot z}$ so that at the receiver the optical intensity can be given by:

$$I(r,z) = I(0,z)e^{-\alpha \cdot z}(e^{-\frac{2r^2}{w^2(z)}})$$

Where $w^2(z)$ is written as:

$$w^2(z) = w_0^2 \left[1 + \left(\frac{\lambda \cdot z}{\pi \cdot w_0^2} \right)^2 \right]$$

and the axial intensity of the beam at the receive lens is:

$$I(0,z) = \frac{2 \cdot P_t}{\pi \cdot w(z)^2}$$

Taking the receive aperture diameter to be D, the total power collected by the receive aperture is:

$$P_{rec} = 2\pi \int_0^{\frac{D}{2}} r \cdot I(r,z) \cdot dr$$

At distances of >300m, atmospheric turbulence effects start to interfere with the beam, so the basic assumptions above may no longer completely hold. Mitigating turbulence is not a part of this thesis, however much work is still ongoing in this area including some that has yielded commercial systems [31]. The transceivers used later in this thesis have a maximum range of about 100m, so the calculations above are accurate in describing their behavior. We can now analyze some design variations on the basic

transmit/receive structure described earlier to look at the various tradeoffs.

What is typically the most limiting component factor in the performance of a FSO link is the sensitivity of the receiver photodiode. At 1550nm (the most common operating wavelength due to the wide availability of EDFAs for increasing the transmit power), receive photodiodes made from InGaAs can offer sensitivities of -55dBm at 1.25Gb/s [32]. Faster diodes have worse sensitivity at the moment, for instance a common 10Gb/s diode [33] used in fiber networks offers a sensitivity of -19 dBm. The next major consideration is the receiver optical design. Since the optics are the heaviest part of a system, airborne nodes want to be able to use components as small and light as possible. Large lenses offer sizable collection power, however they are heavy. Various types of mirror telescopes are also used which are lighter, but typically larger in volume.

On the transmitter side, the transmit lens is typically much smaller than the receive lens, on the order of 1-2" in diameter. An important rule of thumb is that to ensure >90% of the transmitted light exits the aperture, the transmit lens should be at least 2.8 times the beam waist w_0. Because most long distance systems have the transmit signal pass through an EDFA first, the beam exits a fiber-collimator before exiting the transmit lens. The use of fiber-optics sources is preferred because the output beam is almost perfectly circular, as opposed to the elliptical beams coming from most bare laser diodes.

2.2.2 Millimeter Wave RF

In the area of RF communications technology for DWNs, we will restrict the discussion to frequencies that compete directly with FSO, namely the 60-90 GHz E-band. All of this section is also applicable to the popular 60 GHz frequency at the low end of the band, however its lack of significant range in the atmosphere makes it unusable for long range RF systems.

For a transmitter operating at wavelength λ and having a circular transmit aperture of diameter D, the intensity at the transmit aperture is related to the 1st order Bessel Function as:

$$I = 4 \cdot \frac{J_1(\frac{\pi \cdot D}{\lambda} \cdot \sin(\theta))^2}{(\frac{\pi \cdot D}{\lambda} \cdot \sin(\theta))^2}$$

The peak intensity a distance z away from the transmitter having a transmit power P_t and area A is represented as:

$$I_P = \frac{P_t \cdot A^2}{\lambda^2 \cdot z^2}$$

At a distance z away, the transmitted wave intersects the receiver over an angular range of $\theta_R \cong \frac{D}{2z}$. The power collected by the receiver aperture is then:

$$P_r = 2 \cdot I_P \cdot e^{-\alpha z} \int_0^{D/2} r \cdot \frac{J_1(\frac{\pi \cdot D}{\lambda} \cdot \sin(\theta_R))^2}{(\frac{\pi \cdot D}{\lambda} \cdot \sin(\theta_R))^2} dr$$

24

where α is the atmospheric attenuation constant, which is about 0.1dB/km at 80 GHz. Because mmW directional RF systems operate at a much lower frequency than FSO, to get a beam divergence sufficient to ensure a certain data rate over some range, the aperture must be significantly larger than in an optical system.

RF systems cannot transmit and receive at the same time through the same aperture because of interference effects, so they utilize some type of scheduling scheme such as FDMA or TDMA to circumvent this. However, they do not have to worry about the isolation issues that can arise in monostatic FSO systems, since separate TX and RX feed waveguides are used to interface with the antenna.

2.3 Alignment of FSO Transceivers

All of the above calculations make an important assumption about the transceivers, namely that their receive and transmit propagation axes are lined up such that when each transmitter is pointed directly at the other's receiver, all the focused energy falls directly on the center of the detector. Due to the various optical and mechanical imperfections found in any system, this will not be the case. The system must be adjusted to minimize the alignment error such that the receiver can still collect enough power to operate at the working distance. It is understandable then that this alignment is even more important in a dynamic DWN where pointing errors will cause further degradation of the received signal. Considering only optical systems for now, there are two types of FSO designs: monostatic and bistatic. Monostatic systems use a common aperture for transmit and receive, while bistatic have separate ones.

2.3.1 Monostatic Systems

In a monostatic system, behind a common lens sits some type of beam splitting element that separates the transmit and receive optical paths. The transmitter and receiver sit on XY translation stages, typically both fiber mounted devices. Monostatic systems have the advantage of a smaller form factor, less lenses, and easier alignment because both share the common alignment of the main lens. Monostatic systems do have the major disadvantage of narcissus, where improper isolation of the TX and RX paths can cause part of a very strong TX beam to swamp a very weak receive beam. Sophisticated beam splitting arrangements and filters are used to isolate the beams, and some even use separate wavelengths for the two transmitters along with dichroic beam splitters to achieve sufficient isolation.

Alignment is easier than a bistatic system since only a simple corner cube is required as a loopback target. It is worth noting that alignment error, turbulence induced errors, and pointing errors are typically compensated for by a steerable mirror or adaptive optics lens assembly. Figure 2.2 below shows the alignment procedure for a monostatic system.
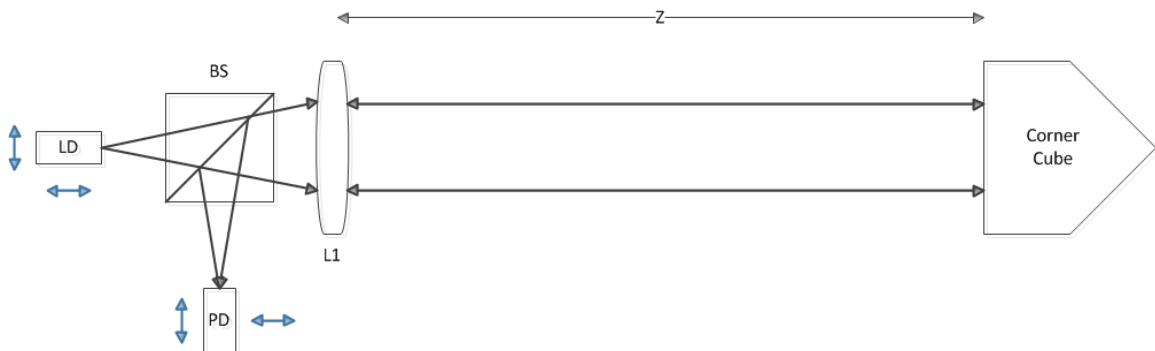
Figure 2.2: Monostatic FSO system alignment setup and procedure

2.3.2 Bistatic Systems

FSO systems were originally developed as bistatic systems, where separate lenses were used for transmit and receive. While requiring more optical elements, a larger form factor, and a more difficult alignment procedure, it offers total isolation between the transmit and receive paths. The alignment procedure is more difficult, especially in systems where the transmitter beam divergence must be kept narrow to work at long range. Figure 2.3 below shows the alignment setup for a bistatic system. The most important element for the calibration is the offset corner cube. This element shifts the transmit beam over by the exact spacing of the transmit and receive lenses, to mimic the function of the regular corner cube used in the monostatic system alignment, while sending an exiting ray out at the same angle as an incoming ray. This must be an extremely precise optical device; otherwise any errors in it will throw off the whole alignment.
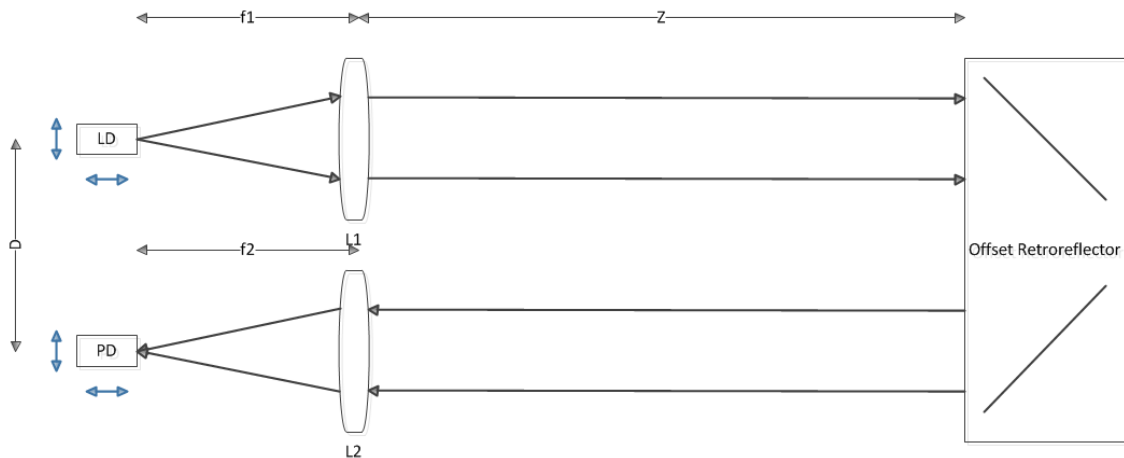
Figure 2.3: Bistatic FSO system alignment setup and procedure. The offset retro ensures that the returning beam has the same lateral separation as the laser and receiver diodes.

To begin alignment, the transmit beam is adjusted by translating the laser diode such that the beam comes out along the transmitter's optical axis. For shorter ranges this can be done with a ruler on an optical table, but at longer ranges a rigidly mounted tube with a test photodiode can be mounted on top of the transmit lens to aid in alignment. Next, the offset retro is placed in front of the beam a reasonable distance away at the same height as the beam, and the receive photodiode is adjusted to maximize the received signal. The procedure tries to make the transmit and receive optical axes as parallel to each other as possible.

There will always be some amount of error in this process, so the acquisition procedure for bistatic links is different from monostatic ones, where the devices are pointed directly at each other and then the receivers are individually adjusted (and in turn adjust their transmit beam). In a bistatic system each transmitter is precisely pointed at the receive lens of the other. If the systems were aligned properly, after the transmitters are both pointed, the beams should fall within the acceptance angle of the receiver lenses, allowing for a good link even if there were small alignment errors. Bistatic systems are not aligned by pointing the transmitter and then optimizing the receiver at the other end, because that could misalign the other transmitter. To illustrate this point, figure 2.4 below shows the results after a calibration of two of the bistatic FSO units used in this thesis. After being aligned using the above procedure, they were aimed at each other 90m apart and then adjusted such that the RSS at each end was maximized. They were then each swept off alignment to look at how the RSS varied on the static unit and the one being rotated off target. As can be seen below, because of the narrow beam divergence

of the transmitter, when it is rotated away, the received signal is quickly lost. However that unit's own RSS stays fairly constant as the acceptance angle of the receiver is much larger than the pointing precision required by the transmitter. Of course, one could make this less sensitive by using a transmitter with a wider beam divergence, but this would require more transmit power or a larger receiver lens.
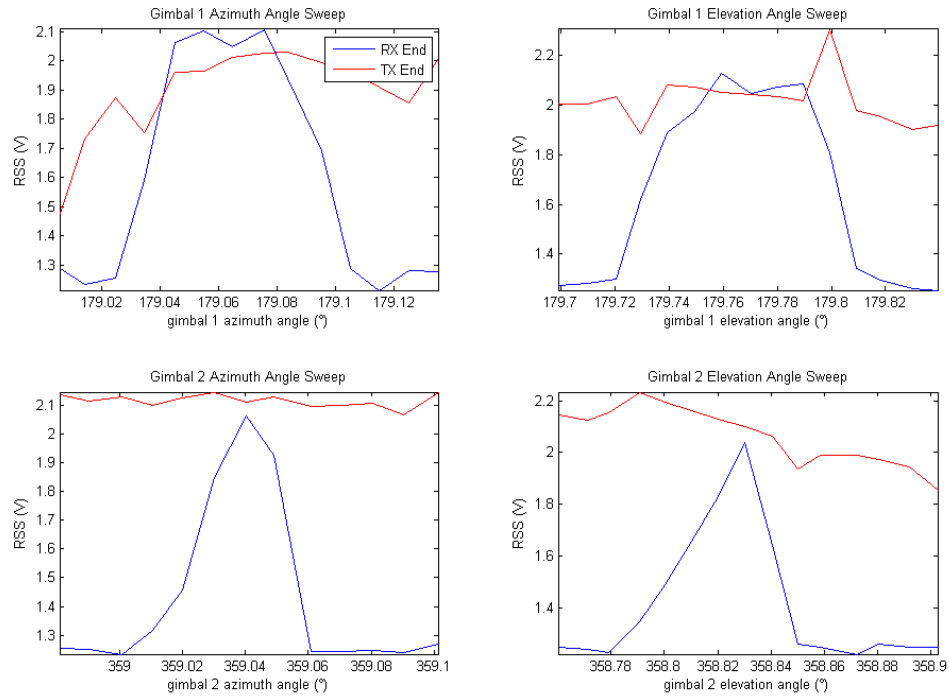
Figure 2.4: Calibration quality measurements from a pair of bistatic FSO transceivers. While the transmitter must be pointed precisely, the receiver has a much greater misalignment tolerance.

2.4 Turbulence

As a laser beam passes through the atmosphere, it encounters regions of different temperature and pressure, which in turn leads to areas with different indices of refraction. These effects change the propagating beam in different ways, such as changes in intensity (scintillation), beam wander, beam distortion, beam breakup, and changes in the phase fronts. Turbulence will cause beam spreading in excess of that expected from diffraction, due to scattering along the transmission path. It will also cause the beam to break up into patches of different intensities caused by the phase fronts interfering with each other. All these effects together will severely degrade the amount of light coming into a receiver, not to mention the quality of the signal over time, as well as the alignment of the beam. Interestingly, turbulence alone does not cause much beam wander; that is mostly caused by pressure gradients that change the refractive index over a wide area.

Beam wander will occur in almost all FSO systems that operate more than a few kilometers apart, however it can be compensated for by the use of a fast steering mirror, provided the deflection is not greater than the mirror's coverage. As for compensating for the other turbulence effects mentioned above, there are a variety of methods used, many of which are still active research areas.

Because turbulence will break a beam into patches of different intensity, it could occur that a receiver will only receive a portion of the beam, or none at all depending on the size and variation of the patches. However, one can use multiple receivers to get past this, a technique known as spatial diversity. In this configuration, multiple receivers are placed farther apart than the correlation distance of the turbulence patches. Thus if one

receiver sees no signal, there is a high probability one of the others will. This is a relatively simple, yet very powerful technique that is used in commercial systems. Another method is called "Time division duplexing [34]." In this arrangement, the same data is sent along the same path, but the beams are cross polarized and one is sent delayed with respect to the other. If this delay is longer than the average fade time of the atmosphere (typically 10ms), then the signals can be compared at the receiver to ensure the proper data is received. A variation on this uses multiple transmitters all sending the same data, but like the spatially diverse receivers, they are spaced far enough apart so their signals remain uncorrelated after passing through turbulence.

A final technique for turbulence mitigation is to use adaptive optics. This area includes deformable mirrors, deformable lenses, fluid-filled lenses, and wavefront correctors. All of these devices and algorithms aim to reconstruct the beam profile of the laser as it was before it passed through turbulence. These systems are still the subject of very active research [35-37], and while there have been various successful tests, their extremely high cost has kept them from widespread use to date.

The effect of turbulence on directional RF is somewhat different. As they propagate through the atmosphere, RF signals are absorbed and scattered by the various particles in the atmosphere. Beam wander is not an issue, but attenuation does degrade the signal. 60GHz is almost completely attenuated after a few miles because it lines up with an absorption band of oxygen. 80GHz is still attenuated, but by a factor of 40 less. While FSO works well in the rain mostly because the rain reduces the strength of the turbulence, it can greatly affect RF. In contrast, RF works well in fog, but FSO is

strongly affected. Some projects propose the use of hybrid FSO/RF systems to give greater reliability, but they have larger size and complexity, which minimizes the types of platforms on which they can be used [38].

2.5 Methods for Acquisition

The initial stage for PAT involves the process of getting both ends of a link to become aware of the other's position in space. In many terrestrial commercial systems, this is achieved by a simple sighting scope, where a user at each end points the unit so that the scope sees the other link in the crosshairs. This is of course limited by how far the boresight can see, and how well it is aligned with the transmit beam.

In longer links, especially in airborne or even aerospace applications, the acquisition process must be either remote controlled or automated. This process must also be fairly quick, since if the link is being repositioned after a break, a long delay in reacquisition can lead to major packet loss in the network. In DWNs, this takes on an even greater importance in the case of physical link reconfigurations. In this situation where a DWN must rearrange the pairs of transceivers to form a new network configuration, the network is typically already in active mode, so users will not be too pleased to see a "please wait" on their screen during mission critical activity. The delay time from network rediscovery processes cannot be changed much at present, so the system must try to minimize the downtime from mechanical repositioning and transceiver acquisition. With modern motors and controllers, the mechanical repositioning time is usually less than one second. In commercial FSO systems, link acquisition time can be in

excess of two seconds. Certain RF units are even worse, some multi channel units taking over nine seconds [47], but most single channel RF units above 24GHz take about the same amount of time as an FSO system. The use of encryption increases this delay even more.

There are four primary methods of node acquisition, each with its own advantages and disadvantages. It is worth noting that after the initial acquisition is made, all systems use some variant of RSS optimization to maintain a signal lock while tracking.

2.5.1 Quad Cells and Position Sensitive Detectors

A quad cell is an array of four photodetectors in a square that will tell the system from which quadrant the beam is coming, and therefore which direction it needs to move in order to center the beam. While certainly not very precise, when coupled with a fast steering mirror, quad cells can be used not only to align beacons, but also the data lasers as well. An extension of the quad cell is the position sensitive detector (PSD). These detectors operate similarly to a regular photo diode, except there are four terminals around the edges of the device. Each pair of terminals on opposing ends measures the photocurrent generated by the incoming light as it passes through a different resistive layer. These two orthogonally placed sensors can give the XY position of the light by looking at the ratios of these currents. For a square sensor of side length L (in mm) outputting currents X1, X2 and Y1, Y2, the position in millimeters can be found by:

$$X = \frac{X1 - X2}{X1 + X2} \cdot \frac{L}{2}, \quad Y = \frac{Y1 - Y2}{Y1 + Y2} \cdot \frac{L}{2}$$

Since PSDs are analog devices, they can give very precise and fast measurements, although they do require more processing electronics.

2.5.2 Focal Plane Arrays

A digital cousin to the PSD is the ever popular focal plane array (FPA). This array of photosensitive junctions gives measurements of incoming light over a grid of points. If the array has proper filtering and is sensitive in the laser's wavelength region, it can act like a digital PSD to determine the light's incoming angle. If multiple points of light hit a PSD at different locations, the PSD will only report the centroid of all those points, whereas a FPA can individually discriminate each point. The limiting factors of the FPA approach are the size of the detector (if the optics are not tailored correctly, extreme angles will walk off the detector), response time, and cell spacing (very small angular changes will fall on the same cell). This can be mitigated in part by using a zoom lens in front of the FPA to achieve angular magnification and thus resolve objects are greater distances, but this comes at the cost of having a heavier and larger optical assembly. With regards to beaconing systems for DWNs, FPAs are usually only used in situations where some image processing is required to pick out a certain pattern for the beacon, for example an array of lights, the outline of a plane, or some other shape. While PSDs and QPDs are used in the fast tracking portion of acquisition systems, the slower

response time (and digital nature) of FPAs make them unsuitable for this task.

2.5.3 Beaconing

Perhaps the simplest form of acquisition is the use of an optical beacon, which could conceivably be traced back to the ancients' use of bonfires to communicate from mountain to mountain. An optical beaconing system uses either continuous or modulated light which falls on either a photodetector or imaging array at the other end. These in turn use the intensity pattern to determine the location of the remote node, and then rotate the platform in order to center the detector on the received light. Beacons are attractive for their low cost and complexity, however their position resolution is relatively poor. For some lower frequency RF systems it may be appropriate, but for most DWNs at ranges greater than a few kilometers it would only be used as an initial guess to save scanning time using one of the other acquisition methods if GPS were not available. The optical beacon is still the most popular way to set up terrestrial links, especially in the many units being installed to boost cellular backhaul capacity.

2.5.4 Laser Beacon Limitations

One could conceivably think of a system with a large receiver and a very wide beacon transmit laser, where the transmitter could scan the sky coarsely and the receiver would quickly pick up part of the wide beam. Beacons lasers also have restrictions on their beam divergence, since enough power must still arrive at the detector in order to

distinguish the signal above the noise.

If we take the receive aperture of area A, transmit power P_t and distance L between nodes, the received power (neglecting atmospheric losses) can be written as:

$$P_{Rx} = \frac{2P_{Tx}A}{\pi L^2 \theta^2}$$

where θ is the transmitter beam divergence. The SNR in this situation is dominated by Johnson (thermal) noise in the receiver, so:

$$SNR = \frac{(\Re P_{Rx})^2 R}{3kT\Delta f}$$

where $\Re$ is the detector responsivity, R is the detector resistance, and Δf is the beacon bandwidth. The bandwidth is typically in the 10s of kilohertz range for beacon lasers, the modulation being higher than the maximum frequency of atmospheric turbulence so the receiver can distinguish between the two.

Figure 2.6 below shows the degradation of the SNR at the receiver as a function of beam divergence. From a designer's point of view, only the transmit power, receiver aperture area, and beam divergence can be changed, so the SNR at the receiver is proportional to these as they are altered. As one can see, the beam divergence term affects the SNR by θ^{-4}, so the SNR gained by decreasing the bandwidth or even increasing the transmit power is quickly lost by the component coming from the beam divergence. While beacon lasers are wider than the data lasers to some extent, they typically do no go wider than 10 mrad for systems operating at ranges from 10s-100s km.
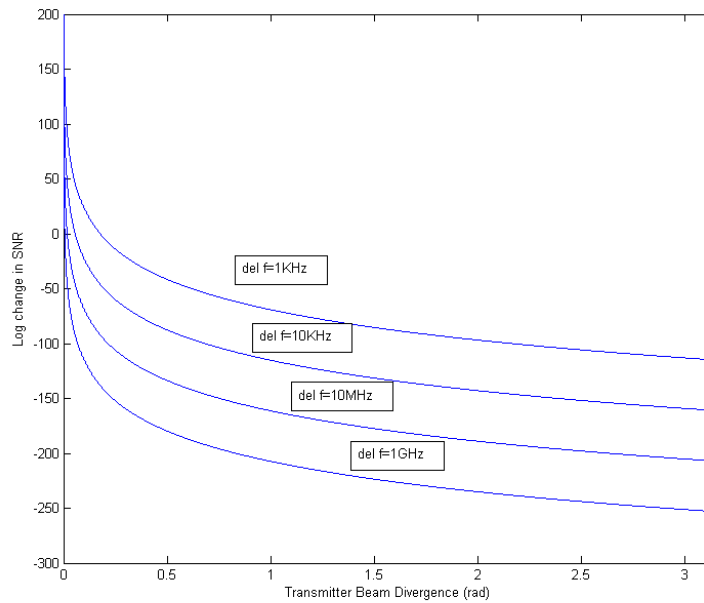
Figure 2.6: SNR vs. transmitter beam divergence. Decreasing the bandwidth improves the SNR, but much slower than the increasing beam divergence degrades it.

2.5.5 Received Signal Strength

A very common method for acquisition is the use of received signal strength. This is the procedure most commonly used for aligning terrestrial systems, for example installing RF backhaul links on cell towers, or FSO units between buildings. After an initial alignment either using a sighting scope or optical beacon, one user raster scans a unit to maximize RSS. The other side then repeats this procedure, and they go back and forth until both sides have an acceptable signal. In automated systems, the procedure is the same, but much quicker and usually with a spiral scan.

2.5.6 Geo-pointing

The last acquisition method is quickly becoming the most popular, mainly because of the advent of sufficiently precise sensors. Geo-pointing is the process of the two ends of a link calculating their azimuth and elevation angles to achieve alignment by knowing their own as well as the other side's position information precisely enough to form a link. Position can be readily measured using GPS (1m accuracy for commercial systems, <0.3cm for some military systems). Pitch and roll orientation angles can be found from inclinometers in static situations, and the yaw angle from a GPS time series, however a new type of sensor called an Attitude Heading Reference System (AHRS) is fast becoming the primary avionic orientation sensor. It combines gyroscopes, accelerometers, magnetometers, temperature and pressure sensors, along with GPS to provide stable and comparatively precise orientation angles even in a dynamic environment. Geopointing has a great advantage of being quicker than all other acquisition methods over a full sphere, since no large area signal scanning is involved. Positioning platforms are also precise enough now that a geopointing system can sometimes be used as the only alignment system in transceivers with sufficiently wide beam divergences. In narrower beam applications, it can still position the beams close enough at the onset to minimize the acquisition times by the fast tracking component of the transceiver.

Geo-pointing does have one disadvantage from a security point of view in that the two ends of the link must transmit their position information to each other over some omni-directional RF channel, potentially leading to the issue of interception and

detection. Since most major military communications networks are already encrypted, this is not seen as much of an issue, unless the delay caused by the encryption was great enough that the calculated pointing vector was no longer accurate once it was received by the platform, or the systems were operating in an environment where even the act of broadcasting anything over an RF channel could compromise their positions.

2.6 Sources of Error in a Pointing System

2.6.1 Mechanical Pointing Error

As mentioned earlier, looking at a transmitter operating with an initial spot size of:

$$w_0 = \frac{\lambda}{\theta_{beam} \cdot \pi}$$

The spot size a distance z away is then:

$$w^2(z) = w_0{}^2 \left[1 + \left(\frac{\lambda \cdot z}{\pi \cdot w_0{}^2} \right)^2 \right]$$

As a measure of pointing performance, one can look at the pointing angle error at which the receiver aperture begins to leave the beam spot. This simple approximation (for $z >> D$) is given by:

$$\varphi(z) \cong \frac{w(z) - \dfrac{D}{2}}{z}$$

Figure 2.7 below illustrates this concept, for beam divergences of 1mrad (red), 100μrad (blue), and 10μrad (green). The log-log plot shows the angular pointing error over distance at which the receiver aperture (here D=10cm) begins to fall outside the transmitter beam spot.
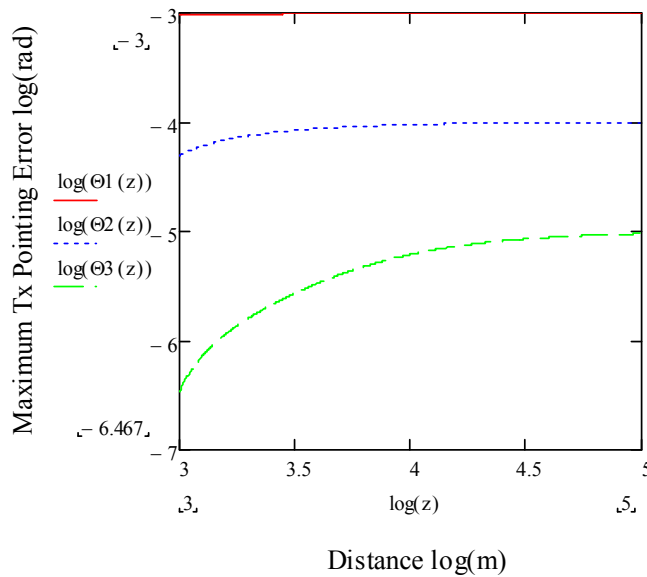
Figure 2.7: Pointing error vs. total receiver aperture coverage. The solid red line denotes a beam divergence of 1mrad, dotted blue represents 100μrad, and dashed green represents 10μrad.

There are several points of interest from this simulation. At close range, the amount of permissible pointing error is very low, but levels off quickly after several kilometers. Only for an extremely narrow beam is a very small pointing error still required at large distances. A FSO system must then find the right balance between

beam-width, transmit power, and platform pointing error in order to maintain the desired BER.

2.6.2 GPS Error

The Global Positioning System (GPS) is a RF-based positioning system based on time-delay-of-arrival (TDOA) measurements of signals from multiple satellites. Depending on the number of satellites, averaging, ground stations, and other techniques, positioning resolution can vary from 15 m down to less than 3 cm. The primary source of error in GPS arises from inaccuracies in the receiver's clock, as it uses this combined with the position and timestamp from multiple satellites to fix its own position. Given the distances between terrestrial receivers and the satellites, even nanosecond errors can cause sizable position deviations. This can be mitigated by using differential GPS, which uses ground station timing signals to reduce the receiver's error. In the USA, the WAAS (Wide Area Augmentation System) network of ground stations allows for an effective measured accuracy of about 1.1m [39], which is what is used in this thesis. GPS receivers will preprocess multiple measurements to give an average position, which also extends to heading data. Figure 2.8 shows the GPS latitude measurement from the Microstrain 3DM-GX3-45 AHRS units [41] used in this thesis, which shows an error of approximately 1m. It is worth noting that the error of GPS measurements is not uniformly distributed over time, so a PAT system using it must account for this variability.

The accuracy of a GPS receiver can be improved even more by using a real time

kinematic system, where a separate base station measures the carrier phase of the satellite signals, and then transmits the amount of offset the receiver should add so that the phase of its internally generated carrier lines up with the satellites'.

The performance of GPS is of great importance for a DWN network as well as a camera network, as these position values form the basis for any pointing operations. In the case of a camera network, the nodes will most likely be fixed, so RTK GPS may be used to get a one-time precision fix. In dynamic DWN networks where platforms are in motion and GPS is used to calculate heading vectors, the system must collect and determine pointing angles quick enough to ensure the GPS measurements do not become out of date.
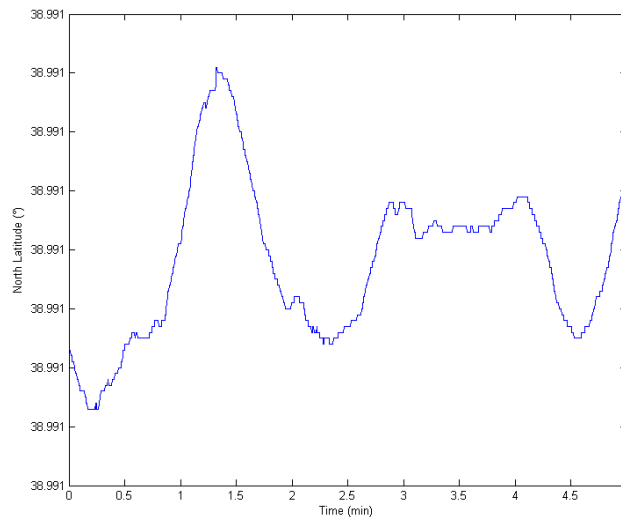
Figure 2.8: GPS Measurements over time. The total error is approximately 1m, but varies over time depending on which satellites are being used by the receiver.

2.6.3 Orientation Sensor Error

There are several methods in use to find one's orientation in space, be it the inclinometer, INU, AHRS, or multiple GPS measurements over time. A very reliable method on terrestrial systems is the inclinometer, which gives the two orthogonal tilt vectors with respect to Earth's gravity vector. From devices that were used in prior work, they offer reliable outputs with errors less than 0.01°. Figure 2.9 below shows a plot of an Applied Geomechanics inclinometer's output [42], where its white-noise profile is clearly visible.
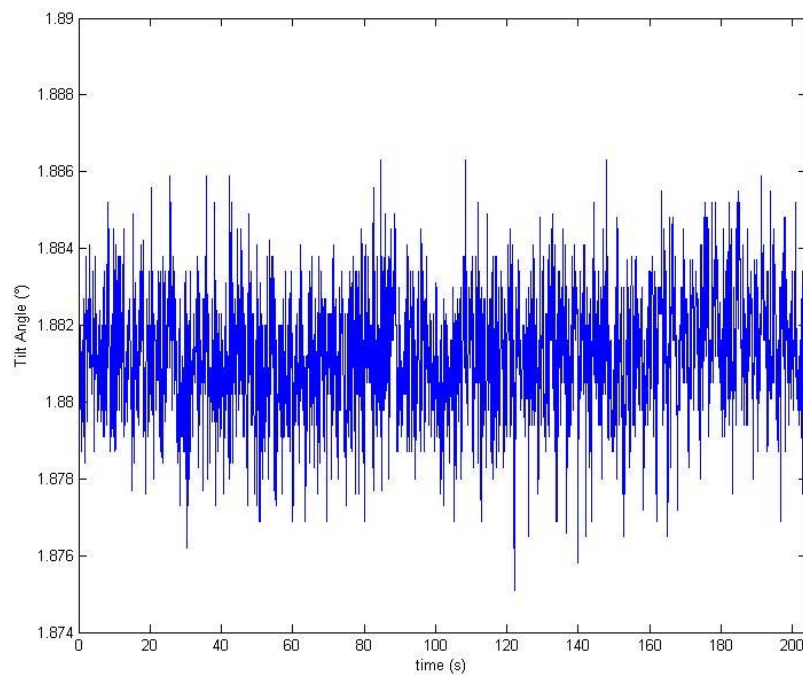
Figure 2.9: Inclinometer angle measurement over time. The white noise profile is clearly visible, and the error is <0.01°.

Using inclinometers on airborne systems has the disadvantage of the change in measurement because of acceleration. This will distort the inclinometer's gravity measurement that it uses for calculating tilt angles. Commercial aviation systems typically use INUs that integrate their angular velocities over time, or by looking at GPS coordinates to establish a heading vector or to correct INU measurements.

Finding the last of the three orientation angles (yaw) can be troublesome, as the time honored method of using a compass is rather inaccurate (the best digital units have repeatability around 0.25° [43]). Another method is looking at gyroscope data over time, however there still can be major drift even if the unit is calibrated and temperature compensated. Figure 2.10 below shows the azimuth angle over time from a calibrated INU designed to output the three orientation angles.
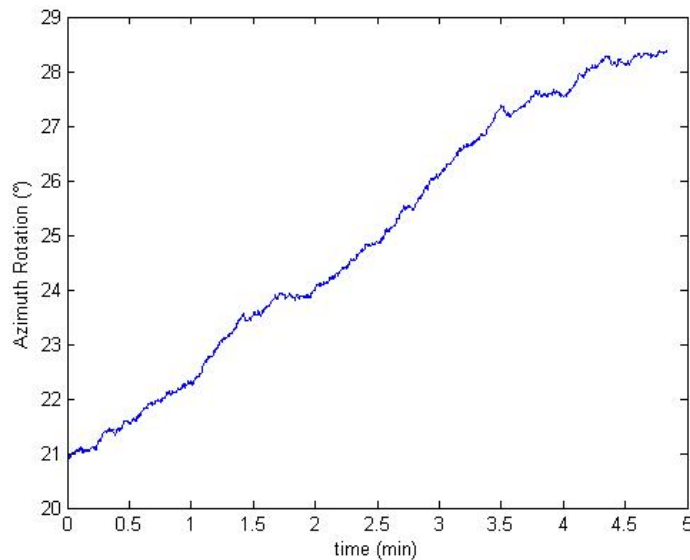
Figure 2.10: INU azimuth orientation angle drift over time. Even in a static situation the azimuth angle measurement is unusable due to gyroscope drift.

2.6.5 The Attitude and Heading Reference System

In recent years a new type of integrated sensor package has been developed to replace the role of INUs in aircraft and other vehicles. The Attitude and Heading Reference System (AHRS) combines MEMS gyroscopes, accelerometers, magnetometers, and GPS to provide a complete package outputting pitch, roll, and yaw orientation angles. The devices use some type of filtering (commonly Kalman filtering) to provide all this information in a sufficiently accurate manner for aircraft operations.

With regard to their use in DWNs, AHRS units are desirable because of their orientation angle format with integrated GPS, eliminating the need for external filtering and processing, as well as a separate GPS processor. They also provide adequate accuracies for most situations, even dynamic ones. Table 2.1 below gives an overview of several types of commercial AHRS units.

	3DM-GX3-45 [41]	IG-500N [44]	NAV440 [45]	MTI-G [46]
Manufacturer	Microstrain, Inc.	SBG	Moog, Inc.	Xsens, Inc.
Interface:	RS-232	RS-232	RS-232	RS-232
Weight:	23 grams	49 grams	580 grams	68 grams
Size:	44x24x14 mm	36x49x25 mm	76x95x76 mm	58x58x33 mm
GPS Accuracy:	2.5 meters	2 meters	3 meters	2.5 meters
Pitch, Roll Accuracy	0.35°	0.5°	<0.4°	<0.5°
Heading Accuracy	1.0°	1.0°	<0.75°	<1.0°
Update Rate:	100 Hz	100Hz	100 Hz	120Hz
Kalman Filter	Yes	Yes	No	No

Table 2.1: Commercial AHRS Comparison

AHRS units have integral inclinometers to provide pitch and roll angles, and use the integration of a gyroscope over time to give the yaw angle. This angular measurement is corrected using accelerometers, magnetometers, and if available, GPS time series. A settling time can be seen when measuring the yaw angle, so its repeatability is noticeably worse than the other two angles. Due to this settling behavior for the yaw angle, it will give errors in the 1-2° range as opposed to the 0.01° average error from the other two axes in static situations. However, while in motion, all axes exhibit about a 1-2° error because the inclinometers cannot be used in the presence of great acceleration. AHRS units also use GPS measurements over time as a correction factors for the orientation angles, but this only works when the platform is moving.

2.6.6 Actuator Error

Any moving mechanical system has certain degrees of error, either from mechanical flexure, slop in gearing, tolerances in bearings, and even how the motors are controlled. Geared motor systems are generally unusable for DWN platforms because of the precision and responsiveness required. DWN transceivers are also lighter and smaller on average, so reduction gearing is not needed. Fortunately, modern servo motors are manufactured with micrometer precision, so any eccentricity of the rotor shaft is so small that is does not contribute meaningfully to the overall pointing error.

One area that does contribute to pointing error is the positioning loop error found in the controller electronics. All servo motors are electrically commutated, and the

cumulative error of the Hall-effect sensors, encoders, and processing electronics affect

the repeatability of the system. The motor control loop process will be detailed later in

this thesis, however it is worth noting here that the best servo motor controllers can

guarantee repeatabilities in the tens of microradians. This is greatly dependent on the

load inertia and rotation speed, but in general it holds over a wide range of payloads.

2.7 Establishment of the Pointing Vector between Two Platforms

Consider the situation in Figure 2.11 below with a transceiver in space (on an

aircraft, for example) with coordinates $X_L=[x_L,y_L,z_L]$ and orientation θ , ϕ , γ pointing

to another remote transceiver at $X_R=[x_R,y_R,z_R]$. The azimuth and elevation angles that the

platform must move to in order to create a link can then be calculated. Also assumed is

that the spacing between the links is large enough that translation offsets in the payload

can be ignored.
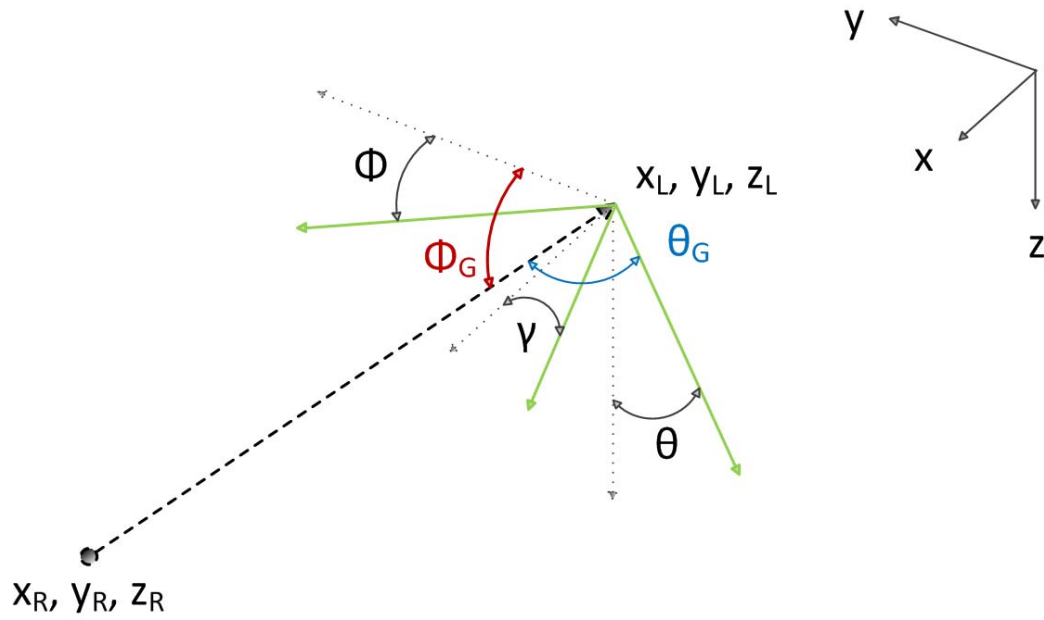
Figure 2.11: Pointing between two platforms. Based on a platform's position and orientation and the target location, azimuth and elevation angles can be calculated to point the transceiver at that distant point.

The transceiver platform's rotation about the x, y, and z axes in matrix form as R_x, R_y, and R_z can put the remote transceiver's position in space in terms of the local transceiver's coordinate system by:

$$X_F = R_x(\varphi)R_y(\gamma)R_z(\theta)[X_R - X_L]$$

where

$$R_x(\varphi) = \begin{bmatrix} 1 & 0 & 0 \\ 0 & \cos(\varphi) & -\sin(\varphi) \\ 0 & \sin(\varphi) & \cos(\varphi) \end{bmatrix}, R_y(\gamma) = \begin{bmatrix} \cos(\gamma) & 0 & \sin(\gamma) \\ 0 & 1 & 0 \\ -\sin(\gamma) & 0 & \cos(\gamma) \end{bmatrix}, Rz(\theta) = \begin{bmatrix} \cos(\theta) & -\sin(\theta) & 0 \\ \sin(\theta) & \cos(\theta) & 0 \\ 0 & 0 & 1 \end{bmatrix}$$

and

$$X_R = \begin{bmatrix} x_R \\ y_R \\ z_R \end{bmatrix}, X_L = \begin{bmatrix} x_L \\ y_L \\ z_L \end{bmatrix}$$

The angles required for the gimbal to point from the local to remote point are then found by the spherical coordinate transformations:

$$\theta_G = \cos^{-1}(\frac{z_F}{r}) \ , \ \phi_G = \sin^{-1}(\frac{y_F}{x_F}), \text{ where } r = \sqrt{(x_F)^2 + (y_F)^2 + (z_F)^2}$$

This process can then be repeated for the remote platform's gimbal so it can point back to the local transceiver.

2.7.1 Angular Ground Truth

One issue that has not been mentioned up to this point is that of the initial calibration of the gimbal encoders. While it is relatively straightforward to find the azimuth and elevation rotation angles for a gimbal based on GPS and orientation sensors, these are based off some initial reference. In other words, if a gimbal rotates to absolute zero, its payload will be pointed directly due north and perpendicular with the surface normal of the geoid at that point. Without this initial calibration, the gimbals have no way to know that they are all pointing based off the same reference system. There are several ways to achieve this calibration, many of which were evaluated and tested in previous group work [53].

49

The elevation angle reference is typically found using a precision inclinometer while in a static situation. These devices give the pitch and roll angles relative to the gravity vector by means of a fluid filled capacitor, and can be precise to within thousandths of a degree. Calibrating the yaw angle is once again more complex. If the gimbal can be precisely mounted on its vehicle pointing at 0 in the direction of travel (towards the nose of a plane, for instance), then looking at the GPS heading vector over time can give an initial reference angle. Another method is pointing at a known beacon on the ground either using the transceiver, or a camera. If the target's GPS location is already known, centering the target in the camera or optimizing RSS in the transceiver can give a calibration when combined with the moving platform's GPS position. The accuracy of this type of calibration depends on the resolution of the GPS measurement, the separation between the units, and the precision of the sighting measurement.

2.8 Methods for Coarse Pointing and Tracking

Once an initial pointing vector has been formed and both sides have enough received signal strength to form a data link, the two platforms must then update their azimuth and elevation angles over time in order to maximize RSS. There are three primary ways to do this, depending on the technology available and transceiver pointing requirements.

The first method, and perhaps the most common, is optimizing received signal strength by adjusting the azimuth and elevation angular velocities of the gimbal motors. Some systems with multiple receive apertures or QPDs can tell you which direction the

signal is moving, thus making the velocity commands rather simple. Rather than guessing which velocity to move at, the common tactic is to use some type of continuous small angle scan to cover a region of interest around the most recent RSS measurement. The spiral scan is most preferred, due to its efficiency in rotating the platform in a smooth, continuous motion. A major disadvantage of this approach is in cases where the signal is lost for a period of time longer than a scan cycle. When this occurs, the system can either widen the scan area, or it must go back into reacquisition mode. If the platform is properly tuned, it would be rare for the system to lose the signal for that long, however this is assuming the moving vehicle as a whole does not make any sudden course changes (like an aircraft diving, for instance).

A variant of the above procedure still relies on RSS to optimize the pointing angles, but instead of commanding angular velocities to the gimbal motors, it commands angular positions. This has limited use outside of FSO, where it can be used to find the pointing vector by looking the received signal beam's spot falling on a position-sensitive detector, which can be related to the azimuth and elevation pointing angles. It would primarily be used in situations that called for a coarse pointing system in order to aid a fast-scanning mirror or adaptive optics setup. It is worth noting that a terrestrial FSO system from Canon [47] uses this approach to compensate for building-sway.

The final coarse pointing method does away with RSS all together and relies solely on the position and orientation sensors at both ends, along with an omnidirectional control network. Exactly as mentioned earlier in the acquisition section, the master node collects position and orientation data from its own sensors and those of the remote

nodes', and then commands the appropriate pointing angles for both platforms. In a pointing system, however, this process is then repeated many times a second to maintain the pointing vector over time as the platforms move. This method has a unique advantage in that even if the received signal is disrupted for a significant period of time, when it recovers the two links will still correctly pointed at each other. The RSS-dependent procedures would still have to enter a reacquisition phase. Of course, in any real system some gauge of the RSS is required, so this approach would still use it as a backup.

Deployable systems (and the one presented in this thesis) typically use a combination of geo-pointing and RSS-based spiral scanning, since the scanning can optimize the pointing in the time in between geo-pointing updates (depending on the sensors' update rates, the node count of the network, and the relative velocity of the two nodes). Geo-pointing is also frequently used in systems with fast scanning mirrors, as the pointing error in the geo-pointing portion can determine how much angular range the FSM must have, and by extension, what its response time should be.

2.8.1 Scanning Patterns for Acquisition and Tracking

Scanning a region of space can be achieved in a variety of manners, for example random scans, spiral scans, raster scans or any other pattern. However, if one wishes to cover the most angular range as quickly as possible while maintaining even sample spacing, the spiral scan is the best choice. It has been used since the invention of radar for scanning the sky efficiently, and is the only real scanning method used in directional wireless for several reasons.

Figure 2.12 shows the basic spiral scan curve and coverage area for a beam of diameter D at some point in space away from the transmitter, and figure 2.13 shows various corresponding raster scans. Depending on the distance away, the resolution of the scan must be changed to ensure complete coverage, and this is also dependent on the divergence of the beam.
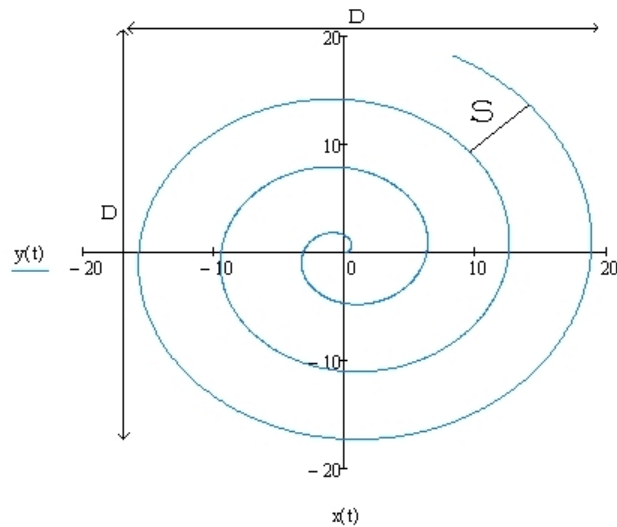
Figure 2.12: The Spiral scan. This plot shows an Archimedean spiral in which the radial distance between arms of the spiral (shown as s) is equal.
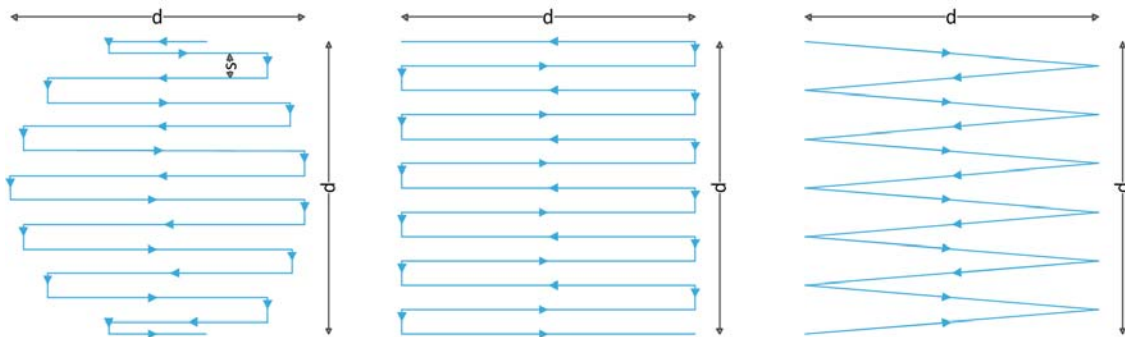
Figure 2.13: Types of raster scans. From left to right: circular raster, square raster, and sloped raster scans, all with a spacing of s.

The second important advantage is mechanical. When executing a spiral scan, the actuator can send simple sine and cosine valued velocity or position commands to the motors, so that neither motor will have to make rapid direction changes or stop/slow severely, as would happen in a raster scan. Therefore the time to cover an area with a spiral scan is usually less than a raster or random scan. Monte Carlo results of a random scan will be detailed in Chapter 4.

An Archimedean spiral (where the spacing between spiral arms is constant) can be given in polar coordinates by:

$$r(\theta) = a + b\theta$$

where a is the starting point (0 starts at the origin) and b is related to the spiral spacing by

$$b = \frac{s}{2\pi}$$

where s is the spacing in radians. The arc length of the spiral for n revolutions can be found using the polar arc length formula:

$$L = \int_{a}^{2n\pi} \sqrt{r^2 + \left(\frac{dr}{d\theta}\right)^2}\, d\theta$$

The path length can thus be found by:

$$L = \int_{a}^{2n\pi} \sqrt{(a + b\theta)^2 + (b)^2}\, d\theta$$

Whereas a square raster scan covering the same FOV would be:

$$L = d + \frac{d}{2s}(2d + 2s)$$

A sloping raster scan is a simpler version, translating in both x and y while covering the

same area. The time to cover an area is less than the square raster scan, however it is less

efficient because of the places it overlaps. The total length for a sloping raster scan

would be:

$$L = \frac{d}{s}\sqrt{s^2 + d^2}$$

Both these two types of raster scans overfill the FOV, but are simpler to characterize and

implement. The last type of raster scan described here more accurately covers the FOV,

and is called a stepped raster scan. In this case the path approximates a disc, and only

overfills the FOV minimally. Its path length is somewhat more complicated, being

represented by the expression:

$$L = 2 \cdot \left[\frac{2r - s}{2} + \sqrt{r^2 - \left(r - \frac{s}{2}\right)^2} + \sqrt{r^2 - \left(r - \frac{\left(\frac{2r}{s} - 1\right)s}{2}\right)^2} + \sum_{k=0}^{k=\frac{r}{s}-1} \sqrt{r^2 - \left(r - \frac{(2k+1)s}{2}\right)^2} \right]$$

Figure 2.14 below shows plots of raster and spiral scans for various resolutions at the

same average velocity where the path length disparity between the types is evident.
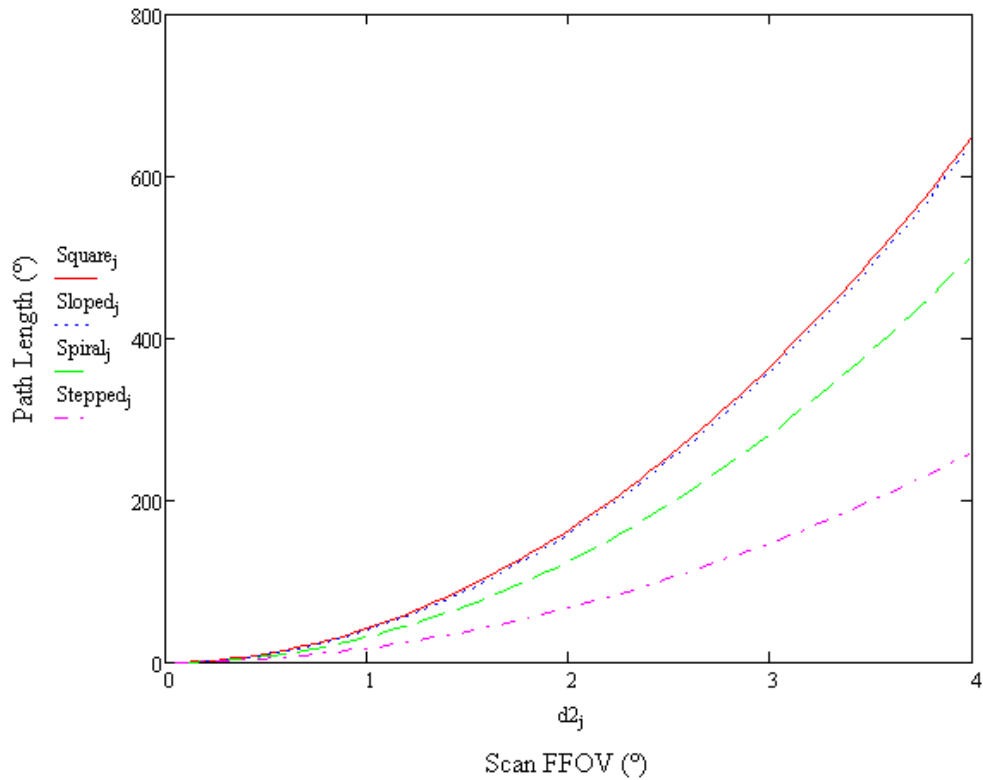
Figure 2.14: Path lengths of spiral and raster scans for various resolutions over a 5°
FFOV with s=0.025°. The solid red line shows the square raster path length, dotted blue
the sloped raster, dashed green the spiral scan, and dot-dashed purple the stepped-circle
raster scan. Even though the spiral scan is not the shortest, its lack of acceleration
changes during motion will actually make it the quickest.

A comparison of the scan lengths for the patterns shown here gives a designer

important information about how to choose a scan, but also that path length is not always

the most important detail. The overfilled square scan takes the most time, not only

because of the path length, but because of the multiple decelerations required at each

corner. While popular in terrestrial scanning systems, it is not used in signal acquisition

because of the slow coverage rate and the fact that it must first move off center to begin a

scan, making it more likely to miss a target completely if the target is moving in the

opposite direction. The sloped scan fares a little better, but still has the same problems.

The spiral scan is significantly shorter in path length, but the stepped raster actually has a

much shorter path length. This result can be deceiving, however. If one takes into

account how the platform would move when executing such a scan, the many changes in

velocity would eventually lead to a longer scan time than a spiral scan, which moves at a

steady rate throughout. Again, the stepped raster has the same problem as the other

rasters in that it does not scan from the center. There is a variation on the spiral scan, the

square spiral which starts from the center, however it has the issue of having many hard

turns which increases the overall time. While it has a slightly longer path length, the

spiral scan is still the primary method for acquisition because of its good fit with the

mechanics of the platforms that run the scan. In airborne systems where the platforms are

already constantly in motion while compensating for platform disturbances, the addition

of a spiral scan of top of this movement presents a much easier mechanical motion profile

than that of a raster or random scan. A spiral scan can be run as part of the platform's

velocity mode control, while the various raster scans would have to be run in position

mode, something problematic because platform stabilization loops are run in velocity

mode only.

2.8.2 Scan Resolution

We can now expand the idea of a spiral scan to include the properties of the

transmitter and receiver, namely spot size and receiver diameter. There are typically

restrictions on the divergence of a beam, since transmitters have finite amounts of power

in a given situation. Therefore they are kept as tight as possible to maximize received

power assuming perfect alignment. Since perfect alignment is never possible in a

dynamic situation, some sacrifice will be made, but it almost always involves increasing

divergence, but also the receiver aperture, and increasing transmitter power as a last

resort.

For a transmit laser executing a spiral scan, if the beam spot diameter at the

receiver is *2w(z)* and the receive aperture is diameter *D*, the scan spacing must be less

than *w(z)*. This is only true at distances such that the beam spot is much larger than the

receiver lens. At the transmitter this corresponds to a scan angular resolution of:

$$\theta_a \leq \frac{w(z)}{z}$$
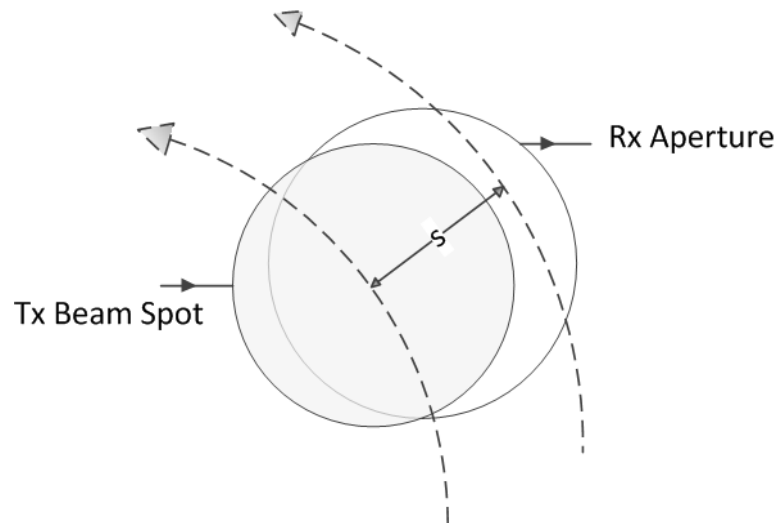
Figure 2.15: Determining the resolution of a spiral scan. The transmitter must be able to
scan at a resolution fine enough to ensure sufficient coverage of the receiver, otherwise
the beam could miss the detector completely.

This is an important result to consider because it changes as a function of range. Thus the resolution required at longer ranges is less than at close ranges, so the pointing system would not need to be as precise.

2.9 Issues Unique to either FSO or RF systems

While this thesis has been generalized to narrow beam wireless networks, there are some technology specific considerations worth mentioning when using either directional RF or FSO transceivers. First, as can been see below in figure 2.16, the beam divergences of different transmit aperture sizes at various RF frequencies are quite different from FSO. This leads to the invariable conclusion that FSO requires more pointing precision, especially as the beam divergence gets smaller in longer range links. Both technologies can suffer crosstalk issues with collocated transceivers; however this is more of an issue in RF because the waves can pass through and reflect off components or structural material to another receiver or be interfered with by a nearby transmitter. To mitigate this issue, some systems are starting to use multi frequency transceivers. Even in FSO there are manufacturers using different wavelengths for the data and beacon lasers. Secondly, FSO systems have an advantage in that their transmit and receive channels operate independently, thus allowing for easier full duplex communications. RF systems can only use the antenna for either transmit or receive at one time, so some type of addressing scheme must be used. For a RF system to achieve the same full duplex data rates as an FSO system, the electronics must be more complicated, and the modulation frequency is typically higher than the OOK modulation frequency of FSO.
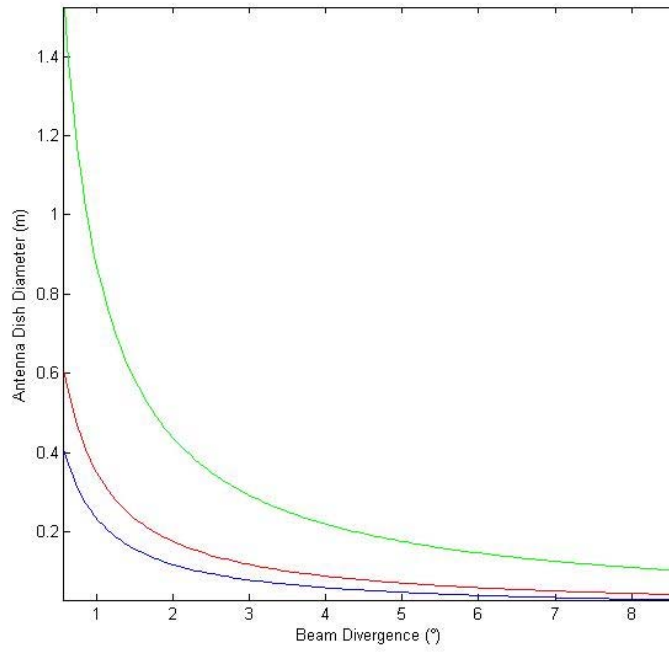
Figure 2.16: Transmitter dish diameter as a function of beam divergence at 80GHz (blue), 60GHz (red), and 24GHz (green). The change in beam divergence is much more pronounced for smaller dishes.

Chapter 3: Hardware and Software Design Considerations for Directional Wireless Networks

3.1 Introduction

As was mentioned in the introduction, the use of highly directional transceivers requires a mechanical means for steering their beams. While some quasi-static systems do exist (phased arrays are one example), even they can sometimes need mechanical pointing depending on the required coverage. The most common and versatile device for pointing these transceivers is the two-axis pan-tilt platform, more commonly known as a gimbal. These devices can rotate a payload in azimuth and elevation, either by rotating to a known angle (position mode) or rotating at a known angular velocity (velocity mode). Gimbals are fairly ubiquitous devices in modern life, though we might not always notice. They can be found on security cameras all over the world, telescopes, robotic assembly lines, cameras at sporting events, radar, and even communications systems. They use a variety of motor and controller technologies depending on the application, and come in great ranges of precision, load capacity, and agility. It was never a specific goal of our group to develop gimbals purely for their own sake; however the lack of affordable units with sufficient pointing precision, payload capacity, and agility led to the design and construction of a series of platforms for different applications. These will be detailed later in this chapter, along with their relevance to DWN research.

This chapter will present a review of current commercial gimbal technologies with respect to terrestrial and airborne DWNs, and current DWN research using these and other custom-made platforms. The requirements for FSO/RF gimbals will then be detailed, and various hardware and software design considerations will be discussed. The control circuitry will then be detailed, along with the FPGA-based control code. The mechanical, optical, and electrical design of the gimbals built for this work will then be explained. The last part of this chapter will deal with the architecture of the secondary control network that links all the platforms together.

3.2 Current Work

Many commercial vendors supply pan tilt platforms for a variety of applications, however only a few could conceivably be used in airborne systems. Most of us are familiar with the ball-shaped units seen on helicopters and some aircraft which can provide stabilized imagery of events on the ground, be it for law enforcement, sports, wildlife management, or traffic monitoring [48-50]. They utilize pan and tilt servo motors which stabilize a payload that in turn is often mounted on a secondary platform that is stabilized by elastic band motors. These motors cannot hold a heavy payload; however their responsiveness allows the platform to compensate for higher frequency aircraft vibrations. Unsurprisingly, these gimbals can cost upwards of $500,000, and typically fall only within the purview of governments and large media organizations. For a FSO system they would be ideal, but their cost makes them a rarity in current research, the few exceptions being the FALCON program at ITT, which uses modified MX12 Skyballs [6],

62

and the FOENEX program at DARPA [3].

Other current research efforts in PAT typically use off the shelf positioning systems, usually antenna or camera positioners [51]. All of these units are sufficiently precise for the applications involved, however they are all quite slow (<30°/sec) and cannot change their direction rapidly or point precisely enough for mobile DWN applications. In a government sponsored deployment on a large scale, perhaps the cost would not matter for purchasing many modified Skyballs, however it was worth investigating and building FSO specific platforms that could test DWN concepts in the field while also providing a cost-effective research platform for our and other groups working in this area. Another area of interest is the construction of devices similar to RF phased arrays, but for optical signals. These use groups of transmitters and receivers to coverage a large FOV, and switch their components on and off depending on the direction of arrival of the signal. While much more complicated optically, they do offer a full coverage solution with no moving parts [52].

Although many groups that focus primarily on transceiver design use COTS gimbals, there are some researching custom designs, especially in the E-band regime. Since these types of transceivers will be mounted on aircraft, spacecraft or the like, size, weight, and power (SWAP) requirements can be quite severe. For example, the recent DARPA Mobile Hotspots Program aims to place 1 Gb/s gimbalized E-Band transceivers on Shadow UAVS, operate at up to 10km apart, and fit inside an 8.5" diameter pod that is 10" long [4]. No commercial gimbal exists that can fit a system like this while providing the agility needed to keep a link connected in such a dynamic environment. Another

program at the Air Force calls for a pair of E-band gimbals that can form a satellite to ground link, the ground link being man portable [5]. As these E-band radio transceivers become more mature, there will be an even greater push for custom positioning systems, along with the algorithms to control them and aid in the formation of networks.

Custom platform research in the FSO regime is more limited, and primarily focused on ground based systems. A group in Japan has developed gimbaled mirror platforms to achieve ground to train FSO links while the train is in motion, and also hand off from gimbal to gimbal so the train has continuous connectivity [53]. Several projects at the Naval Research Laboratory (NRL) have taken a unique approach to FSO communications by using modulating retro-reflectors to act as a non-mechanical beam steering device, so the moving platform only needs to have a fixed optic on it. This only allows one way communications, but for a UAV sending video to the ground, it is a very efficient method [54]. NRL has also demonstrated ship-to-ship FSO communications using very large COTS platforms at modest ranges as well as in some air-ground scenarios [55].

The overall trend in the PAT platform area is towards the development of smaller, more agile gimbals for both laser and RF communications systems, with the intention that most of these units will be mounted on unmanned vehicles. Judging by current government efforts, this area will become even more active in the next few years.

3.3 FSO Platform Design

Due to the inherently narrow beams in DWNs, transceivers must be precisely aligned with each other in order to ensure that enough power falls on the receiver. When the requirement is added that the transceivers must be mobile, a method must be found to steer the beam in some fashion. Some narrow beam RF systems use phased-arrays to accomplish this, and while they lack moving parts and can supply high data rates reliably, they are prohibitively expensive in most situations and can be quite heavy. In the case of FSO, some work has been done on a similar concept involving arrays of lasers that communicate to different areas in space, making alignment much easier [45]. These systems are greatly limited in range due to the wider beam divergences of their lasers, but they can be very effective in indoor applications. The most common way to point a DWN transceiver is with a gimbal, and many companies make a variety of them for applications such as antenna dish pointing, surveillance systems, and weaponry. Only a handful make units that could be used for DWN systems, but none are really suited for RF systems.

The requirements for a DWN gimbal are significantly different in a few areas that make them unique from all other platforms to-date. The most important capability is that of agility. DWN gimbals must be able to continuously make quick acceleration and direction changes in order to maximize received power in the face of its transport platform experiencing various shocks, vibrations, and other movements. These movements can sometimes be at rates over 5Hz. To achieve such performance, the type of motor and controller used in the gimbal is of critical importance. The stepper motor is

known for its precision movement and high load capacity. However the nature of the gearing that gives it such characteristics also makes it quite slow. Stepper controllers that also generate a current profile before moving are also undesirable for a DWN gimbal, because a new positioning command cannot be issued until the previous one is completed. Stepper motors also have significantly slower acceleration than similarly sized motors from those in the next family of motors, servos.

Servo motors are much more common in the robotics community because of their high peak torques, direct load coupling, and precision motion control. The most noticeable feature of modern servos is that of electrical commutation. While older model servos used brushes to let the motor know the position of the rotor in order to correctly apply power to each of the stator packs in the correct order, these brushes reduced efficiency and also the lifetime of the motor. Almost all servo motors today use Hall-effect sensors instead of brushes. These sensors tell the orientation of the magnetic field coming from the rotor magnets, which is then fed into the commutation electronics that along with an angular encoder comprise a complete closed-loop positioning system.

Servos in which the load is directly coupled to the rotor are known as direct-drive motors. These are popular due to their compact design, lack of gearing, and high peak torque values [46]. Coupling the load to the motor with a gear can increase torque and load bearing capacity, but the backlash in the gearing will reduce the resolution of the system as well as prevent rapid direction changes.

Servo motors come in a variety of shapes and sizes; however there is one particular form factor which is important in gimbal systems, the axial flux servo motor.

These motors have large pancake like rotors where the magnets extend more out the radius than the more common radial flux motors that have the magnets extending down a shaft all at the same radius. Axial flux servo motors have a lower continuous torque rating than radial flux motors, however their peak torque is several times higher [56]. This high peak torque allows a gimbal system to be much more agile, and also allows for a more compact platform structure.

As mentioned earlier, a complete servo positioning system includes some type of rotational angle sensor. Some systems use angular resolvers, but most use optical encoders. These coded wheels have small holes that pass an optical signal through to a receiver, and the series of pulses can be read off as the position. Modern encoders have resolutions of over one million pulses per revolution (ppr), and the ones used in the motors in this work were 20 bit absolute encoders. Absolute encoders are much preferred because they retain their position after being powered off, as opposed to incremental encoders, which reset to zero after losing power.

How the servo motors are controlled is also of critical importance in a DWN system, as one must achieve low latency, high responsivity control with minimal overshoot and high accuracy. The basic servo motor controller is a Proportional-Integral-Derivative (PID) type, with three nested loops: current→velocity→position. Typically the end user only directly controls the position loop; however the two others must be precisely tuned for the position loop to perform well. Figure 3.1 below shows a block diagram of the basic control structure.
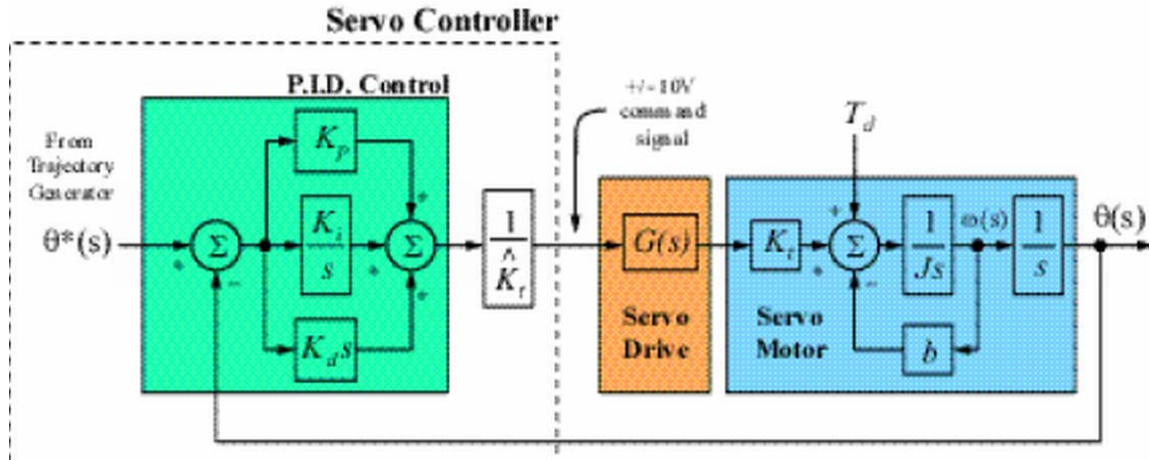
Figure 3.1: Servo motor control loop [57]. The goal of the PID loop is to minimize the difference between the motor's current position and the commanded position.

The overall goal of the servo control loop is to minimize the position error (or velocity error if running in velocity mode), defined as the difference between the current encoder position, and desired encoder position (or difference between measured and commanded velocity while in velocity mode).

As seen above in figure 3.1, there are many parameters that can be adjusted in a servo control loop, depending on the application. Systems rotating a motor at a constant and precise velocity will pay more attention to the velocity and current integral gains, while quick positioning systems will focus more on differential and proportional gains to ensure rapid, precise movement with minimal overshoot.

3.3.1 Mechanical Design Considerations

Gimbals come in all shapes and sizes, but there are several important mechanical design considerations that all must take into account. First is that for maximum performance, the platform and its payload must be weight balanced. That is, when no power is applied to the motors, the payload will rest at its zero position. This has several important benefits. First, as direct drive motors always draw current when energized, if the system is balanced when not moving, the servo motors must only use a minimal amount of power to hold position. Second, when the motors do move, their response time is improved as they do not have to first overcome the forces from an uneven load. Lastly, a balanced load presents a more predictable object to move for the motors, so the servo control loop as a whole is more responsive, both in rapid accelerations, and slow steady rotations.

The next important consideration is that the platform be as compact as can be allowed, so that it can fit in the smallest imaginary cube possible. This reduces the moment of inertia seen by the motors, again improving control responsiveness and power consumption. Ungainly platforms will exhibit under-damped rotations in many cases, and can even cause the things they are mounted on to become unstable. It is for good reason that the camera platforms seen on helicopters are small, spherical devices.

The mechanical structure must also be as light as possible without allowing for major flexing of elements. Even small distortions in a payload's mount could throw a narrow laser beam off its target many kilometers away. Another device used to minimize unintended payload movements is the slip ring. These rotational joints allow the cabling

in the platform to rotate freely about the motors' rotational axes without causing cable drag. Cable drag appears to the controller like some unknown (and uneven) load on the motors. The servo motors will attempt to compensate for this, but since the cables will not always move predictably, this will cause erratic performance in the servo motors. Slip rings also prevent cable overlap, where if a motor axis rotates more than one revolution, the cables could be torn out. Many platforms have hard limit switches to prevent this, but slip rings offer an added layer of protection in case of a major electrical failure in the controller.

Whether a platform holds a FSO or RF transceiver can make a big difference in how the platform is designed. Since FSO systems are usually driven by EDFAs some distance away from the steerable portion of the transmitter, the gimbal must either have a fiber-optic slip-ring, or some type of cable management to prevent the fiber from getting a bend radius so small that it loses light containment. E-band RF platforms must deal with the difficulty of taking signals through a waveguide structure and getting them to a steerable antenna. This could include using flexible waveguide, mounting the radio and PA directly behind the dish (which can dramatically increase the payload weight and inertia), or using some other antenna design where the waveguide does not have to move at all [58]. All of these options are under consideration in the various active research programs, and minimizing the mechanical complexity of the moving portion of the platform is of critical importance for the agility and reliability of a deployed system.

3.3.2 Platform Design for This Thesis

      For the work featured in this thesis, a different type of platform was required, as it had to hold both a camera and FSO unit, but also have integrated control for both and stabilization capability as well. As the camera could be used either as a beacon finder (or house a laser beacon instead) or as a surveillance camera, it had to share the same elevation axis as the FSO transceiver. In this setup, each payload sat on opposite ends of the elevation motor, allowing the weight of the elevation motor to sit directly above the rotational axis of the azimuth motor. As the payloads were significantly lighter than the elevation motors (3 lbs as opposed to 11 lbs), centering the elevation motor minimized the inertia seen by the azimuth motor, thereby reducing power consumption and improving response time. Since stabilization was required, the motors were directly coupled to their load and no gearing was used. The lack of gearing allows for rapid small and large movements, limited only by the acceleration limit of the motor. While gearing is advantageous in super-precise pointing as well as holding heavy, unbalanced loads, the mechanical slop and inability to change direction quickly makes them unsuitable for stabilized platforms. Table 3.1 below gives the specifications of the six completed platforms, and Figure 3.1 shows the finished platforms.

Feature	Specification
Motor Type	Brushless AC Direct Drive Servo Motors [59]
Encoder	20 bit, absolute
Slip Ring Type	Axial, 24 circuits, gold plated brushes and rings
Gimbal Form Factor	T-Style, common elevation axis
Payload Capacity	35lbs
Slew Rates	>360°/s in azimuth and elevation
Positioning Repeatability	±0.002°
Azimuth Angular Range	0-360° continuous
Elevation Angular Range	-25° to 205°
Weight	30lbs (with current payload)
Dimensions	6.5" x 11.5" x 12"
Control	Spartan-6 FPGA [60] mounted on custom I/O board

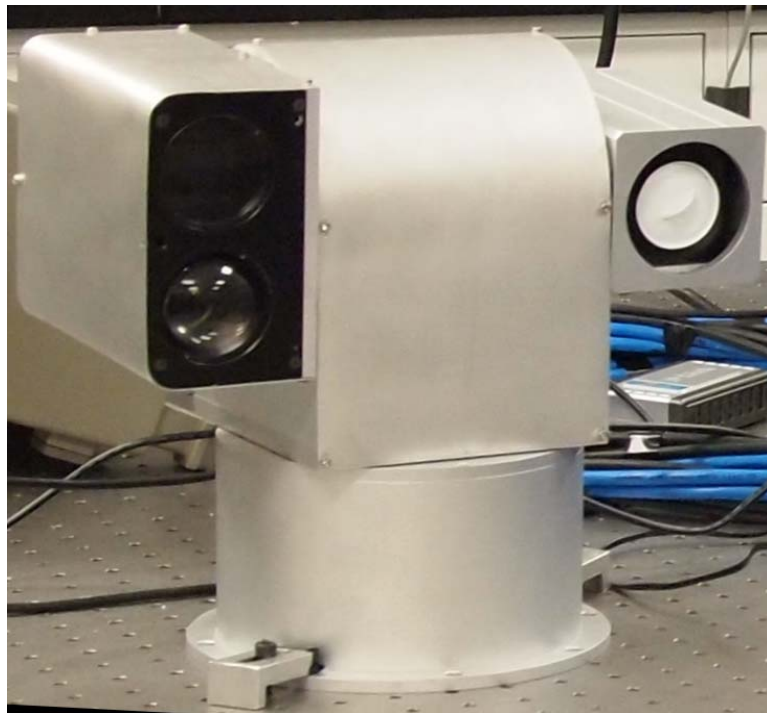Table 3.1: Platform Specifications

Figure 3.2: One of Six Completed FSO/Camera Stabilized Platforms

3.3.3 Prior Work in Stabilized Platforms

The platforms seen in this thesis were not created entirely out of a vacuum, as they are the latest in a family of platforms built over the last seven years for various applications. The lessons learned from these other projects were critical in the success of this current work. These platforms have a unique combination of speed, precision, agility, load carrying capacity, and cost effectiveness not yet seen in the commercial market.

In Figure 3.3 below, a pair of platforms is shown holding a long range camera system using machine vision cameras tied to 22x computerized zoom lenses with 16 bit precision encoders on their zoom and focus elements. This ability to know the positions of the both the lens elements as well as the payload itself were used in experiments to test a FSO control channel implementation [61] as well as dynamic camera calibration and real-time target tracking with two movable cameras [62,63].

Figure 3.4 below shows another gimbal holding an E-Band antenna. The gimbal was built to hold an antenna from ARA as part of a project for a man portable gigabit uplink, or as a ground/aerial node for and E-band backhaul network [5]. The platform is only 8.5" across and 10" tall without the antenna and weighs 29lbs.
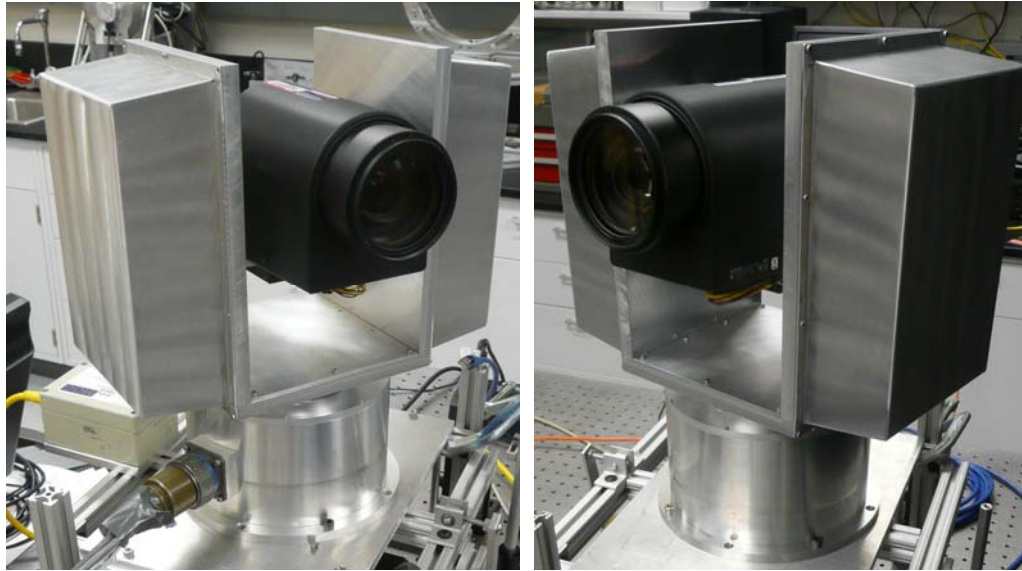
Figure 3.3: Cooperative stabilized long range camera platforms

Figure 3.4: E-band platform with antenna and controller

In Figure 3.5 below, a set of four servo stabilized gimbals can be seen holding 5.8 GHz patch antennas, which connect to a radio below the platform. These gimbals were built several years before the ones seen above, so they do not have slip rings. These were used in a physically reconfigurable network to test how common routing hardware would respond to a morphing physical layer. Because of the fairly large beam-width of these antennas (9°), the motor encoders were not as precise as the other platforms (20,000 PPR compared to 1,024,576 PPR). This allowed for even more cost effective platforms that did not sacrifice performance. The results of this experiment will be detailed for the first time in section 4.7.
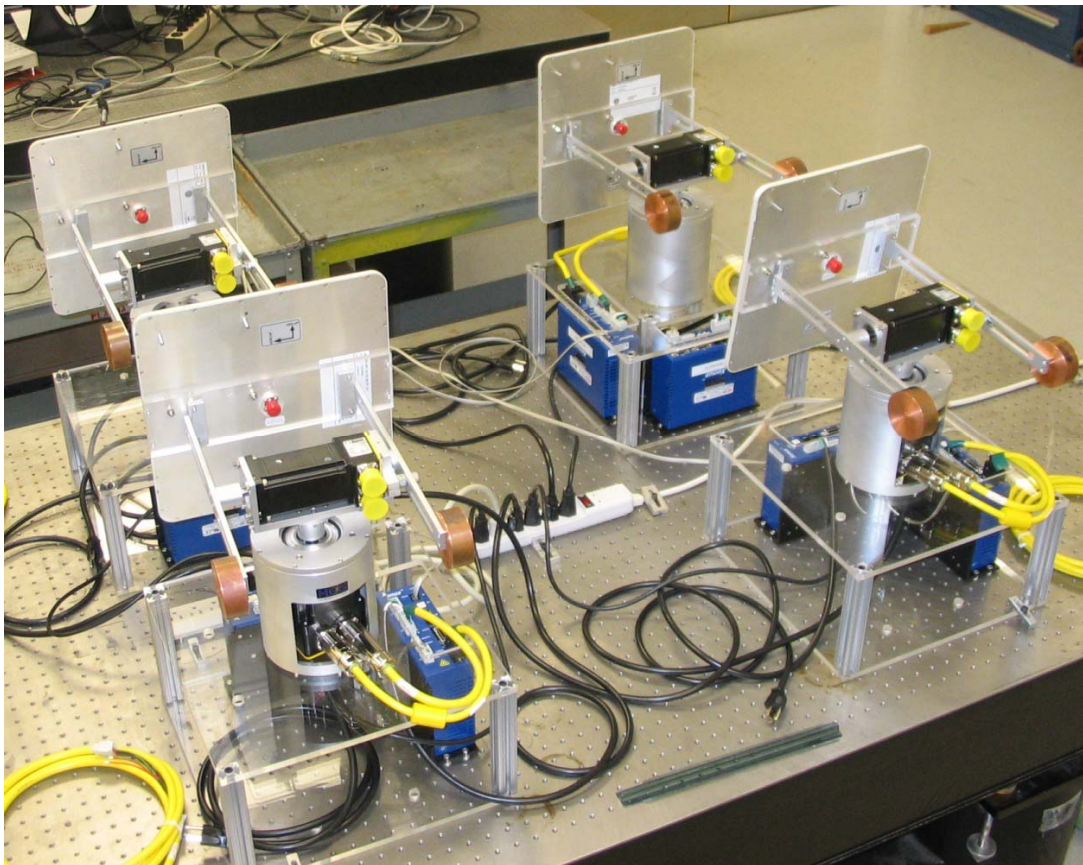

Figure 3.5: 5.8 GHz patch antenna platforms

3.4 Implementation of the Platform Controller

Once the platform is mechanically complete, a controller must be designed to collect information from the various sensors involved in the PAT process, and then generate appropriate pointing commands to both the local and remote platforms. There are many options for how the platform controller is actually implemented, be it x86/ARM based computers, microcontrollers, CPLDs, FPGAs, or even ASICs. Since the control channel, sensor controllers, sensor fusion algorithms, motor controllers, radio controllers, and user interfaces are all running simultaneously, the target platform must be able to handle all these processes in an efficient manner. When one considers that the processes mentioned above may all be running at different clock rates, the notion of parallel processing becomes desirable. While most of the architectures mentioned above are capable of parallel processing, how efficiently that can be achieved along with how easily it can be implement is starkly different between the options.

The familiar programming languages associated with x86/ARM processors (C,C++, etc..) are perhaps the easiest to implement, and parallel processing is typically handled automatically by the lower level threading functions that the user does not have to program directly. The disadvantage to this approach is that you need a computer to run it, which increases the space required as well as power. Since many of the sensors involved do not use regular computer interface standards, some type of custom interface board would also have to be fabricated. From a prototyping point of view computers are the friendliest, but they are not always practical in confined spaces with stringent power and weight requirements (an UAV, for example). Microcontrollers are also a viable

possibility because they can be programmed in C, and require little external circuitry. However, a single microcontroller generally is a serial instruction device, so commands must be done sequentially which can slow down a system with many processes greatly. A set of microcontrollers operating together could provide a level of parallelism, at the expense of increased circuit complexity.

For an integrated control channel system, motor controller, and sensor fusion algorithms, only a FPGA has the parallelism and computational power to easily achieve all these tasks. Each module can run at a separate clock rate, and update its variables appropriately without interfering with other modules. Modern FPGAs also have enough logic slices that they can even mimic computers with soft-core processors if needed. Because interfacing to external signals is done at the logic level, one can easily use a variety of standards (RS232, RS422, RS485, SPI, I^2C, TTL) either directly to pins on the FPGA, or through simple level shifter ICs.

With these considerations in mind, the controller hardware and software implemented in this thesis can now be detailed. Based on previous experience designing the controllers for the other gimbals seen above, a Spartan-6 FPGA from Xilinx was chosen. It has the appropriate number of I/O ports, logic slices, clock generators, and onboard RAM for this implantation. In order to reduce PCB complexity and design time, an integrated module from Opal Kelly [60] was employed, which includes the FPGA, flash ROM, RAM, clocking, power supplies, and USB programming port all on one module.

The external circuitry to the module can be seen as a block diagram below in

figure 3.6 and the completed control board in figure 3.7. The differential line drivers and receivers are critical for interfacing with the servo amplifiers, which put out significant electrical noise. The differential lines offer excellent noise cancellation, which is essential for getting accurate readouts of the encoder signals. These drivers also output the position pulse trains in differential format, making sure no spurious movement pulses are received by the motors. It was learned during interfacing the cameras seen on the gimbals in this thesis that the servo amplifiers output large amounts of RF noise at about 6 MHz. This was enough to distort the analog component video signals coming from the camera to render them unusable, even with the addition of RF chokes. Part of the future work for this thesis will be to build a separate video processing board that sits directly behind the camera, allowing it to tap the digital differential outputs from the camera, as opposed to the noise-susceptible analog video signals. The video input and output sections of the circuitry seen in the bottom center of the PCB board will be moved behind the camera, along with a separate video processing FPGA.

3.4.1 Controller Architecture

The overall controller architecture is a series of semi-independent modules that process various sensor inputs, a core that aggregates all data and outputs pointing angles, and external interfaces to control motors, talk to other gimbals over RF or serial connections, and a TCP/IP based diagnostic and control interface. Figure 3.8 below gives a block diagram of the controller architecture, highlighting the parts that exist as VHDL code inside the FPGA.

The section that controls the motors is perhaps the most straightforward. In order to move a certain number of steps, the FPGA generates a pulse train of 1 pulse/step with the period of the pulses determining the velocity (a basic PWM signal). A second channel sets the direction of the rotation with a 0 for clockwise and 1 for counterclockwise. The motion control core in the FPGA finds the shortest path between the current and commanded position, taking into account the prohibited zones of the elevation motor's range. The servo amplifiers handle the rest, turning these values into the appropriate current profiles to send to the motors.

The various soft UARTS seen in the diagram convert the level shifted inputs from the various sensors into the common 8-bit serial packets used in RS232 and RS422. An onboard serial device server converts one RS232 UART in the FPGA into a TCP/IP socket connection that is accessible over the IP network. This allows for external user control and data collection.

The most important part of the controller is the DTCN core, which takes all the sensor information from both local and remote nodes, computes pointing angles based on the current network topology, and sends this information back out over the RF channel. While the FPGA can process this data at hundreds of megahertz, the GPS update rate of 4Hz limits reconfigurations, while the AHRS update rate of 100Hz is much higher than the bandwidth of the servo amplifiers for stabilization purposes (typically about 5Hz maximum). For a three node network as seen in this thesis, the control channel can update at a maximum rate of 20 Hz given the data capacity of the RF modems.
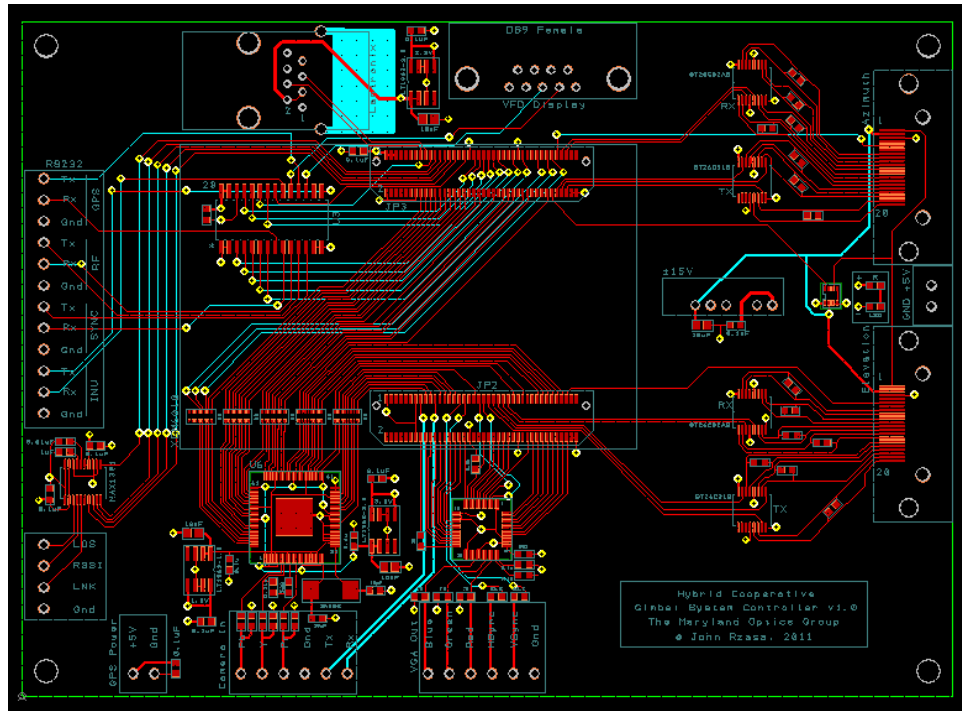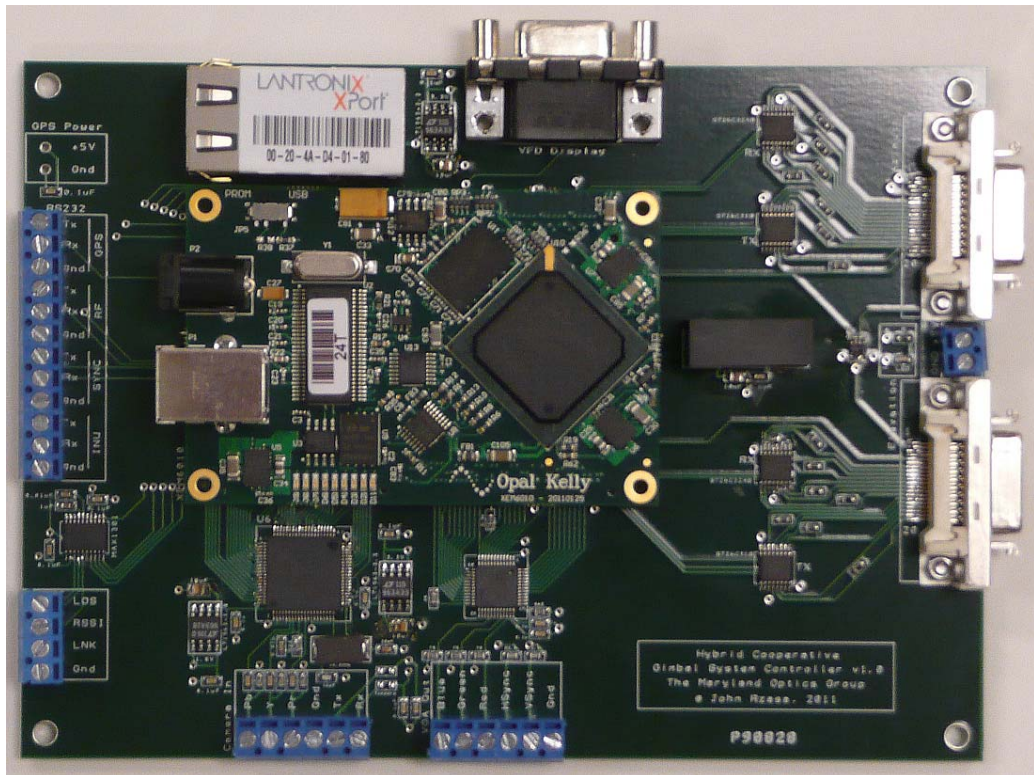
Figure 3.6: PCB layout of platform controller

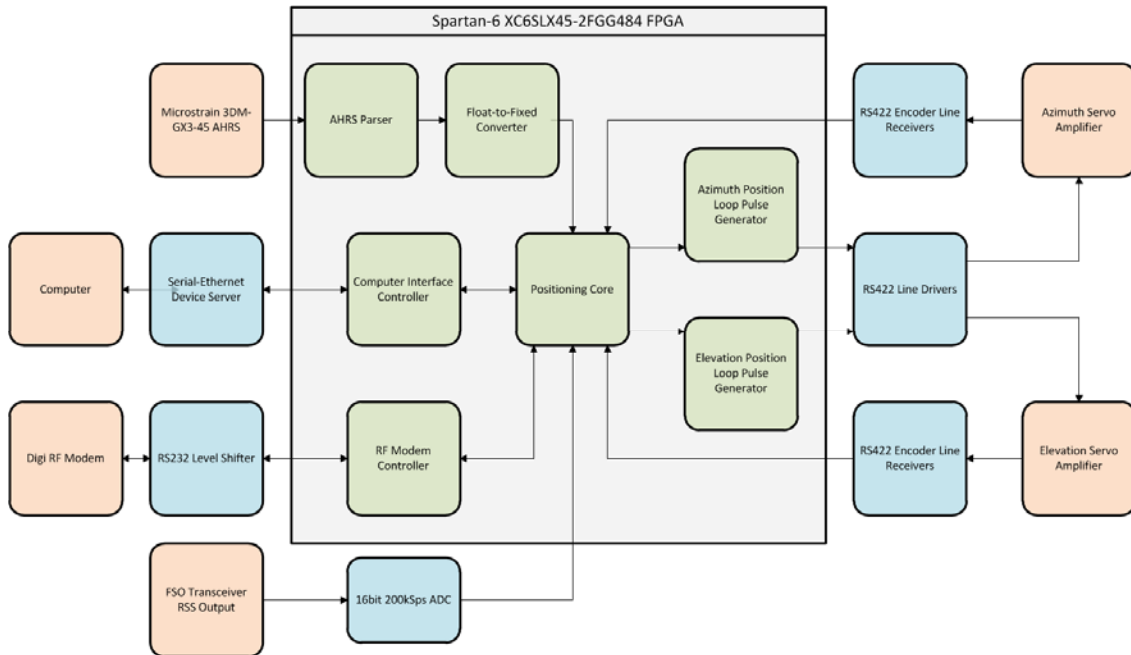Figure 3.7: Completed platform controller board

Figure 3.8: Control system architecture. The blocks in green are VHDL code modules in the FPGA, the blue blocks are ICs on the circuit board, and the orange blocks are external devices. The control board runs on a Xilinx Spartan-6 FPGA at 100MHz.

3.5 Free-Space Optical Communication Transceiver

In order to evaluate PAT in FSO systems, and for DWNs in general, a transceiver was needed to mount on the pan-tilt platforms. While FSO was not necessarily a requirement, cost and ease of use made it a feasible solution. Fortunately, our group was in possession of a large quantity of 100Mb/s FSO transceivers from a company named Lumenlink [64]. These are small units with a bistatic optical design, running off 5VDC with a 100Mb/s Ethernet interface as well as analog RSS and LOS signals. Their compact form factor allowed for easy mounting on the platforms, with some modifications.

3.5.1 Optics

Each Lumenlink uses a standard 1310nm laser diode transmitter, with an output power of 5mW. This sits behind an 8mm FL asphere collimator lens that gives a beam divergence of about 1 mrad. On the receiver side, a 50mm diameter asphere with a 49mm FL collects the incoming light onto a 1.25 Gb/s photoreceiver with integrated TIA, which has a 75μm diameter active area and -28dBm sensitivity. Since the electronics board could not be changed, swapping out the diodes was not an option, and the receive lens had an acceptable FOV, so it was not changed either. However, the transmit lenses on each unit were not consistently aligned, and the very narrow beam divergence made them unsuitable for PAT applications where one transceiver had to be able to connect with any number of other transceivers. The transmit and receive diode mounts were replaced with a custom translation mount, as well as a new adjustable, lockable z-mount for the transmitter in order to set the beam divergence to 1.5 mrad, which still allowed the units to work at 100m, but widened the beam enough to give a more comfortable margin for pointing. All six units were then aligned with themselves using the same test rig in the lab, to ensure consistent alignment of all the units. Without this alignment procedure, the units could not be guaranteed to work with any other unit during reconfiguration tests. Alignment of a bistatic transceiver requires the use of an offset retro-reflector, which reflects the incoming ray in the same direction, but laterally spaced by the same amount that the transmit and receive axes are separated by.

The receive lens and photodiode were simulated in CodeV to verify the acceptance angle of the receiver, and to see at what angle a signal lock could no longer be

achieved. Figure 3.9 below shows the power collection percentages of the lens for various incoming ray angles.
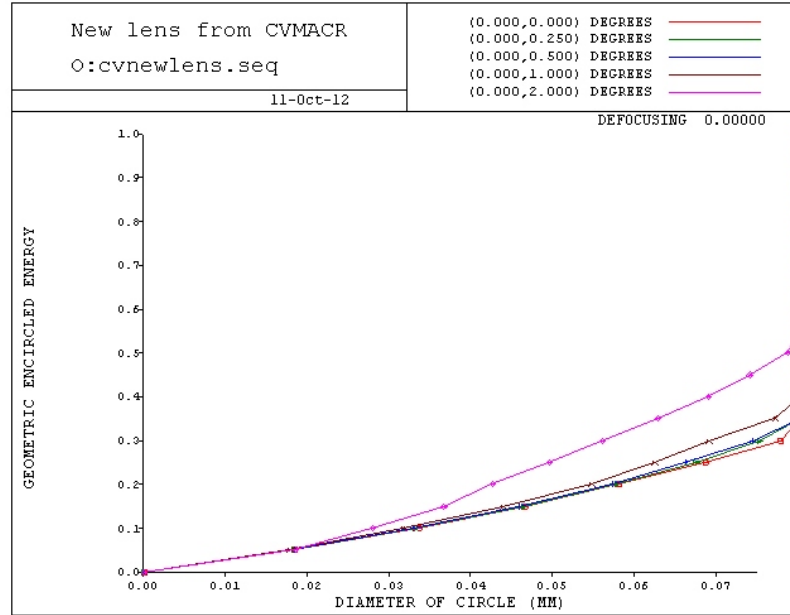

Figure 3.9: Power Collection vs. Angle for FSO data photodetector and lens

This can be compared to an experimental scan of one of the receivers at 90m, as seen in the spiral scan below. The FOV in this plot is ±0.5°, which fits well with the CodeV simulation. The scan appears oval in this plot because the transmit laser is slightly elliptical. Using a bigger receiver lens and wider diverging laser could increase the FOV, however the laser power would have to be increased which is not always possible depending on system limitations. The laser diode current supply in the Lumenlink could only handle 5mW lasers, so the laser diode power could not be increased for this thesis.
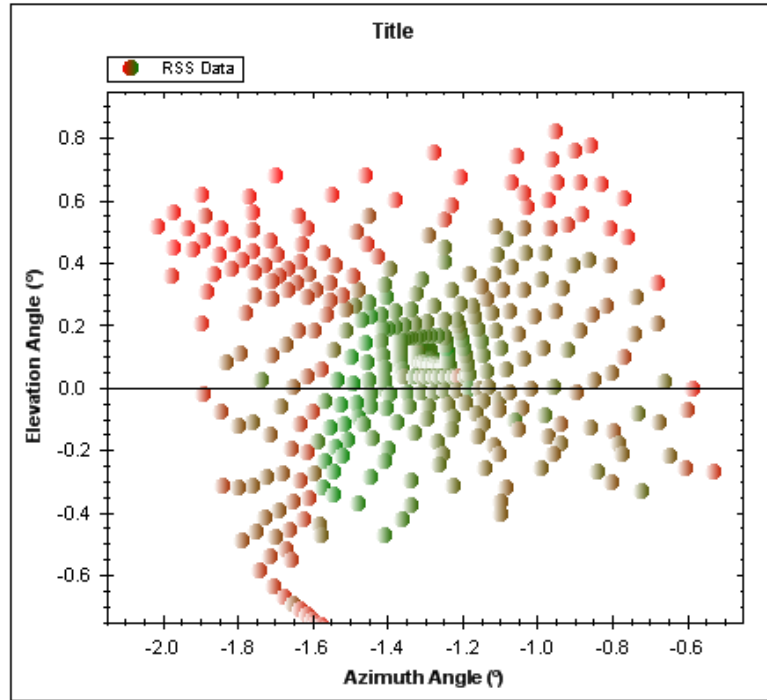
Figure 3.10: Measured FOV of lumenlink receiver (red points denote no received signal, green points denote a received signal above the detection threshold)

The unit as originally designed was intended for links up to 250m apart. Since the relatively narrow beam divergence and bistatic design, each unit had to be precisely pre-aligned in the lab with the use of an offset retro-reflector and adjustment of translation stages holding the laser diode and photoreceiver. After this process was completed, the translation stages were glued in place. Unfortunately, some of the units were not aligned properly, and were thus unusable. Compounding this issue was the fact that the transmit lens was an asphere with a very short (8.0mm) effective focal length, which made alignment incredibly sensitive. To help mitigate this issue, the lens was placed in a new optically threaded adjustable tube that could be locked. The beam was then measured with a photo-detector 2.25m away to determine the beam divergence by looking where

the optical power decreased to $\frac{1}{e^2}$ of the peak value. Figure 3.11 shows a profile of the beam at 2.25m, the measured power shown in solid blue and the $\frac{1}{e^2}$ point in red marks. All the transceivers were then set to have a beam divergence of 1.3mrad.
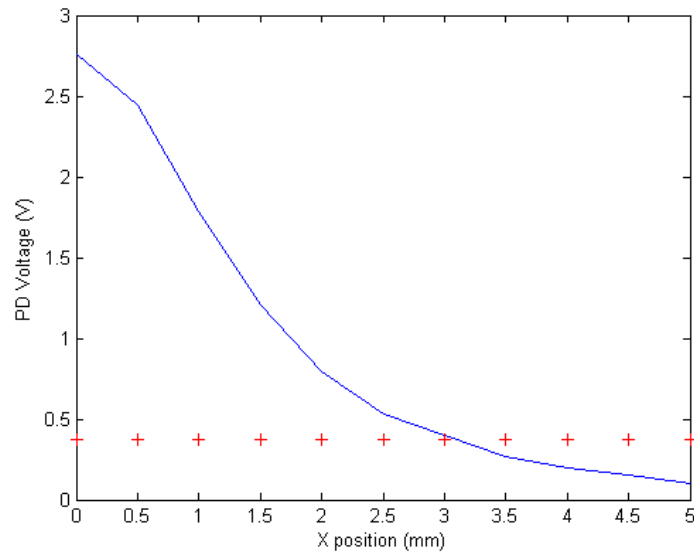

Figure 3.11: Measured beam profile in blue with the $\frac{1}{e^2}$ line in red crosses. The beam divergences can be seen as 3mm/2.25m, or 1.3mrad.

 Secondly, the laser diode and photoreceiver were mounted in a custom built alignment mount, which included translation stages with locking screws. Now when the pre-alignment was completed, the diode mounts could be locked in place with screws rather than glue, in case the procedure needed to be repeated. Figure 3.12 below shows a photo of the new optical head of the transceiver.
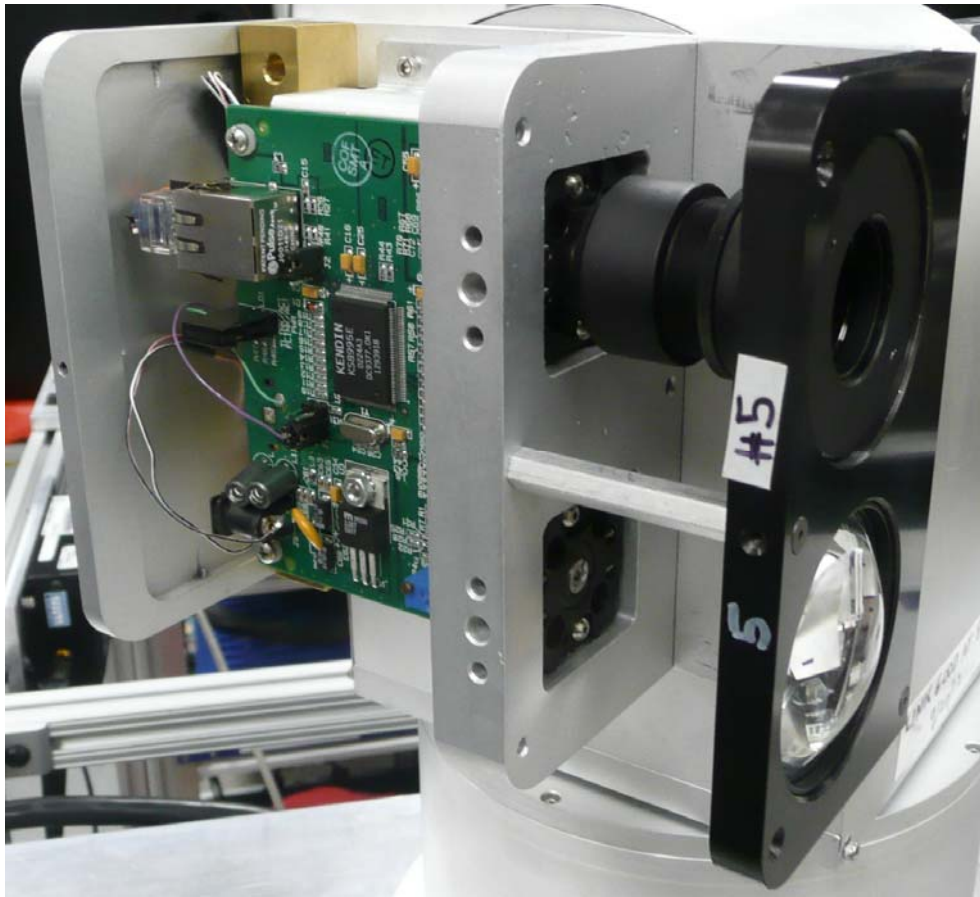
Figure 3.12: Completed new optical head (with cover removed). The black tube at the top right is the tx lens mount which can be rotated in and out to set the beam divergence. The green PCB is the media converter board which also holds the laser and photodiode.

3.5.2 Laser Beacon

Since the data laser in this and many other FSO systems is very narrow, using it as an alignment source even over a small FOV can take inordinate amounts of time with a coarse positioning platform. Therefore the use of a wider beacon laser coupled with a larger and slower photodetector was used as a coarse alignment tool.

For the purposes of this work, a 5mW 650nm laser diode module was employed,

which could be driven and toggled directly from the FPGA. For the receiver, a 1cm^2 wide-area silicon photodiode was used, mounted behind a 50mm diameter PCX lens with a 49mm FL. This setup was simulated in CodeV to determine the operational FOV of the beacon, and ensure that it had a much wider acceptance angle than the data laser. Figure 32 below shows the CodeV results which display a ±10° FFOV, much greater than the ±0.5° FFOV of the data receiver. Finding the operational FOV of the beacon is simpler than for the data laser, since any light falling on the beacon detector above the noise level will let the receiver know that the beacon is hitting the unit. Given that the detector is a 10mm square, a basic geometrical analysis of the lens-photodiode setup in CodeV shows that the FFOV is about 20° (figure 3.13).
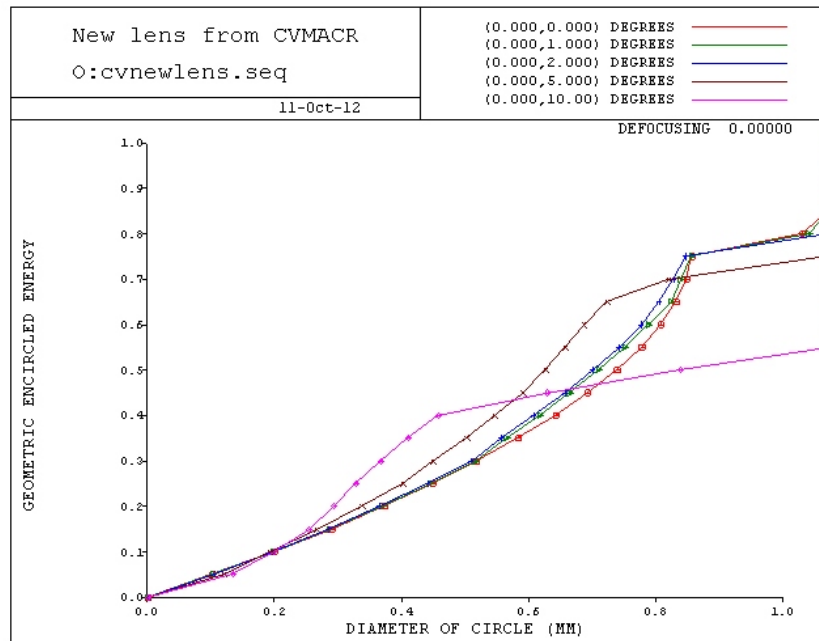

Figure 3.13: Received Power vs. beacon input angle

8.62   MM
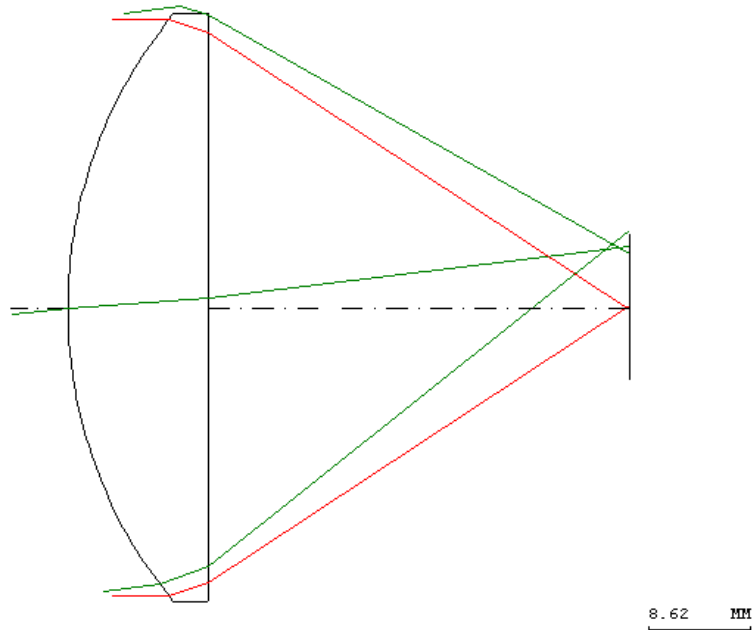
Figure 3.14: Beacon FOV simulation (red rays are for normal incidence, green for 10°
incident rays). The black bar on the right is a representation of the size of the
photodiode. Light falling outside of this line will not be detected.

Figure 3.15 shows the completed beacon. The photodiode was run in direct

photovoltaic mode without transmitter modulation, however in longer range situations

where turbulence plays a role, the transmitter would have to be modulated to distinguish

itself from atmospheric modulations, and the receiver would also have to be amplified to

pick up the weaker signal.

Figure 3.15: Completed beacon assembly. The laser is on bottom in a rotation stage, while the large-area photodiode is mounted above, sitting behind a PCX lens.

3.6 Platform control network

3.6.1 Introduction

One part of the research presented in this thesis is the simulation and development of an omni-directional RF control channel that brings together all the DWN nodes in a particular network. This control channel has several purposes including diagnostics and topology control, however the main purpose is to aid geo-pointing of the nodes so that they do not have to blindly scan the sky with their beams to find their partners. Geo-pointing is not a particularly new concept, one could even think of ancient mariners using the stars to guide their ships as a form of geo-pointing. This concept does take on a new complexity when dealing with networks of DWN transceivers all needing to link up correctly, stay linked up, and recover from disturbances as quickly as possible in order to minimize network downtime.

3.6.2 Geo-pointing

As mentioned earlier, the math used to direct two gimbals to point at each other in space is rather straightforward, but the quality of the sensor data used to implement it in a real system can be troublesome. The essential data needed to align two units are their GPS positions and their pitch, yaw, and roll angles. Common AHRS units which output all this data together follow almost the same formatting rules, floating-point 32 bits per orientation angle and 64 bits per GPS position field (latitude, longitude, altitude) [44-46]. Since the orientations angles can be applied locally by the gimbal when pointing, only the

GPS position must be transmitted to the master controller node. Modern AHRS systems

output GPS information no faster than 4Hz, so the capacity requirements for the control

are rather modest, as will be seen later.

Given the various errors in modern GPS and attitude sensors, an insight into

pointing using these devices can be gained by simulating how they affect overall pointing

error at various ranges and sensor error levels. Figure 3.16 below shows how the

maximum angular error varies for different GPS accuracies at different ranges. This also

shows that for some very long range links, the most precise types of GPS (RTK, WAAS

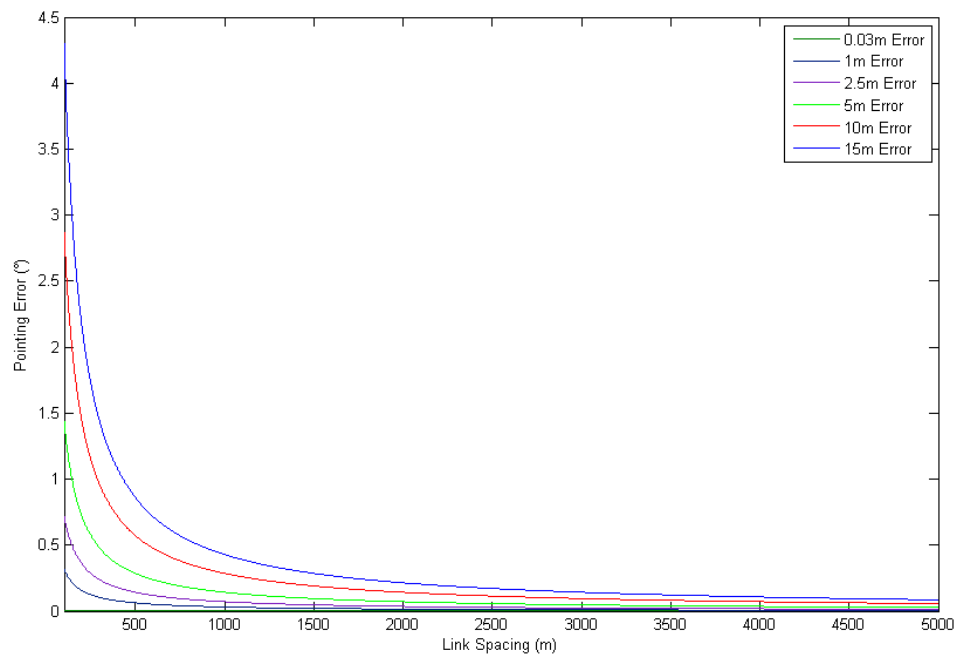enabled) are not necessarily required for pointing such links.

Figure 3.16: Pointing error vs. range and GPS accuracy. Even for very poor GPS
accuracy, at ranges of several kilometers the angular error is small enough to allow quick
alignment of RF transceivers or FSO transceivers with beacon lasers.

In dynamic situations, AHRS units will guarantee orientation angles within ±1° in the

worst case, so this extra error can be added onto the plot above. This can be a significant

source of error especially for FSO systems, but not E-band units at longer ranges since

their beam widths are large enough that they can still get an initial signal lock before

going into their spiral scan optimization mode.

3.6.3 Operational Modes of the Control Channel

When setting up the control channel, there are several possible modes of

operation, each with its own unique features. It is important to note that the control

channel does not operate continuously in most cases, only in a housekeeping mode to

keep nodes appraised of their counterparts' positions in case the DWN signals are

blocked causing the RSS based scanning optimization to fail. Figure 3.17 below shows a

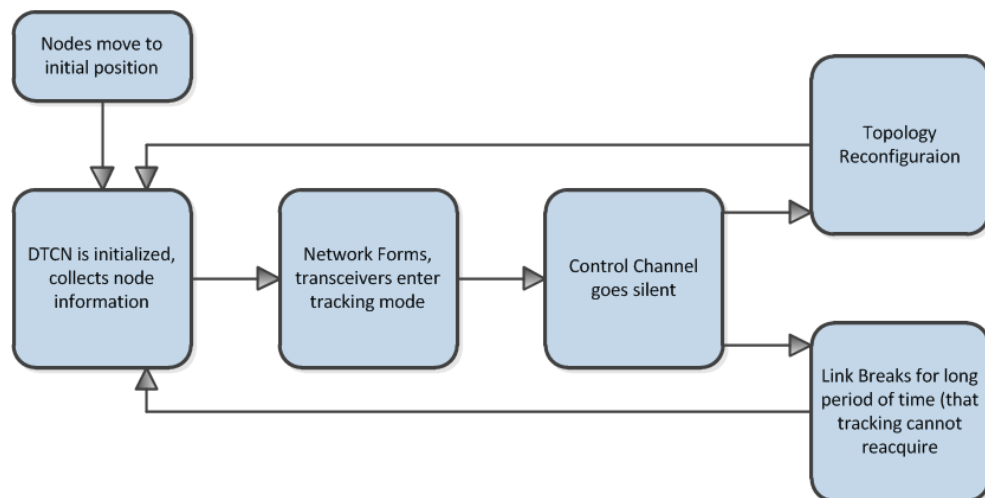flow chart of when the control channel would be used.

Figure 3.17: Operational modes of the control channel. This runs at the initial network
configuration and anytime the network must reconfigure, or when a link unexpectedly
goes down.

The most common architecture is that of the designated topology control node (DTCN). In this scheme, one node is selected as being the master, and it in turn gathers all the GPS positions of the remote nodes. It then takes this information and combines it with the desired topology to tell the nodes where to move and in which direction the gimbals should rotate to find their partner. The remote nodes receive this information and combine it with their local orientation information to generate the proper pointing angles. This architecture is the most common because of its simple setup, low bandwidth requirements, and for security reasons as the control channel is activated only when a reconfiguration or regeneration of the network is required. If the DTCN is lost for whatever reason, a new DTCN node is designated and the process continues. The major problem with this approach is in terms of scaling. In a very large network, if the DTCN receives the GPS data from each node one at a time, it could happen that by the time it has received all the data, computed the topology, computed the pointing angles, and sent the information back to the remote terminals, the nodes will have moved enough to be out of range of the beacon/transmitter beams, which can happen quite quickly in a DWN. As can be seen from the simulation in section 4.2, if two planes are passing laterally with respect to each other 10km apart at 400kph relative to each other, a laser with a 100 μrad beam divergence will leave at 10cm receive aperture in 8.6 milliseconds. Figure 3.18 below shows a diagram of the DTCN architecture.
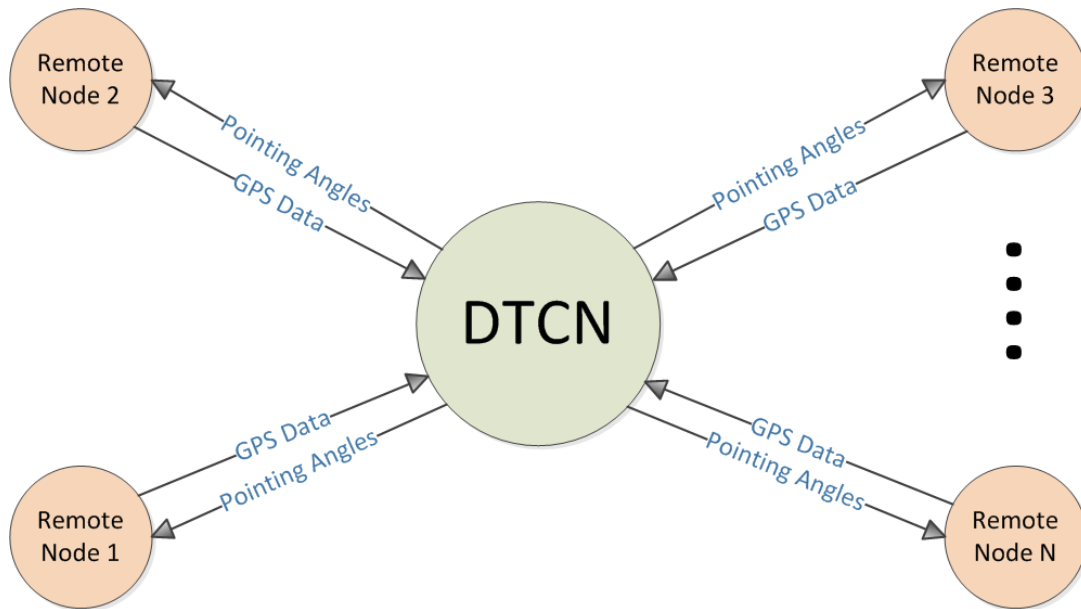
Figure 3.18: The Designated Topology Control Node (DTCN). The DTCN aggregates the positions of all the nodes and tells them where they should point to find their link partner.

A related approach for larger networks is that of distributed designated control nodes (DDTCN). Much like the internet has control routers all over the world, a DDTCN has DTCNs running smaller partitions of the network in order to reduce the delay in the control channel. When a network gets large enough, there will be nodes that are so far apart that they couldn't conceivably communicate with each other anyways, so the control network does not need to take them into account at the same time. Each DDTCN will overlap some nodes with another DDTCN, so these interactions will keep the entire network together. Figure 3.19 below shows a diagram of the DDTCN configuration.
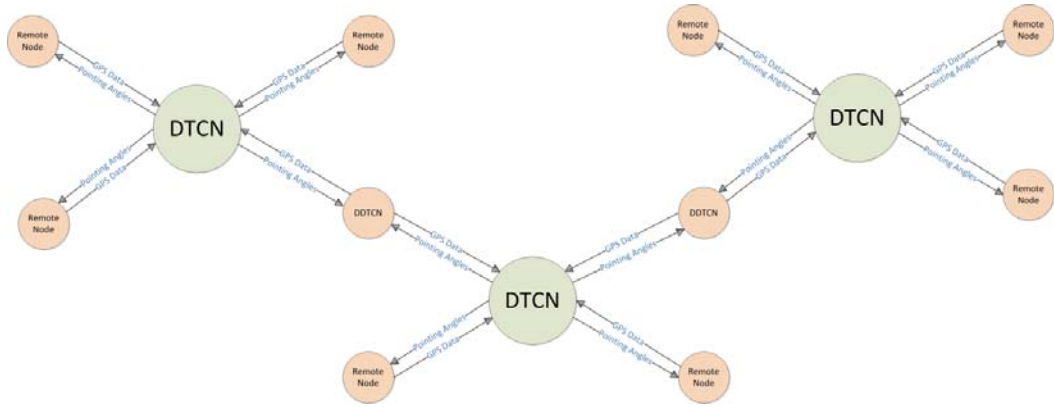
Figure 3.19: The Distributed Designated Topology Control Node (DDTCN). Sections of the network that cannot talk with each other due to range or operations limitations can be partitioned in order to speed up the discovery process.

There are situations where the use of a control channel could be forbidden, either because of jamming or requirements for radio silence. This would call for some type of beaconing approach to find the other end of the link, or other blind scanning method. Both of these methods are very slow in their point-to-point implementation and even more so in a larger network. The ultimate goal of the omnidirectional control channel is to quickly form a network and then minimize network downtime by giving all the nodes an accurate last known good coordinate of their partners in case the received signal is lost for too long a time. One other option is to form the network using a RF channel while still in friendly airspace, and then fly the already connected network into the operational theatre, where it could then morph to service its end users. GPS housekeeping information could then be sent over the directional links, so that if one link went down, the others could have a good estimate of where to scan their transceivers to look for the lost node.

95

3.6.4 Control Channel Implementation

In order to test the PAT concepts presented in this thesis, a control channel was developed to link the six FSO transceiver platforms built for this work. It consists of a set of 900MHz ISM band RF serial modems, which transmit RS232 transparently over the air [65]. One platform was designated the DTCN and thus controlled the RF channels to the other platforms. Since each node was bi-connected, only one gimbal on each platform was radio enabled, with the other one exchanging data to the radio gimbal via a null modem cable.

3.6.5 Data Structure

The DTCN node receives GPS information from the remote nodes, parses it, and then sends the remote nodes the azimuth and elevation angles back for each of its two platforms. As mentioned before, the GPS data comprises three 64bit floating point values. Using a simple header and footer arrangement, the remote nodes transmit their position data string (PDS) to the DTCN node in the format:

PDS = [2 byte header][24 Byte GPS data][1 byte terminator]

The DTCN would then transmit move angles back to each node in the form of a position command string (PCS):

PCS = [2 byte header][2.5 byte azimuth 1 angle][2.5 byte elevation 1 angle][2.5 byte azimuth 2 angle][2.5 byte elevation 2 angle] [1 byte terminator]
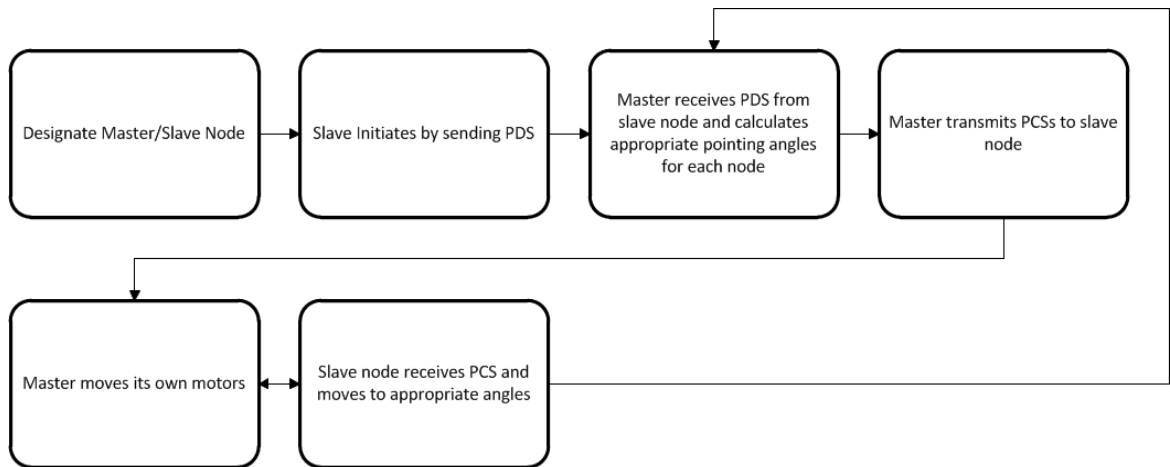
Figure 3.20: Control channel operational flow. This process runs constantly while the control channel is active.

The remote nodes would then apply their local orientation angles to the received angles to determine how the gimbals should rotate. This process would repeat either at some regular housekeeping interval, when the nodes lost their received signal for a certain period of time, or in the case of some ongoing research, when the network was perceived to be about to fail [20]. With a control channel data rate of 19.2Kbps, the theoretical highest update rate of the control channel in this thesis would be 30Hz. This will be slower in practice due to processing delays in the embedded controller, but it is ultimately limited by the update rate of the GPS data (4Hz) and number of nodes. If the network became large enough, the update frequency would go below the GPS output frequency. Figure 3.21 below shows a simulation of the maximum update rate for larger number of nodes, assuming the DTCN polls each one in order, and then sends out pointing angles at the end successively to each node. Depending on the beam widths and distances involved, the GPS and pointing angle precision can both be reduced in order to

increase the network capacity. While it would be advantageous in terms of recovering

from network failures more quickly, most operational scenarios have the control channel

only being active at the initial network formation, and then going silent afterwards until a

refresh is needed. Even if the control channel is encrypted, the simple act of transmitting

RF could alert the enemy to the nodes' locations.

The maximum repositioning update frequency for a network of N nodes

(neglecting processing delays which are negligible compared to the RF channel data rate)

can be represented by:

$$U_R = \frac{B}{N(T + R)} \; (\text{Hz})$$

where B is the effective channel data rate in bps, T is the master PCS packet size (in bits),

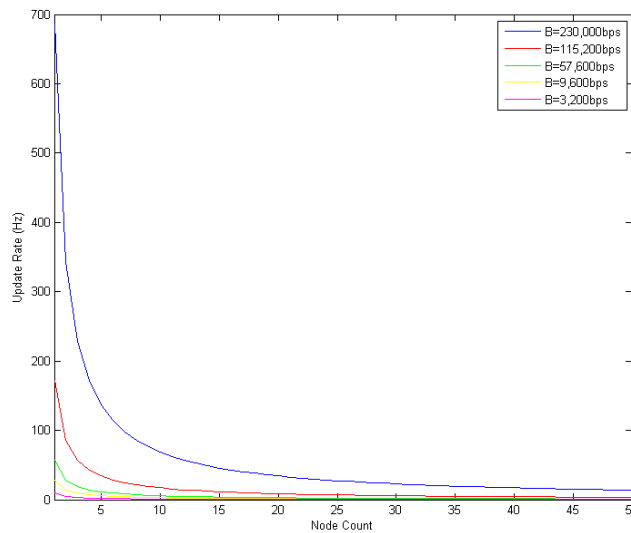and R is the host PDS packet size (in bits).

Figure 3.21: Control channel update rate as a function of network size. For very large
networks the update rate decreases dramatically, limiting the velocities and beam
divergences of the transceivers to ensure the two links will point at each other even after
the DTCN's processing delay.

3.6.6 Analysis

The use of a control channel in PAT is a well studied concept and has been implemented in several fielded systems [6,22,23]. It significantly speeds up the acquisition process, and uses already existing communications networks. Given that it is only used to form a link at the beginning, the data capacity requirements for the control channel are quite modest. Even a HF radio operating at 6.4kbps could be used to form a link, provided the two ends weren't moving very fast relative to each other. While the benefits of this arrangement are frequently recognized and this scheme used, there are some disadvantages when talking about security and also larger networks.

Even if the control channel is encrypted, the simple act of broadcasting data with an omnidirectional antenna will give away a node's location to all who can receive its signal. There could be situations where the network has to be completely silent while in operation, so it would either have to be formed outside the operational area and then moved in already connected, or some blind configuration would have to take place. The other major issue with a control channel is that of scale. Over a limited capacity channel, forming a network of 10 nodes might be feasible, but for a network of 50 nodes, by the time the DTCN has aggregated all the node information, the pointing angles it generates may be out of date. As mentioned earlier, distributed DTCNS can be used in this situation, but that could require a tertiary control channel, because the frequencies and capacity used by the secondary control channel will be occupied. These issues may not become implementation problems for several years, however they are worth considering now as part of the general concept of how large directional wireless network form.

Chapter 4: Simulations and Experimental Results

4.1 Introduction

In an ideal directional wireless network in which two nodes want to form a link, they would rotate by some angle, acquire the received signal, and then begin transmitting data. While this is still what every real-world implementation tries to achieve, how it gets to that point is a rather complicated process. The combination of errors from position and orientation sensors, pointing platforms, and transceivers leads to many variables that must be optimized in order for the system to achieve the desired level of performance. The process in which the network forms in the first place is also a major issue, since the method of geo-pointing using a secondary control channel might not always be available. Even the control channel has its own limitations, so all of these various issues must be considered simultaneously when designing a directional wireless network.

While previous members of our group have focused extensively on cost function optimizations for the placement and movement of backbone nodes to maintain sufficient coverage for a set of terminal nodes, it was always assumed that the PAT portion of this process was ideal. That is, when node A needed to point to node B, this operation had no pointing error, happened instantaneously, never went out of alignment during movement of the nodes, and atmospheric effects only reduced RSS by some predetermined amount. Many real-world implementation issues make the overall network coverage problem much more complex, something that few have worked on to date.

To investigate some of these issues, a series of simulations were run in order to look at the challenges inherent in PAT. The first set examines how platforms point at each other while their nodes are in motion. Any type of mechanical positioning system can change its orientation at some given rate, and this determines the compensation bandwidth of the system. This applies to both the coarse and fine positioning systems.

The next set of simulations demonstrates the usefulness of the PAT calculator. The relationships between the various design variables are explored, and some important observations made about the characteristics of FSO/RF PAT systems. The final simulation section looks at a PAT scheme for forming links when no control channel can be used. These results are also compared to Monte Carlo simulations of two nodes randomly scanning the sky looking for each other.

4.2 Pointing Between Moving Platforms

Consider two nodes that are moving at velocities v_1 and v_2, the maximum acceptable time delay between repositioning operations in order to keep the receiver aperture always within the beam spot can be calculated. If the relative lateral velocity between the two nodes is taken as v_{1p}-v_{2p}, then the time interval at which the receiver aperture would lose the beam spot (assuming the aperture was in the center at t=0) is given by:

$$T_{max} = \frac{w(z) - \dfrac{D}{2}}{\left| v_{1p} - v_{2p} \right|}$$

Figure 4.1 below shows a log-log plot of how the repositioning time depends on a range of relative platform velocities for a beam-width of 100μrad at distances of 1km (red), 10km (blue), and 100km (green). At great distances the beams are generally wide enough that pointing error is not as much of a concern as atmospheric effects are.
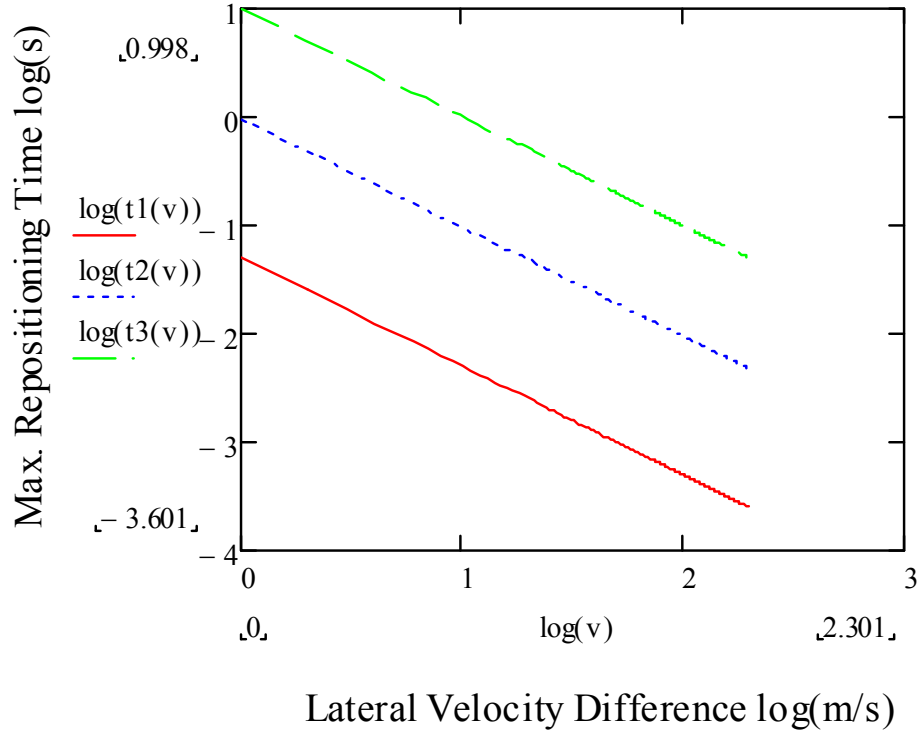

Figure 4.1: Relative platform velocities vs. maximum acceptable repositioning time. The solid red line denotes a link spacing of 1km, dotted blue a spacing of 10km, and green a spacing of 100km. As links get farther apart, the angular rate of change between them decreases, so the platforms do not have to reposition their beams as rapidly.

At great ranges, the coarse platform will not need to rotate as fast in order to ensure coverage from a geometrical pointing perspective, however all the platform disturbances that affect the local transceivers' orientation will magnify the pointing error

102

seen at the other end. When the platforms are both in motion this can become even more pronounced, especially if a node must do evasive maneuvers, but still maintain connectivity. In dynamic situations an agile platform is required, primarily for its own stabilization rather than basic pointing operations. In a RF system, this platform is responsible for all the pointing and tracking, but FSO systems have the additional fast tracking stage that must also be steered. The platform doing the coarse positioning of the transceiver must be able to rotate quickly enough to keep the laser beam within the FOV of the fast scanning mirror while the platforms are in motion, otherwise the signal will be lost and acquisition will have to begin again.

Figure 4.2 below shows the relationship between range and relative lateral velocity for a FSO transceiver operating at 1550nm with a beam divergence of 10μrad. As can be seen, the relationship between these two presents a wide array of repositioning times required for the platform, so a plot like this can give mission planners a map for how nodes should be spaced and what their relative trajectories should look like.
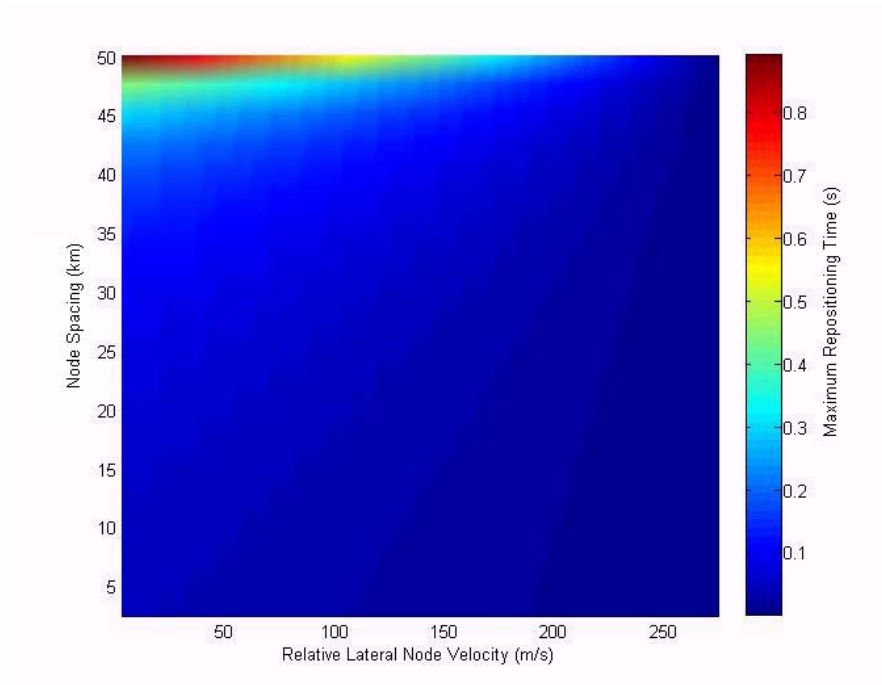
Figure 4.2: Maximum repositioning time vs. range and relative node lateral velocity (red denotes a longer time between required platform adjustment, blue a short time). Smaller relatively velocities mean that repositioning speeds of the platforms can be relaxed.

4.3 PAT Performance Calculator

It is quite important that a PAT system know the error characteristics of all the sensors involved and the characteristics of the transceivers that affect PAT. For example, the total angular error is in the platform will give the beaconing/fast tracking components of the system an estimate of how much angular coverage they must have in order to acquire the other end of the link. The various properties of the transceivers such as beam divergence, transmit power, and receive aperture size must also be considered in order to ensure that unreasonable pointing precision is not required, or FSMs with too large an angular range that would reduce bandwidth.

With the above considerations in mind, a calculator tool was devised to provide a designer with a method for examining the limitations in a PAT system at a given point in time for a given architecture. For example, in a situation where GPS accuracy has degraded to ±5m, orientation angle accuracy is at ±2°, the nodes are 10km apart, the gimbal has a pointing error of ±0.01°, the receive aperture diameter is 10cm, and the transceiver is operating at 1550nm with a beam divergence of 100μrad, the required transmit power to ensure that -55dBm is collected by the receiver can be calculated. One can imagine a host of variations on this situation, and also how the parameters could change over the lifetime of a network. Fast angle scanners/beaconing lasers have inherent limitations that are set in the hardware design phase and cannot always be changed, so it is important to have a metric for overall PAT performance to help decide these details before a system is built, to tell the user/controller when the limitations will be hit in a deployed system, and how to mitigate them. In RF systems a similar issue is the diameter of the dish antenna, a critical parameter that is generally desired to be as small as possible in airborne systems.

The output of the PAT calculator is the amount of received power collected by the receive aperture. This is the quantity all systems are trying to maximize, and is the quantity that will be degraded by pointing errors, turbulence effects, and transceiver design parameters. Being able to account for many of the factors influencing the received power will give users a powerful tool in designing not only dynamic FSO systems, but also directional RF systems, which are widely expected to be deployed in operational situations within the next few years.

From Chapter 2, for a FSO system operating at wavelength λ with a beam divergence θ_{beam}, and transmit power of P_t, the initial spot size is written as:

$$w_0 = \frac{\lambda}{\theta_{beam} \cdot \pi}$$

The optical intensity at the receiver can be given by:

$$I(r,z) = I(0,z)e^{-\alpha \cdot z}(e^{-\frac{2r^2}{w^2}})$$

Where the intensity of the beam at the receive lens is given by:

$$I(0,z) = \frac{2 \cdot P_t}{\pi \cdot w(z)^2}$$

and $w^2(z)$ is written as:

$$w^2(z) = w_0{}^2 \left[1 + \left(\frac{\lambda \cdot z}{\pi \cdot w_0{}^2}\right)^2\right]$$

Taking the receive aperture diameter to be D, the total power collected by the receiver is:

$$P_{rec} = 2\pi \int_0^{\frac{D}{2}} r \cdot I(r,z) \cdot dr$$

where $\alpha = 0.44 dB/km$ at 1550nm on a clear day.

If a pointing system has an error of β radians, the offset of the beam at the receiver would be:

$$r_{offset} \cong z \cdot \beta$$

where β would take into account mechanical pointing error, GPS error, and orientation angle error. As GPS altitude measurements are frequently much worse than horizontal measurements, the error from common barometric altimeters is used, which is the standard in most aircraft.

The total received power including the effect of the transmitter pointing error would then be:

$$P_{rec} = 2\pi \int_{0}^{D/2} r \cdot I(r + \beta, z) \cdot dr$$

If we also consider an RF system with pointing errors, we start again from Chapter 2 with the intensity at the transmit aperture, given by:

$$I = 4 \cdot \frac{J_1(\frac{\pi \cdot D}{\lambda} \cdot \sin(\theta))^2}{(\frac{\pi \cdot D}{\lambda} \cdot \sin(\theta))^2}$$

The peak intensity at the receiver is found by integrating the above intensity over the full hemisphere in front of the aperture:

$$I_P = \frac{P_t \cdot A^2}{\lambda^2 \cdot z^2}$$

At a distance z away, the receiver intersects the transmitted wave over an angular range of $\theta_R \cong \frac{D}{2z}$. The power collected by the receiver aperture when also accounting for an

angular pointing error β is then:

$$P_r = 2 \cdot I_P \cdot e^{-\alpha z} \int_0^{D/2} r \cdot \frac{J_1(\frac{\pi \cdot D}{\lambda} \cdot \sin(\theta_R + \beta))^2}{(\frac{\pi \cdot D}{\lambda} \cdot \sin(\theta_R + \beta))^2} dr$$

The attenuation constant $\alpha = 0.1 dB / km$ at 80 GHz on a clear day.

RF systems have the great advantage of being able to use coherent detection in a heterodyne arrangement, so the sensitivities of the receivers are much better than the direction detection (DD) optical receivers (below -100dBm as opposed to ~-55dBm). RF is also much less susceptible to atmospheric effects, with the exception of 60 GHz that coincides with an absorption band of oxygen, and which limits the operational range of 60 GHz transceivers.

We can now look at how the different combinations of design variables can give us insights into how FSO and RF systems can be designed and how they would function in operational situations.
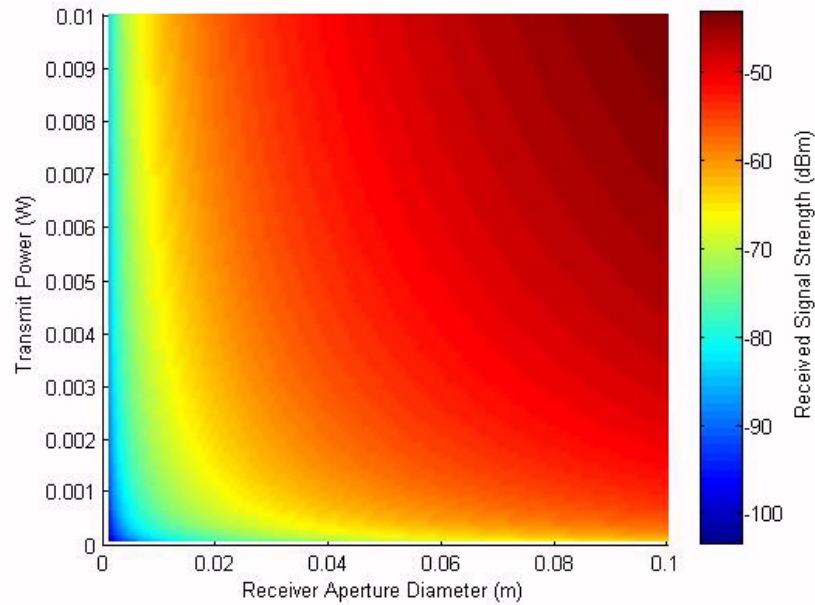
4.3.1 PAT Characteristics in a 1550nm FSO Link

Figure 4.3: RSS vs. RX aperture size and TX power (z=10km, θ=100μrad, no pointing error). Increasing the receive aperture will improve performance moderately more than increasing the transmit power at a comparable rate.
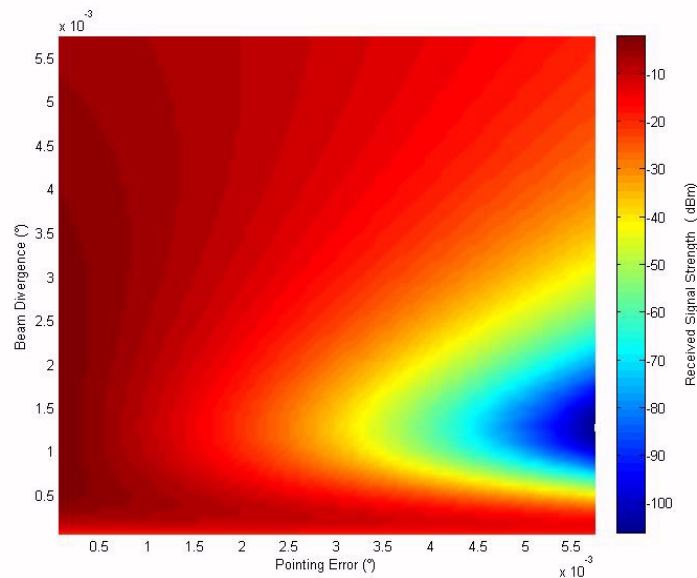

Figure 4.4: RSS vs. beam divergence and pointing error (z=1km, P_t=1W). For very small beam divergences at close range the beam will not completely fill the receiver, so increasing pointing errors can cause the received power to drop off in certain configurations.
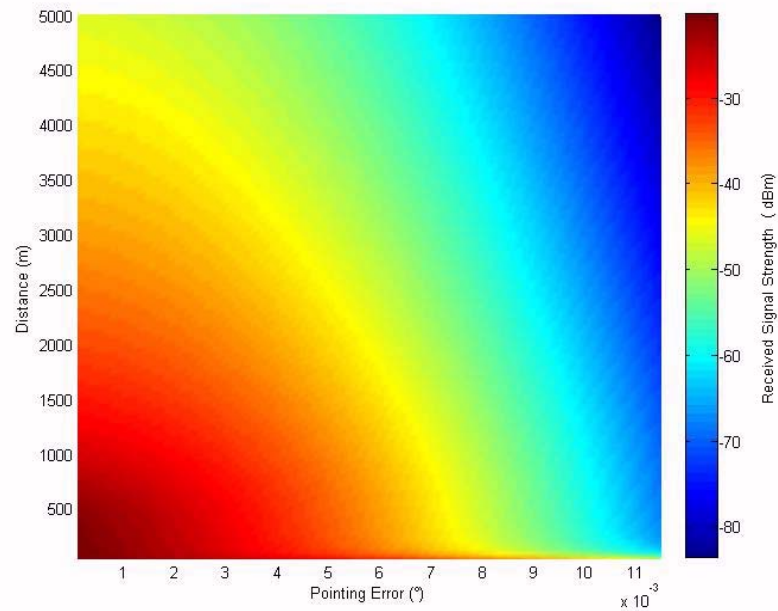
Figure 4.5: RSS vs. distance and pointing error (P_t=10mW, θ=100μrad). The percentage loss of power is greater at shorter ranges, but if the link margin is sufficient, the pointing requirements can be relaxed.
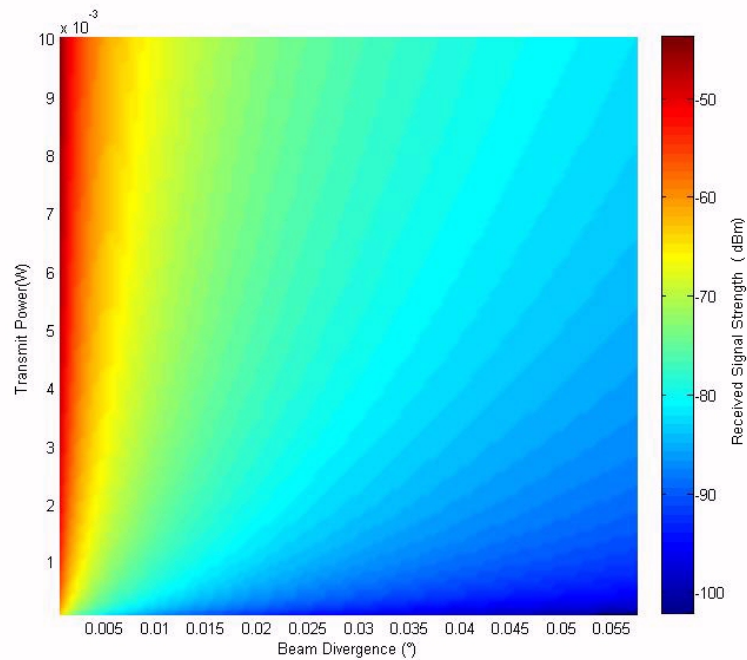

Figure 4.6: RSS vs. TX power and beam divergence (z=10km, D=10cm, no pointing error). For very narrow beam divergences, increasing the transmit power does not improved the received power much.

110

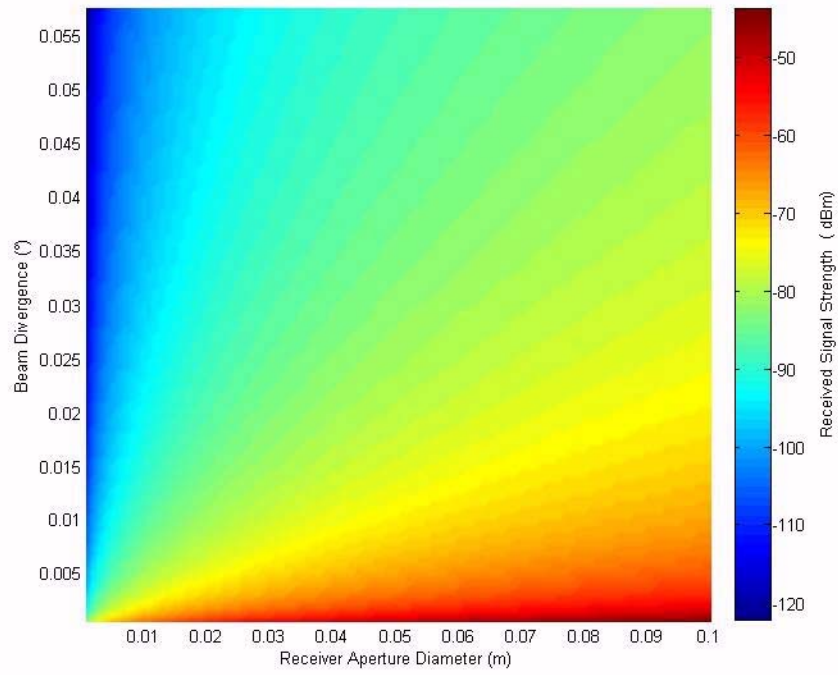Figure 4.7: RSS vs. RX aperture size and beam divergence (z=10km, Pt=10mW, no pointing error). Beam divergences and receiver aperture size affect the received power in approximately the same manner.

4.3.2 PAT Characteristics in the E-band at 80GHz
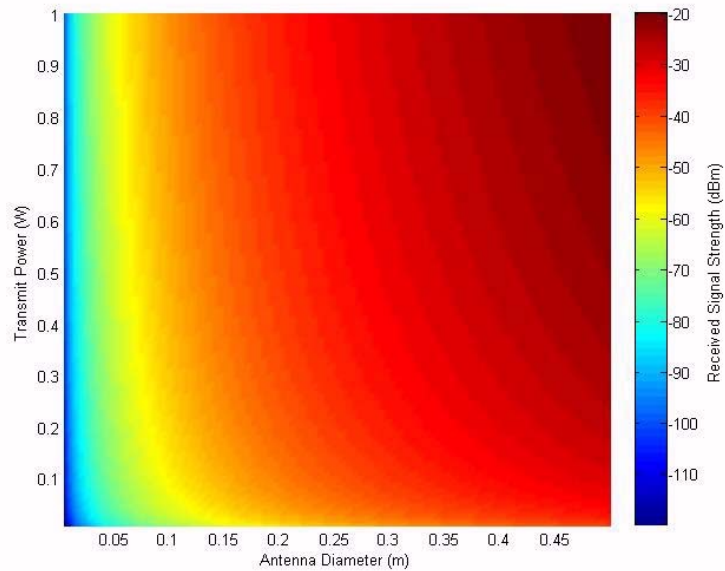
Figure 4.8: RSS vs. Antenna Diameter and Transmit Power (z=10km, no pointing error). Very large dishes produce very narrow beams and also collect more received energy. Small dishes collect less power but are less sensitive to changes in transmitted power.
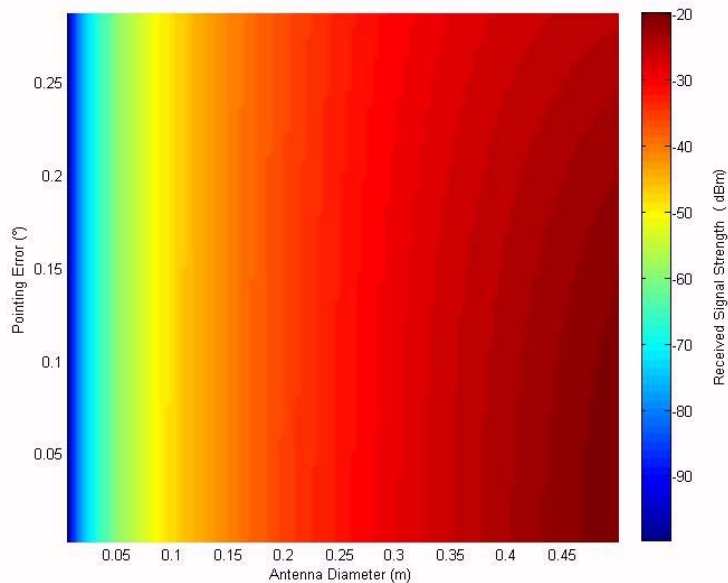
Figure 4.9: RSS vs. Antenna Diameter and Pointing Error (Pt=1W, z=10km). Large dishes produce very narrow beams which are more susceptible to pointing errors. Smaller dishes receive less power but are less susceptible to pointing errors.

112

Figure 4.10: RSS vs. Distance and Pointing Error (Pt=1W, D=30cm) For an appropriately sized dish, pointing error changes affect the received power much less than the loss from spreading over longer and longer distances.

Figure 4.11: RSS vs. Distance and Transmit Power (D=30cm, no pointing error). Changes in transmit power cause only slight improvements in received power compared to decreasing the range between two links.

4.3.3 Analysis

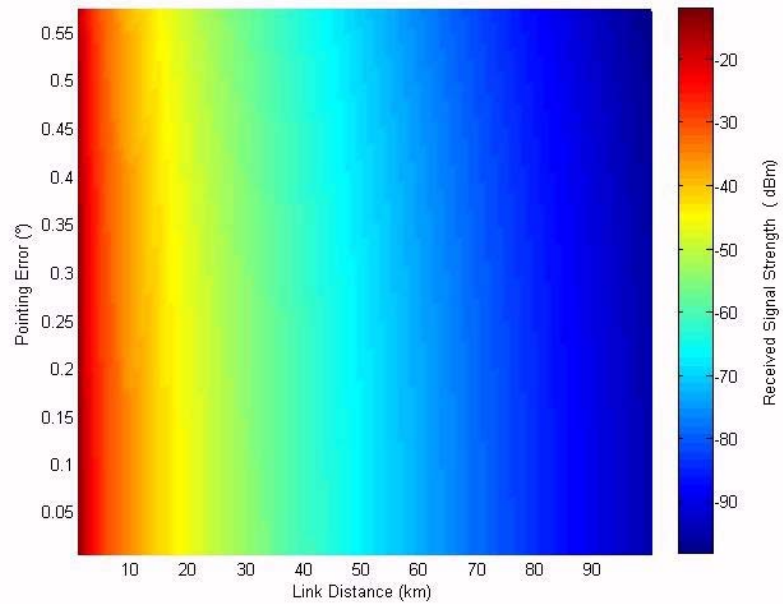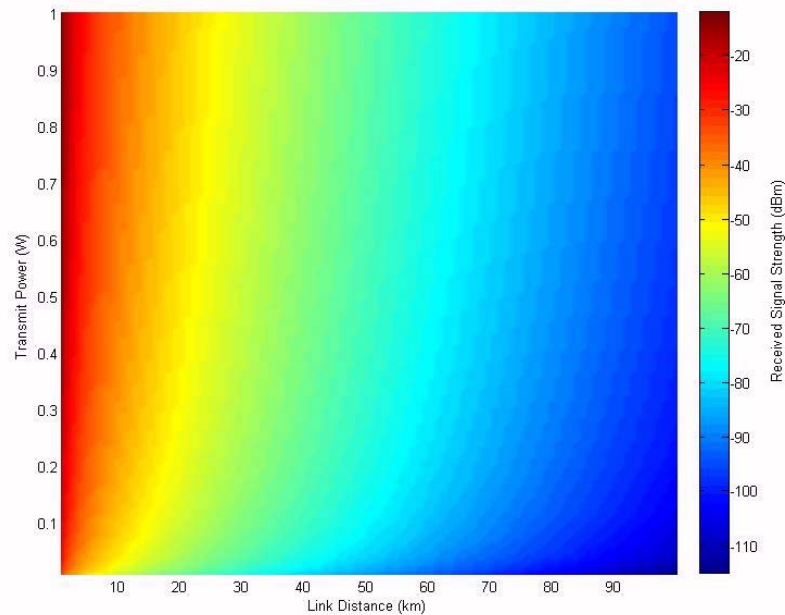There are many more combinations of variables that could be considered beyond the ones plotted in the previous two sections, and in a system design all of them would have to be optimized simultaneously. Some important observations can now be made from these figures.

First, for both FSO and RF systems, perhaps the most important parameter is the beam divergence. This value influences the size of the transmit aperture, the working range of the link, and the required transmit power and receiver sensitivity. One would like to have the divergence as narrow as possible, but this could lead to very large transceivers, severe turbulence effects and possibly unusable pointing precision requirements. All of the design variables are closely related, but because of the power loss caused by beam spreading related to the beam divergence, it is usually kept as narrow as possible before adjusting other specifications.

A second important observation is related to pointing precision and distance. Once a beam travels far away and spreads out, the pointing requirements get less stringent if the beam divergence is increased. If a platform for some reason can only provide a certain pointing precision, the operational capability of the system can be improved if the beam divergence is widened. Unlike cameras trying to focus on a small target from far away, beam spreading can actually be a benefit for designing positioning systems. On the other hand, as links get farther apart, atmospheric effects become worse, requiring more responsive adaptive optics.

Finally, there is one very interesting difference between how FSO and RF

transceivers are designed. Because the initial size of an FSO transmitter aperture is relatively small (<5cm in diameter) due to the much smaller operating wavelength than in RF, more room can be left for a large receiver, but the transmitter can still project a beam with a small divergence. In the case of an RF transceiver, however, because the same dish is generally used for transmitter and receiver, when the beam divergence is set, the receiver's collection ability is also set. Many commercial systems use very large antenna dishes to narrow the beam enough to ensure enough power at the receiver, but without having to resort to large transmit powers. Power amplifiers for E-band radios are still an emerging technology with limited gains, so using large dishes has been the stopgap measure to date. While the U.S. government is investing in new E-band radios and gimbals, a large part of their funding is still going into the design of small E-band RF power amplifiers to supply up to 10W, because in order to use these systems as desired on UAVs, the antenna dish diameter will have to be much smaller than the current terrestrial units (20cm as opposed to 60cm).

4.5 Alignment using a Chirped Spiral Scanning Algorithm

In the most extreme of cases, it might be required to form and maintain a link in which it is impossible for the links to have any communication with each other, the only knowledge they have being that the other link simply exists somewhere in space (and hopefully in range). As mentioned before, a relatively simple method of link formation is by optimizing RSS. However, without prior coarse alignment (by eye, camera, beacon, etc…), some automated method must be found to align the transceivers. Conceivably the

two platforms could be set to move in some type of raster scan through the environment, but with their narrow beams it yields a high probability that the two links might never find each other.

What is proposed in this thesis is a scanning technique in which wide beam divergence beaconing lasers are used to scan the environment, but whenever a link is briefly formed during a scan, a burst of information is sent over the beacon link with the position and orientation of the remote platform at that moment. The receiving link can then use that information to restart its scan, but using the last known good position of the other link. With both nodes doing this back and forth, a good coarse alignment can then be found for the narrow-beam data transceivers to start alignment using their fast steering mirrors. This method is much slower than the geopointing method described earlier, but it does have the advantage of being almost completely covert. If this link were to go down at any point, the network downtime would be significantly longer. In forming a larger network of nodes, care must be taken to ensure that each pair of transceivers will link up only with their partner. This is achieved by giving each platform a unique ID which it transmits during the chirped scan. Again, this can slow down the network formation if a link has to go through several of these scans to find its partner. Once the network is formed, however, the data network can be used to disseminate last known good positions and orientations of all the links to aid in downtime recovery and physical reconfiguration. It should also be noted that these blind scanning concepts always involve the use of a receiver with a wide FOV, otherwise the method could become time consuming to the point that it was unusable.

Ideally, one could think of a situation where a wide beam divergence transmitter beam falls on a wide FOV receiver. Since neither would have to scan a large area of the sky with great precision, the process could be relatively quick, even if both were engaged in a random scan. However, this idea will fail fairly quickly once the units become spaced farther apart and the receiver can no longer pick up enough signal from the very large beam spot of the transmitter at that distance, especially since the SNR goes down by the fourth power of the beam divergence. Also, there are limits as to how much the beam divergence of the transmitter can be changed given limitations on the aperture size and space for optics behind it, especially if the beaconing laser shares some of the optics of the data laser. In fielded systems to date, the beaconing laser typically has a beam divergence of 10 mrad [6]. Because the beaconing system operates at a substantially lower data rate than the data laser, not as much received power is required, allowing for a larger photodiode on the beacon, thus increasing the usable FOV. Even with the same lens as the data photoreceiver, the FOV of the beacon can be increased by several times.

The procedure for the chirped scanning method can be given as follows:

1) Once the platforms are in their desired locations (as determined by the aircraft), a start scanning signal is sent to the platform.

2) One platform is designated the host before takeoff, and the other is designated as the remote terminal.

3) The host terminal remains fixed at a certain pointing vector for a certain period of time, looking for a signal on the beacon receiver.

117

4) During this same period, the remote beacon strobes the sky rapidly, covering its entire operating region.

5) If the host detects a signal, the links exchange position and orientation information over the beacon laser, move to point at these coordinates, and then initiate the data laser alignment procedure.

6) If no signal is found after a certain period of time, the host beacon moves to a new pointing vector, and the remote laser repeats its scan. This is repeated until a signal is detected.

How quickly this procedure succeeds is mostly dependent on the receiver FOV and transmitter beam divergence, but it can also be sped up if the aircraft can be given some very basic information about what region of the sky their counterpart will be in during the flight, using terrain landmarks, the position of the moon, or even star maps at night. This could be programmed in advance and does not require radio transmission between the two units.

The last situation for blind scanning is where both platforms are in a completely GPS denied environment with access only to some internal synchronized clock in each aircraft and their own orientation information. The initialization and scanning procedure is the same as in the previous section, however when the host node does receive a signal, instead of exchanging position and orientation information to get a last known good fix, the nodes only exchange orientation information and the host node tells the remote node

to halt scanning and hold its current pointing vector while the host node optimizes its received signal strength. Once this is complete, the data lasers proceed to start their alignment using fast beam steering. The procedure just outlined is very similar to the previous one, with one major difference. If, for some reason, the nodes lose each other's signal completely during the beacon alignment phase, without the last known GPS position the nodes must initiate a much larger scan to reacquire the beam (depending on the length of the link break), since they have no knowledge of where the other node might be now. Of course, if the beam is lost only for a short period of time, the beacon can quickly reacquire, however for longer times it essentially becomes like starting the process anew. The aircraft will be not only changing their positions over time, but also their orientations, and if a node is not aware of how the other's is changing during a loss of signal, it cannot make an estimate as to where to start scanning again.

Figure 4.12 illustrates the drastic difference in acquisition times for this fully-blind chirped acquisition algorithm (assuming a strobe revolution time of one second and gimbal slew rate of 360°/s). Only for very wide beacon lasers does this system become usable, but it will allow two systems to connect eventually if all other forms of communication between the nodes are forbidden.
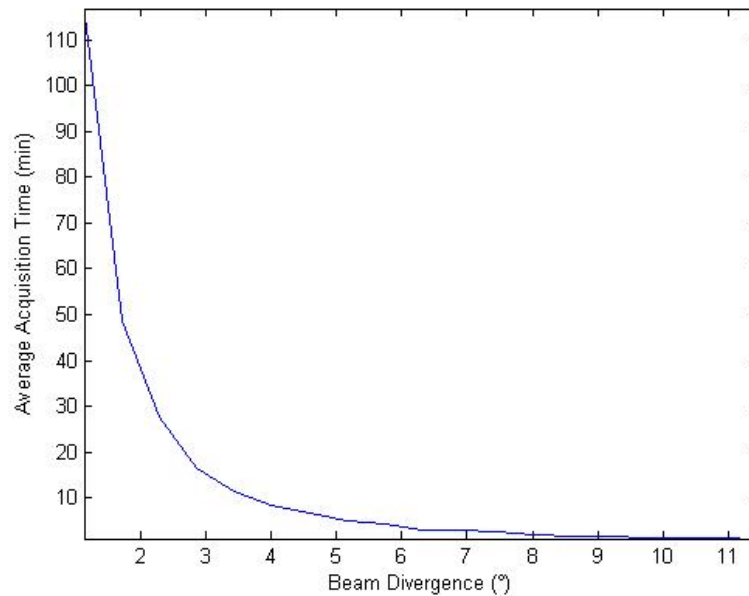
Figure 4.12: Average acquisition time for randomly placed nodes as a function of beam divergence. For beams on the order of modern FSO and RF systems, random acquisitions could take hours. However, if very wide beams could be used, the acquisition could be quicker than a spiral scan.

4.6.1 Monte Carlo Simulations

Another way to look at the problem of totally blind acquisition is to conduct a Monte Carlo simulation of the process. Namely, if we choose random azimuth and elevation angles for both transceivers at a resolution fine enough that the beam can hit the receiver, how long on average would it take for the two links to point at each other? For instance, figure 4.13 below shows the average time to form a link with 0.05° pointing precision over different angular coverages. As one can see, even at 2° it takes an average of 30 minutes to connect with a platform slew rate of 90°/s.
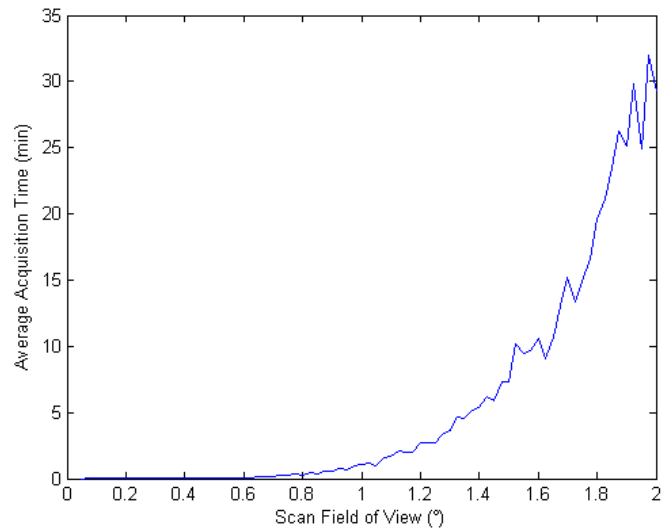
120

Figure 4.13: Average acquisition times for a random scan. Scans for FOVs greater than a degree become intractable for practical systems.

For further comparison, we can look at different scan resolutions over the same

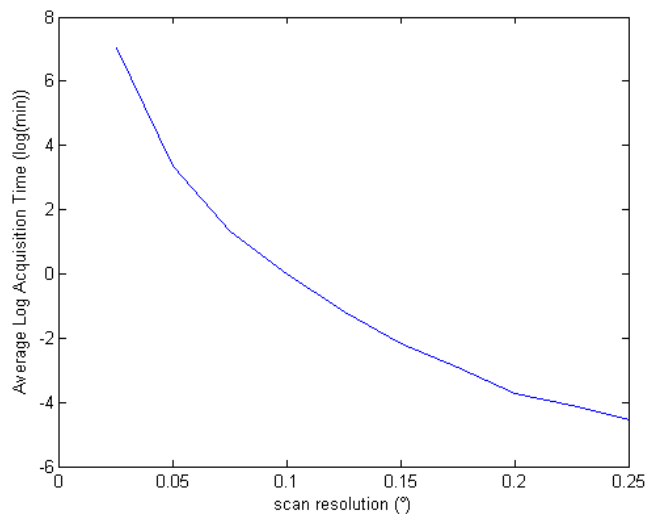maximum angular range of 2°, shown in a log plot in figure 4.14.

Figure 4.14: Average acquisition time for random scan vs. scan resolution. If very wide beams could be used, thereby allowing wide scan spacings, random scanning is a feasible alternative.

For any scan type, random or patterned, an important note is that the scan resolution should never be finer than necessary, since it does not provide any noticeable improvement in pointing and acquisition times, but in fact will increase the time it takes to form a link. As mentioned in chapter 2, there are limits to how wide the divergence of a beam can be and still have it deliver enough power on the receiver, and this in turn limits how coarse a scan can be. It would be ideal to scan the sky with a 90° wide beam, however at any practical distance, the SNR would be far too low for this approach to be feasible.

4.6 Experimental Results

With the systems that were detailed in Chapter 3, several experiments were undertaken to evaluate some of the algorithms that were simulated earlier in this chapter.

The first experiment involved characterizing the FOV of both the data transceiver and beacon system. These experiments gave a measure of how much coverage the scanning algorithms must have in order to guarantee acquisition.

The second experiment tested how long it took the system to complete a scan using various scan resolutions. Depending on the beam divergence, link spacing, and receiver aperture size, the scan resolution can be adjusted appropriately in order to maximize efficiency.

After this, two acquisition experiments were conducted on an indoor test range 90m long, using an Ethernet cable between the two ends to simulate the chirped scanning

concept since the FSO units could not be configured to exchange the signal information directly. The first measured the total acquisition time for two data lasers depending on their initial misalignment. Depending on the quality of the initial pointing (by GPS, beaconing, or some other means), the data laser will have to scan some certain area to guarantee acquisition. While in most FSO systems this is done with a fast steering mirror, the lack of them in these transceivers requires that the acquisition be tested using the gimbal. The next experiment measured total acquisition times for the beacon system as a function of initial misalignment, but deriving these angles from a range of GPS errors and the distance between links. This experiment provides very illuminating results about what kinds of performance characteristics beacon systems actually need.

Finally, all the systems were taken outside into a parking lot and deployed in a small FSO network. The system gathered GPS information, generated pointing angles, and then let each node use its spiral scanning capabilities to acquire and maintain connectivity. This experiment was not completely successful, however the control channel and data laser acquisition components were completed.

4.6.1 Pan-Tilt Platforms

Part of the preliminary work for this thesis was to design and build prototype pan-tilt platforms that would have sufficient performance to function as coarse pointing units for mobile FSO networks, directional RF transceivers, or camera systems. The platform must have the proper combination of pointing precision, smooth low and high speed velocity control, minimal backlash, appropriate load carrying capacity, and small size in

order to be useful in mobile applications.

Figure 4.15 below shows the six completed platforms along with their control

units. Figure 4.16 gives an inside view of the control unit. The two large beige boxes are

the servo amplifiers, and the FPGA control board can be seen at the top right.

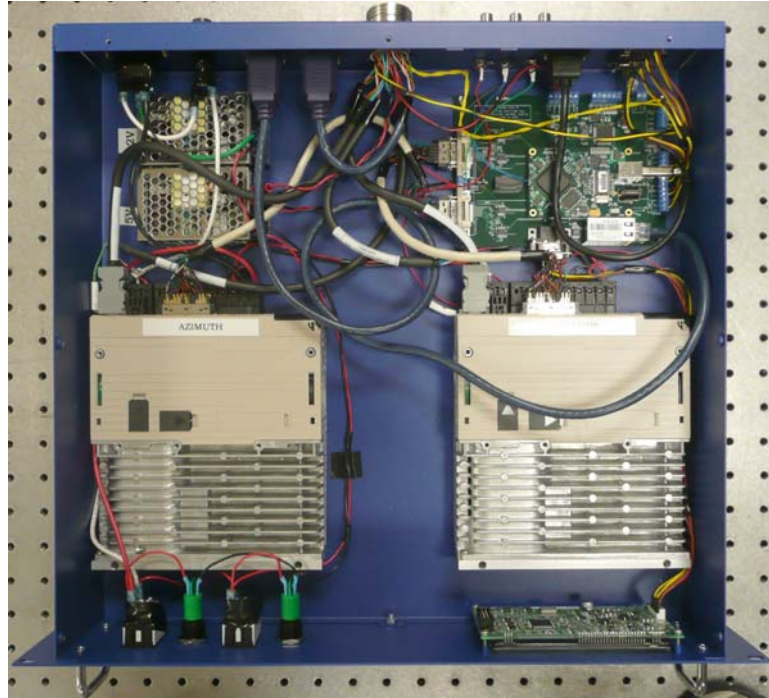Figure 4.15: Completed FSO/zoom camera pan-tilt platforms.

Figure 4.16: Detail from one of six completed control units. The beige units are the auto-tuning servo amplifiers running in position mode.

In order to verify and test the various acquisition and alignment algorithms shown in this paper, an unobstructed area about 100m long was required (the range being limited by the transmit power of the data lasers). Fortunately, access to the second floor service corridor in the Kim Engineering Building was gained for the experiments. The platforms were spaced 90m apart and connected to each other with a long Ethernet cable to simulate the chirped laser beam concept, while also recording data from both ends.

Figure 4.17: 90m Testbed for acquisition tests

4.6.2 Beacon scanning results

As mentioned in Chapter 3, the beacon lens and photodiode were simulated to give a FFOV of 20°. To experimentally verify this, all the units were manually aligned with a beacon laser incident on the center of the beacon receive lens, 90m from the laser source. A spiral scan of the receiver was then initiated, and the beacon RSS was measured at each azimuth and elevation angle coordinates. Figure 4.18 below shows a plot of one of the tests, where the FFOV can be seen as 14°. The disparity from the simulated value is due to the lens not being at the center of rotation while the platform is scanning, and this translation error in effect reduces the FOV. Since the focused beam

walks off the detector at larger angles, the change from a good beacon signal to none at all is quite abrupt, as opposed to the data laser where the received spot at the plane of the detector is larger than the detector active area, so there is a comparatively more gradual rolloff, albeit over a much smaller FOV. To give an idea of how the FOVs of the beacon and data receivers compare, figure 4.19 below shows simultaneous scans of the two receivers on two platforms, the left two plots are at the FOV of the data laser, the right two the beacon laser. The top two plots are the data RSS, the bottom two the beacon RSS. It is evident that the disparity in FOV lends an FSO system to requiring some type of intermediate alignment process in-between geo-pointing and fine scanning. The use of the beacon lets the fine angle component operate over a much smaller area, and much quicker too. Secondary beacons like this are not used in RF systems, as their larger beam divergences allow for the data beam to act as a beacon simultaneously. However, if initial geo-pointing is unavailable, other types of beacons may be used to give an initial pointing estimate.
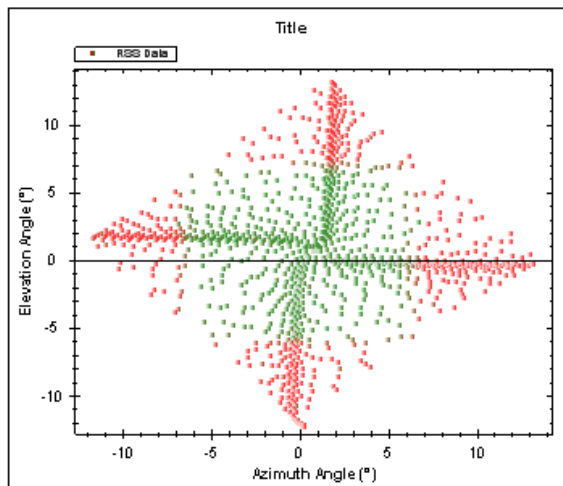

Figure 4.18: Beacon FOV RSS measurements. Green denotes a sufficient beacon signal, red denotes no signal. The FFOV can be seen as 14°.
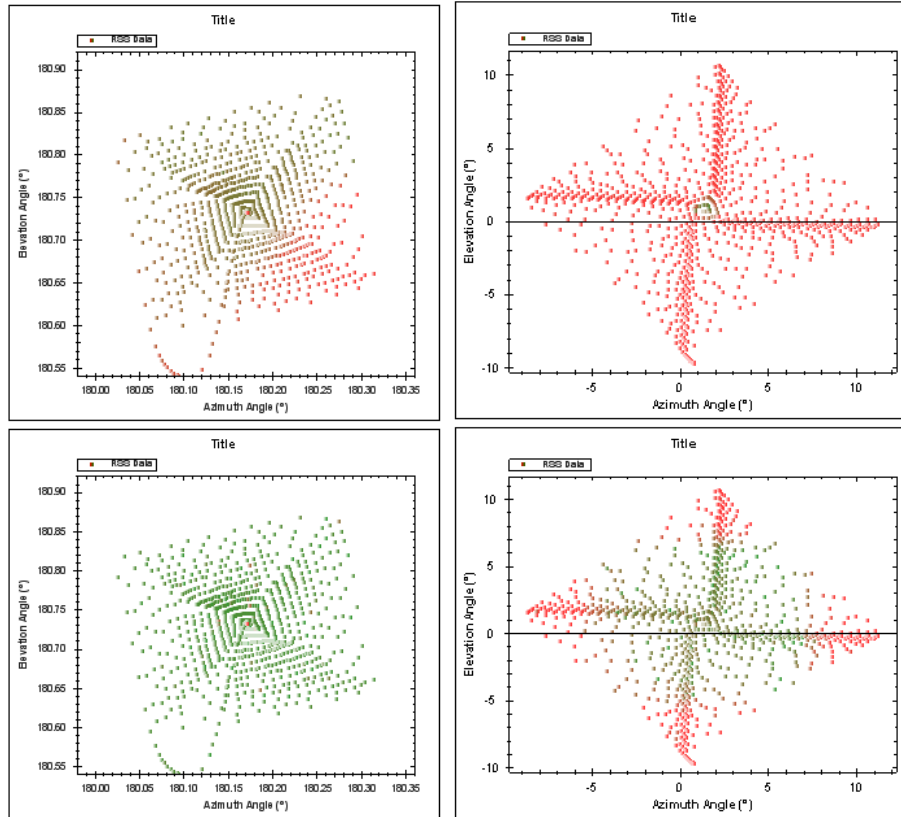
Figure 4.19: FOV comparison for beacon and data receivers (red points denote no received signal, green points denote a received signal above the detection threshold). Note the difference in scale between the data laser (top) and beacon laser (bottom) over the two ranges (1° on the left, 20° on the right).

4.6.3 Fine Angle Data Laser Scanning

Since the beacon laser is intended to take care of the intermediate region between geo-pointing and data laser scanning, the data laser scan algorithm can be fixed to a set resolution and FOV, assuming the beacon has a consistent error. Based on the earlier CodeV simulations, the FFOV of the data laser is 1°. Because the receive lens is 50mm in diameter, at 90m the transmit beam must be pointed to within 0.031° to ensure it hits

the receiver lens. Figure 4.20 below shows the results of a scan where the transmitter was aligned on the receiver, and then the RSS at the receiver was measured while it executed a spiral scan. The FFOV was measured as 0.9°, which fits well with the simulation prediction of 1°.
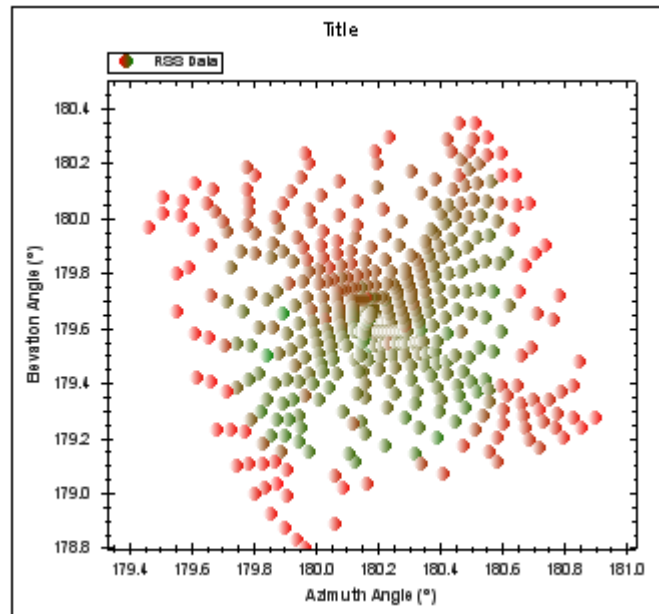

Figure 4.20: Receiver FOV measurements at 90m (red points denote no received signal, green points denote a received signal above the detection threshold). Compared to the 14° FFOV of the beacon, the data receiver has a FFOV of 1° on average.

Because the transmitter scan resolution is determined by the range and beam divergence, different scan resolutions will be required depending on the link separation. Figure 4.21 below shows experimental results of the scan times over ±0.5° for various scan resolutions. As can be seen, for very fine scan increments the process can take several minutes, which could be infeasible in a dynamic situation. It is therefore an important design consideration to make the geopointing and beacon pointing as precise as

possible to limit the scan range, but also to keep the beam divergence as wide as possible.
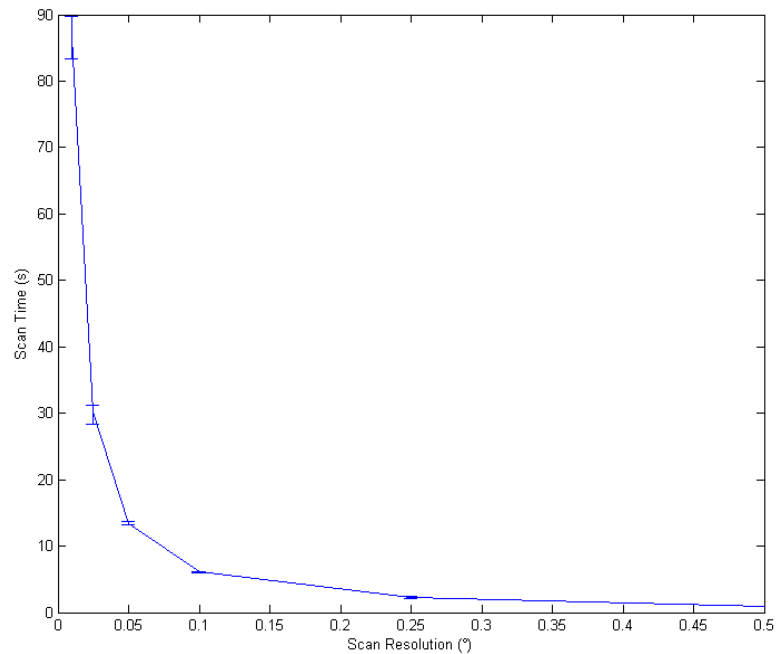

Figure 4.21: Average fine angle scan times over ±0.5° at various scan resolutions (scan velocity of 90°/s). Keeping the data laser beam as wide as possible will make the acquisition time only a few seconds long.

4.6.4 Automatic Two-step chirped spiral scan acquisition

The first acquisition test was to evaluate the performance of a two-stage chirped scanning method. In this method, one platform scans its transmit beam in a coarse spiral scan. When the receiver end sees this beam, it sends a modulated beacon beam back with the RSS it saw at that time. One could think of this like using a retro-reflector to get a return signal. When the scan is completed, the transmitter can see where the other

receiver found a peak, and then move to it. The units then switch roles and repeat. After

this, the data lasers repeat the process, but over a much smaller FOV and with a finer

resolution. While something of a simplification for monostatic systems where a FSM can

steer the transmit beam along the same optic axis as the receive beam, this experiment

provides a platform for evaluating various beacon parameters, laser parameters, and

scanning algorithms.

   Since a spiral scan produces a large set of data points, only signals above a certain

level are used, and the centroid of those points in the azimuth/elevation plane is used as
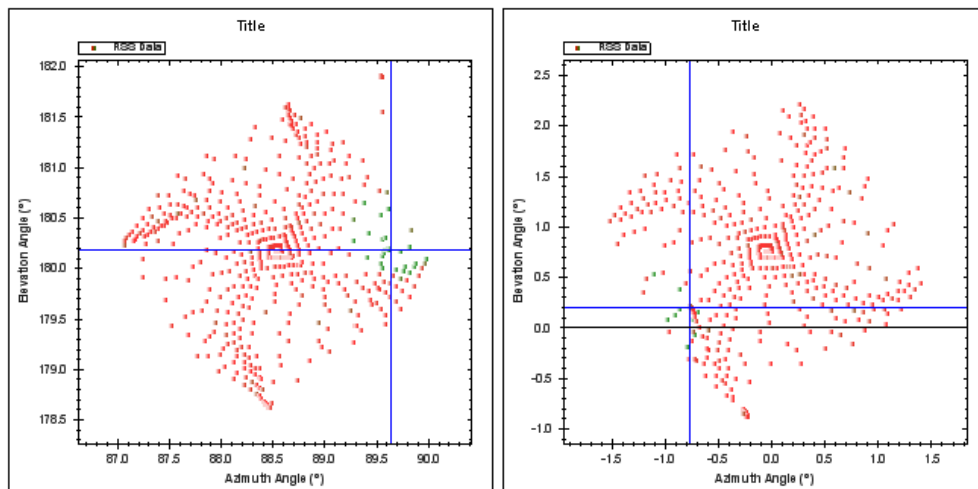
the pointing angle.

Figure 4.22: Centroid determination of RSS for alignment. Once the spiral scan has
found a cluster of good RSS measurements, it will rotate to the centroid of those points
and then remain fixed as the other end of the link completes its scan.

Figure 4.23 shows experimental results for data laser acquisition times as a function of the initial misalignment.
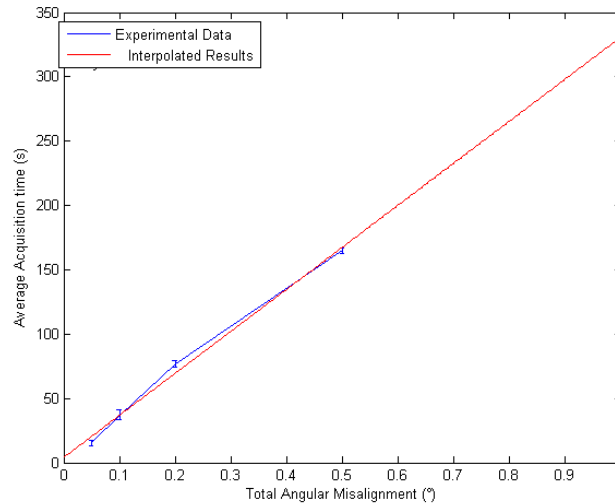

Figure 4.23: Average Acquisition Time vs. initial alignment error (using a 0.01° scan resolution and a scan velocity of 90°/s). Note the linear trend of the scans, which is quicker than a constant velocity spiral scan. The scans used here are run in position mode, so the platforms accelerate between in each waypoint, thereby decreasing the acquisition time.

One would expect the scan time to increase faster than linearly as the angular misalignment increased, however the system used in this work has a fundamental difference from a velocity-based spiral scanning system. Because this thesis uses gimbals that run in position mode, the gimbal moves to a set of waypoints to form a spiral-like pattern out of a series of linear moves. During each of these moves the motors accelerate and decelerate. As the spiral gets larger the motors have more and more time to accelerate, and will never (at least in the realm of the scan ranges used in this thesis) hit their acceleration limit at which they would go into a constant velocity mode like a typical spiral scan. For the scan ranges involved here, the increase in scan time as a

132

function of FOV can be taken to be approximately linear. This acceleration mode has the advantage of being quicker, but the disadvantage of that at larger angles, the number of RSS samples per angular sweep goes down. While this could conceivably become a problem in some situations using very fast scans, the ADCs used on the control board sample fast enough (200KSps) to compensate for the increasing scan velocity.

4.6.5 GPS Assisted Pointing with Spiral Scan Acquisition

Modern WAAS enabled GPS offers a best case position error of 1.1m [39], or up to 15m in the worst case [66]. RTK GPS can give 3cm position error [67]. To look at how these errors affect acquisition times at various ranges, the test-bed was setup that the initial angular misalignment was calculated by a simulated range and GPS error.   The beacon scan then ran, acquired, and this process was repeated to get an average acquisition time.

Figure 4.24 below shows the tests at different simulated ranges. At 1.1m error the beacons would lock on immediately at 5km, and the beacons would align automatically at 25km in the case of 15m GPS error.
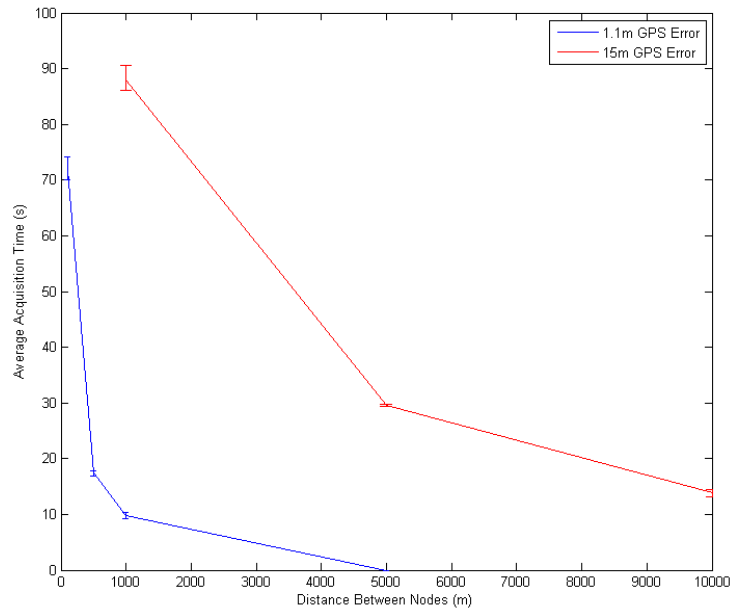
Figure 4.24: Average beacon acquisition for best and worst case GPS error vs. range (using a scan resolution of 0.05° and a scan velocity of 90°/s). Even for large GPS errors, the acquisition time can take only a few seconds at long ranges typical of the operational scenarios for these types of systems.

These experiments validate some very important points about the pointing and acquisition of narrow beam transceivers. When dealing with FSO systems, for links that go 10s to 100s of kilometers, using a sufficiently wide beacon laser can allow one to cover an angular range equivalent with the worst case GPS area quite effectively, even with a slow platform. Even in the case of an aircraft, which one would think requires very agile platforms, a slow stepper motor system could even be used, provided the aircraft did not make rapid direction changes. Since this is always a possibility, servo stabilized platforms are usually employed, however they do not need to have extreme performance specifications. FSO can avoid this issue because the bulk of the beam

134

tracking is done by a fast steering mirror. As long as the coarse platform can get the beacon to within several milli-radians, the fast steering mirror will do the rest.

The same cannot be said for directional RF systems. Because these transceivers do not use a separate beacon beam and are unaffected by turbulence the way laser beams are, all their tracking abilities must be in one platform. E-band transceivers are only intended to work in the kilometer-10s kilometer ranges, so the scanning times seen in the above experiments become much more relevant. Even with the wider beam divergences involved, these platforms must be quite agile in order to keep airborne platforms locked while being comparatively close together.

Finally, the above experiments show why it is very important to have some type of initial pointing method other than a blind scan. Even in the RF domain, executing spiral searches over more than a few degrees can take an unacceptable amount of time, and could be fruitless when the two links are moving in space and go out of each other's FOV before their scans complete. Taking into account the aircraft dynamics, link ranges, operational scenarios, and available transceiver features are essential when designing a platform and PAT control system for a given communications technology.

4.6.6 Router Performance in a Physically Reconfigurable Network

Another DWN project was also conducted in the course of research for this thesis, involving the characterization of fixed infrastructure network routers, and how they would handle DWN links reconfiguring themselves without being able to tell the router they are doing so. A major assumption in almost all DWN projects is that for the actual network and routing portion, existing hardware can just be plugged right in and work seamlessly with a physically reconfigurable network. As far as can be determined from current research, no one has actual tested how routers would perform. Namely, it was desired to see if the routers would be able to find a new path, how long it would take, and if it would detect the shortest path consistently.

To help answer these questions, a four node DWN was constructed, using custom made direct-drive servo gimbals (figure 4.25 below) which held 5.8 GHz patch antennas and radios [68]. These units offered 20 Mb/s data rates at full duplex, and at a range of about 3 miles. Each of these was connected to a Cisco 2400 router that was running the OSPF routing protocol. The update timer for the router was set to its minimum of one second. In other words, the router would check all of its ports every second to make sure they were still responding. Each of these nodes was placed on one of four different buildings on campus, shown below in figure 4.25.

Once these platforms were deployed, they were linked together with a series of high data rate fixed FSO and RF directional transceivers that served as the control channel. Figure 4.26 shows a block diagram of the full network will all the hardware. One node was set as the DTCN, which then commanded the platforms to go through a

136

series of rotations to form different network configurations. During this whole process, the computer at each node would ping the others every 100ms to see which paths were active. As the platforms reconfigured, the downtime of each path was measured. This measurement could be separated into three parts: mechanical rotation time, radio resynchronization time, and router discovery time. The mechanical time was always about 1.5 seconds, as it was set beforehand. The radio resynchronization time was 9 seconds on average, the long delay due to the built in encryption and the fact that each link actually consisted of 24 sub-channels that all had to reconnect. Figure 4.27 below shows the results of the router reconnect time measurements over 100 trials, and figure 4.28 shows the radio resynchronization time over the same 100 trials.

This experiment proved a very important point about DWNs: fixed link routers with no knowledge of the network around them will successfully adapt to link breakages and reconfigurations, and find the shortest path between two nodes, regardless of the technology involved or control channel in charge of the links. In fact, besides the delay time from the radios (which goes down to under one second in single channel 80GHz and FSO systems), the limiting factor in network convergence was the hello-packet interval of the router, which could not be set to less than one second. Typical routers set this to 30 seconds or one minute, as fixed networks generally do not change very often. In deployed systems that could possibly reconfigure, a modified firmware allowing for hello packet intervals in the hundred millisecond range or less would make the downtime from topology changes even less. Future experiments will expand to larger networks that can do more sophisticated reconfigurations, as well as testing newer DWN transceivers.
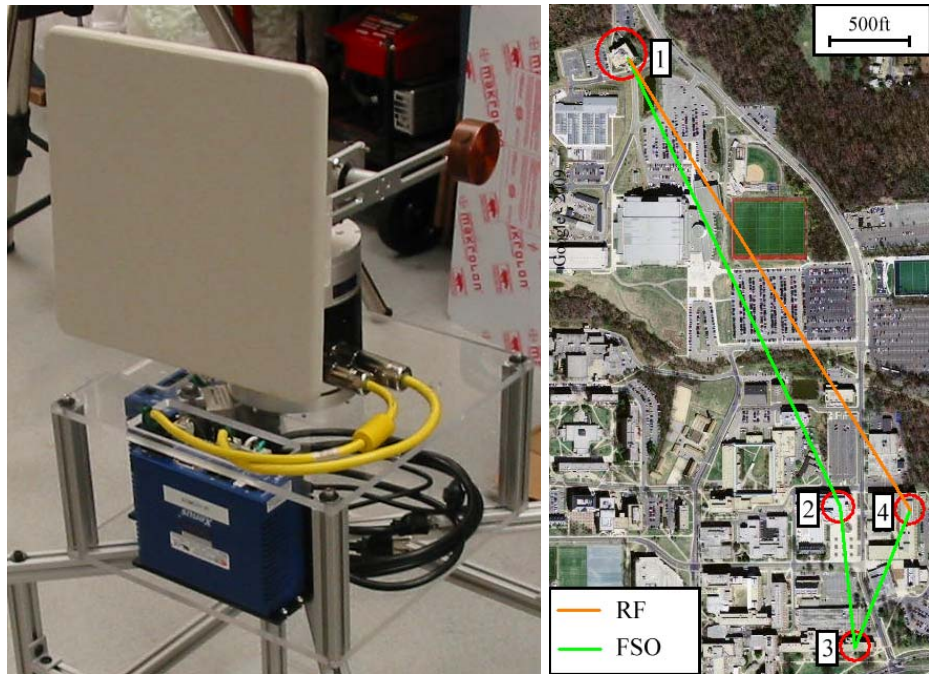
Figure 4.25: 5.8 GHz Directional RF gimbals and test-bed. The gimbal used direct drive servo motors with a resolution of 0.018°. The platforms and routers were placed in radomes on four buildings on campus.
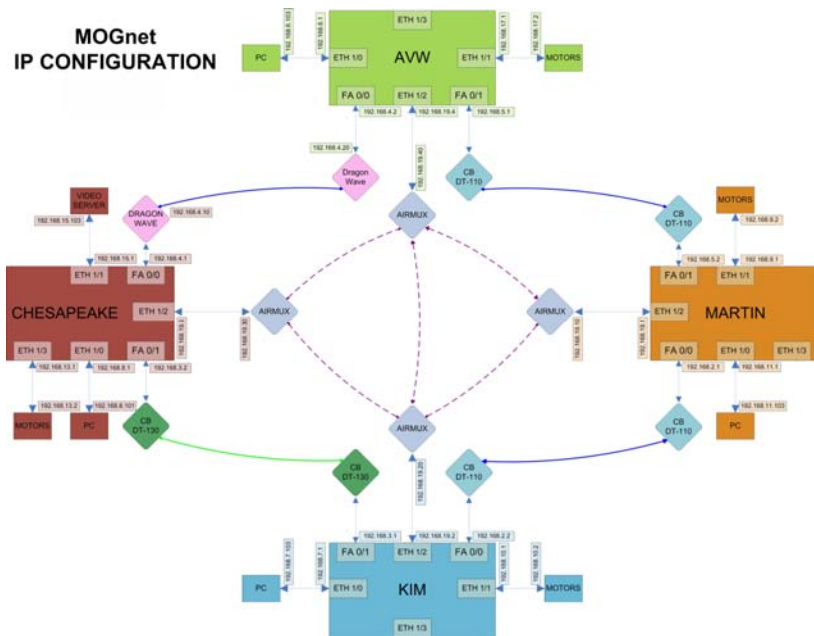

Figure 4.26: Network configuration. The large blocks denote the routers with all their interfaces present. The four diamonds in the middle represent the steerable radios.
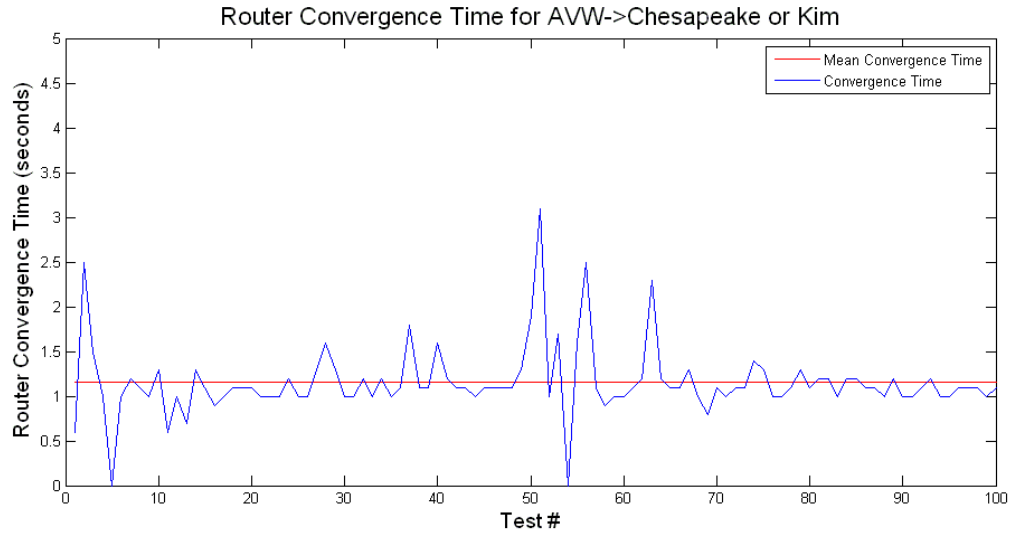
138

Fig. 4.27: Average router convergence time. With a hello packet interval of 1s, the convergence time was 1.2s, averaged over 100 trials.
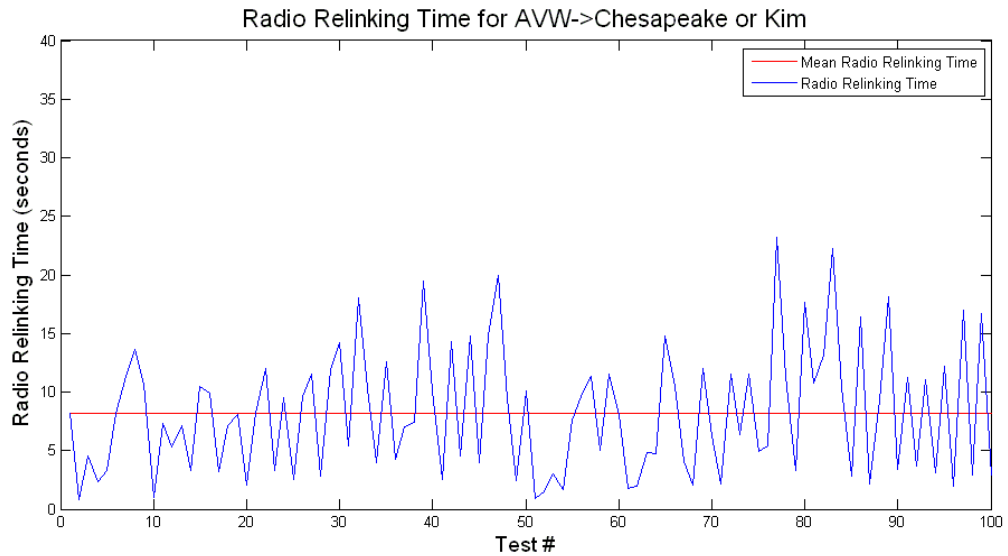

Figure 4.28: Average radio resynchronization time. The average time was nine seconds, but this was a characteristic of the radio that could not be changed. Single channel systems at higher frequencies have resynchronization times under one second.

4.6.7 Platform Angle Calibration

Before a network of DWN nodes could initiate geo-pointing operations, each platform's azimuth and elevation angles must be calibrated so that they agree with a common coordinate system. In most cases, that is chosen to be the geodetic coordinate system used by GPS, where locations are measured by the well known latitude/longitude/height above the ellipsoid values. For the purposes of the three-node network in this thesis, a fourth GPS location was measured and all the units pointed their beacon lasers at that point. The angles made to that point were combined with the units' GPS positions and the calibrator targets' GPS position to put the platforms in the common coordinate system. Figure 4.30 shows a diagram of the alignment procedure.
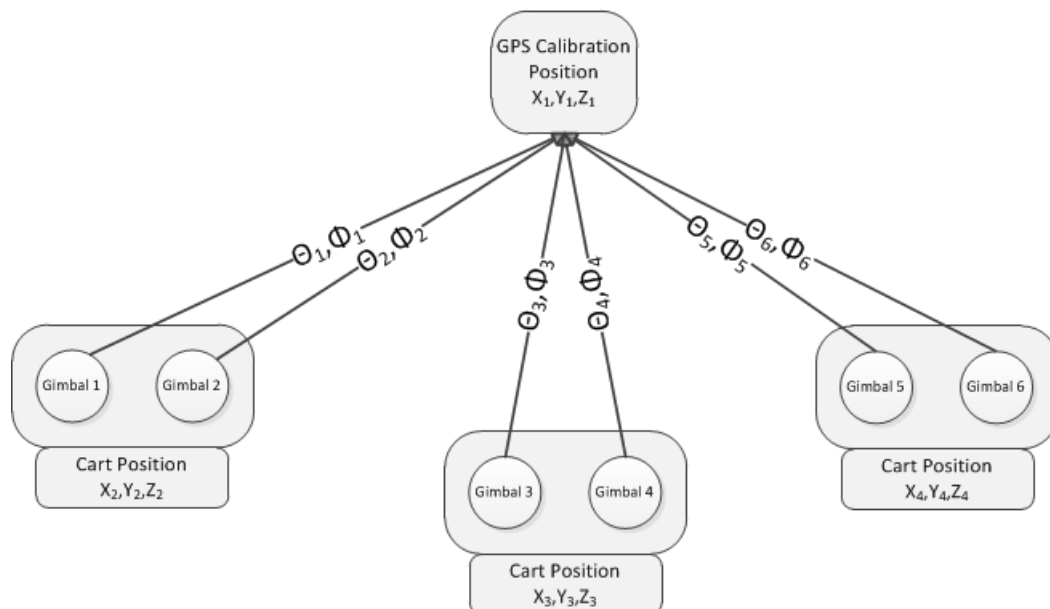

Figure 4.30: Initial angle calibration

4.6.8 Full Network Acquisition

The six FSO platforms built for this thesis were separated into three bi-connected nodes on carts and taken into the parking lot next to the Kim Engineering building, spaced approximately 60m apart in a triangle, and manually aligned to verify all links were active. Figure 4.29 shows the outdoor test-bed. The system should have then geo-pointed, aligned its beacons, and then aligned its data lasers. Unfortunately due to a design flaw in the beacons that was found too late to correct (a lack of filtering so the beacon could be distinguished from background light), the system could not be fully utilized. The RF network and PAT control was successfully verified during indoor testing, but the final outdoor experiment using real-time GPS measurements will not be completed until a later date. Figure 4.30 shows a screen capture from the auto-alignment procedure of the data lasers that was successfully completed during the outdoor experiment. The top two plots show the receive signal strength of the data laser as a function of platform angles, and the bottom two plots are of the beacon signal.

Figure 4.29: Outdoor test-bed. The node in front was the DTCN, sending pointing commands to the other two nodes.
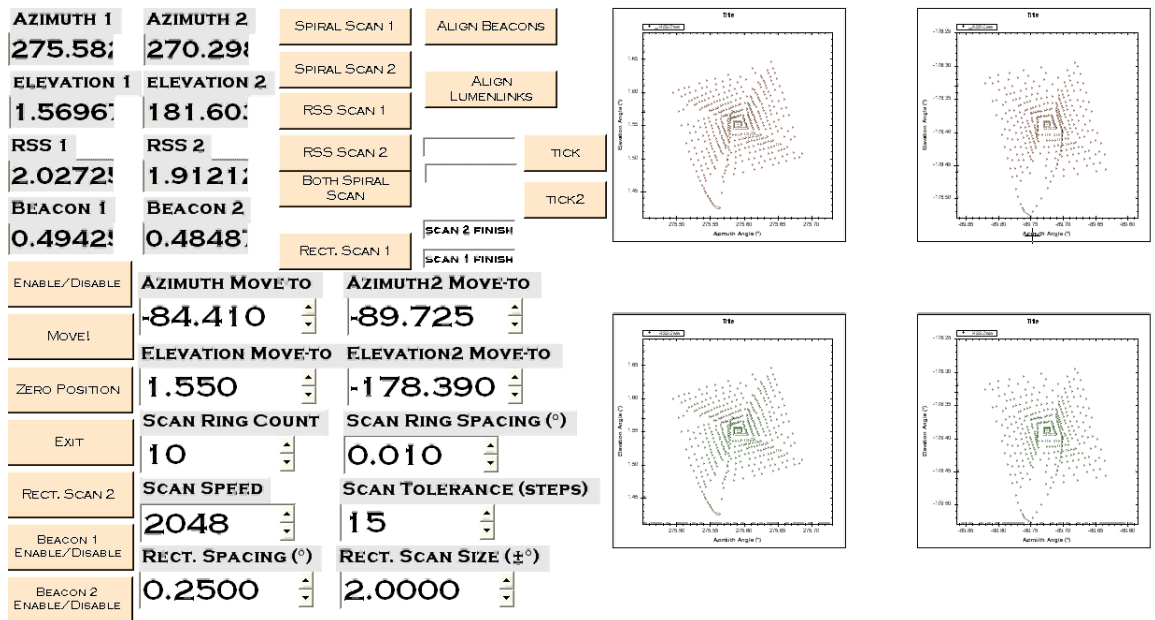
Figure 4.31: Data laser acquisition during outdoor experiment. The top two plots are of the data laser RSS of the two ends of a link, the bottom two the beacon laser RSS.

Chapter 5: Conclusions

Forming a directional wireless network involves the cooperation and interaction of many different components, all of which must perform to specification for the system to work. As has been shown in the preceding sections, each of these subsystems has different design considerations that must be taken into account when creating a network. There are several observations that can be taken from the design of this type of system that uses a secondary control channel for pointing, and a two level scanning stage for acquisition.

First, from a scaling point of view, the main limiting factor is the omnidirectional

142

control channel. Once the initial pointing angles are transmitted to all the platforms, each pair of nodes can execute its acquisition algorithm, independent of all the others. In other words, regardless of the size of a network, once all the nodes know where their partner is, the network will form in about the same amount of time. Using distributed DTCNs, higher bandwidth control channel radios, or potentially lower resolution sensors (transceiver pointing requirements permitting) are all possibilities for mitigating the scaling issue.

Second, unless RTK GPS systems where the accuracy is <3cm become affordable, FSO transceivers will always require an intermediate alignment mechanism, typically using a beacon laser. While this adds to the overall acquisition time, it adds a layer of robustness to the link, as it is easier to track a 10mrad laser than a 10µrad one. The coarse platform and fast steering mirror both have limitations as to how fast and how large of disturbances they can compensate for, so using a beacon of some sort helps alleviate these requirements.

How the control channel is implemented is also an essential design consideration. The implementation used in this thesis is fairly simple in that the DTCN polls the remote nodes in order to collect the data and then sends pointing angles back out. However, it could be possible that some nodes have a built-in priority where they and their partners must be linked first, or these priorities could even change as a network grows, leading the control network to determine pointing command dissemination strategies. The control channel must also be designed as to whether it will be always active, active intermittently, or used only once at startup. These types of choices will determine how

the control channel is used, and how robust the overall network will be.

Finally, knowing what information can be assumed to be available is also important. As mentioned earlier, completely blind acquisitions are possible, but they are only really feasible if some information can be sent over the scanning beam. With regards to pointing, knowing the update frequency of the GPS and orientation sensors will determine the limits of the angular rates between nodes that be tolerated, which also influences the design of the fast steering systems, or in the case of RF, the platform itself.

In this thesis, many aspects of PAT in directional FSO and RF networks were analyzed and simulated, specifically the various methods for undertaking the acquisition phase. Simulations were conducted on several methods for scanning, and their advantages and disadvantages were analyzed. A test-bed of six high performance FSO platforms were designed and constructed to allow for evaluation of these algorithms, and also to serve as a base for future experiments in cooperative camera surveillance and RF/FSO directional wireless networks. These platforms were then used to test several acquisition strategies for both single links and a larger network. Another set of platforms were used to test the response of fixed link routers to changes in a physically reconfigurable network.

Chapter 6: Future Work

While the experimental work presented in this thesis is primarily directed at FSO communications networks, there are several other applicable areas where it might find a use. An immediate use would be in directional RF systems, specifically E-band (60-90 GHz) systems. Almost all of the technology presented in this thesis is directly applicable to this type of system, and it is expected that the expanding use of E-band will in fact accelerate the development of deployable FSO systems.

Another related area is that of autonomous distributed surveillance systems. Many of the PAT concepts in this thesis can also be used to precisely point cameras and track targets. Similar platforms have already been used to test these concepts on a small scale [61], but they can certainly be expanded. The use of multiple steerable camera systems that relay target information over an omnidirectional control channel is of great interest in situations where dispersed cameras cannot be effectively wired together, but who must still be able to operate together in some fashion. This could be very useful in dynamic situations where cameras are placed in various locations or even on mobile nodes, and then must autonomously track targets without the use of a central processing node, during a large event in a major city for example.

With regards to the FSO systems presented in this thesis, there are significant improvements that could be made. Perhaps the most important would be the development of a custom FSO transceiver with features built-in specific to mobile platforms. The units used in this paper were bistatic transceivers, which feature significantly easier to manufacture optical assemblies, as well as the absence of narcissus

issues. However, the added mechanical complexity of two optical axes can make them more difficult to align. When only one link exists, this can be mitigated by doing minor mechanical adjustments to optimize the alignment. However, when one transceiver may have to connect to any number of other ones, consistent alignment can become very difficult. The common solution to this is the use of a monostatic transceiver. While one must carry out a much more careful optical design, the alignment is significantly easier and more consistent from unit to unit with the use of a fast steering mirror. It is hoped that the construction of such a transceiver along with improvement for greater range, more accurate RSS measurement, more compact and rigid construction, an integrated chirped beacon, 1550nm operation (to allow the use of an EDFA), and gigabit speeds will allow for many of the experiments to be rerun at greater ranges and with a greater variety of platform dynamics. Some of the platforms described earlier were also initially designed to hold high definition color zoom cameras for surveillance applications, and it is hoped that these can be deployed to evaluate their use as an autonomous distributed tracking system with a RF control channel to exchange target information to each platform having non overlapping FOVs. It is also hoped that an E-band demonstrator transceiver can be constructed to evaluate many of the concepts in this thesis, while not necessarily requiring a complete gigabit radio.

Bibliography

[1] http://www.darpa.mil/Our_Work/STO/Programs/Optical_RF_Communications_Adjunct_(ORCA).aspx

[2] http://cictr.ee.psu.edu/facstaff/kavehrad/Papers/BAA04-03(ORCLE].pdf

[3] https://www.fbo.gov/index?s=opportunity&mode=form&id=3e0a98a1c71f7f3f3301b567d380c896&tab=core&_cview=0

[4] http://www.darpa.mil/Our_Work/STO/Programs/Mobile_Hotspots.aspx

[5] http://www.afsbirsttr.com/TopicPreRelease/Profile.aspx?pk=21070

[6] Cunningham, J., Foulke, D., et al., "Long Range Field Testing of Free Space Optical Communications Terminals on Mobile Platforms," Proc. IEEE MILCOM, 2009

[7] Llorca, J., Milner, S., Davis, C., "A Force-Driven Mobility Control Algorithm for Joint-Coverage Connectivity Optimization in Heterogeneous Wireless Networks," Proc. SPIE, 6709, 2007

[8] Anguita, J., Cisternas, J., "Turbulence strength and temporal correlation in a terrestrial laser communication link," Proc. SPIE 7814, 2010

[9] Yuksel, H., Harris, J., et al., "Aperture averaging and correlation function measurements in strong atmospheric turbulence for optical wireless communications," Proc. SPIE 7091, 2008

[10] Fletcher, T., Cunningham, J., et al., "Observations of Atmospheric Effects for FALCON Laser Communication System Flight Test," Proc. SPIE 8038, 2011

[11] Kanno, I., "Development of Deformable Mirror Composed of Piezoelectric Thin Films for Adaptive Optics," IEEE Quantum Electronics, 2007

[12] Chen, G., "Light-beam stabilizing control in long-distance transmission systems

subject to mechanical vibrations," Proc. ICMA, 2010

[13]   http://www.dragonwaveinc.com/products/packet-microwave/horizon-compact

[14]   http://bridgewave.com/products/60ghz.cfm

[15]   Llorca, J., Desai, A., et al., "Reconfigurable optical wireless sensor networks," Proc. SPIE 5237, 2003

[16]   Llorca, J., Desai, A., et al., "Optimizing performance of hybrid FSO/RF networks in realistic dynamic scenarios," Proc. SPIE 5892, 2005

[17]   Milner, S.D., Llorca, J., and Davis, C.C., "Autonomous Reconfiguration and Control in Directional Mobile Ad Hoc Networks," IEEE Circuits and Systems 9(2), 10-26 (2009)

[18]   Llorca, J., Milner, S.D., and Davis, C.C., "Mobility control for joint coverage-connectivity optimization in directional wireless backbone networks," Proc. IEEE MILCOM, Nov. 2007.

[19]   Llorca, J., Milner, S.D., and Davis, C.C., "Molecular System Dynamics for Self-Organization in Heterogeneous Wireless Networks," Eurasip Journal on Wireless Networking (2010)

[20]   Coleman, D., Armacost, K., Davis, C.C.; Milner, S.D., "A molecular-inspired approach for predicting topology change in directional mobile wireless networks," ISSNIP, 2011

[21]   Llorca, J., "Self Organizing Directional Wireless Backbone Networks," University of Maryland, 2008.

[22]   Walther, F.G., et al, "Air-to-Ground Lasercom System Demonstration," Proc. SPIE 7814 (2010)

[23]   Young, D.W., Juarez, J. C., et al, "Multichannel high-data-rate optical transmission between ground and airborne platforms," Proc. SPIE 6457, 2007

[24]   Bagley, Z., Hughes, D., et al., "Hybrid optical radio frequency airborne communications," Optical Engineering, 2012

[25]   http://bridgewave.com/products/80Ghz.cfm

[26]   http://www.lightpointe.com/607080ghzradio/airebeam7080ghz.html

[27]   Franco, J. C., Rzasa, J., Milner, S. D., Davis, C. C., "Transmission of high definition imagery using hybrid FSO/RF links for real-time surveillance, event detection, and follow-up," Proc. SPIE, 6709, 2007.

[28]   Wan, D., Zhou, J., "Stereo Vision using Two PTZ Cameras," Journal of Computer Vision and Image Understanding, 2008

[29]   Lu, Y., Payandeh, S., "Cooperative Hybrid Multi-Camera Tracking for People Surveillance," Canadian Journal of Electrical and Computer Engineering, 33, 145-152, 2008.

[30]   Broaddus, C., Germano, T., "ACT-Vision: Active Collaborative Tracking for Multiple PTZ Cameras," Proc. SPIE, 7345, 2009

[31]   http://www.nova-sol.com/products-and-services/compact-optical-interrogator

[32]   http://www.atoptics.com/ProductDocs/AOR31510BL.pdf

[33]   http://www.jdsu.com/ProductLiterature/rxpmgrtl097-ds-oc-ae.pdf

[34]   Trisno, S., "Design and Analysis of Advanced Free Space Optical Communication Systems," University of Maryland, 2006

[35]   Dagel, D., "Large-stroke MEMS deformable mirrors for adaptive optics," IEEE Jour. On Microelectromechanical Systems, 2006

[36]   Lee, S., "Focal tunable liquid lens integrated with an electromagnetic actuator," Applied Physics Letters, 2007

[37]   Sinefeld, D., **"Wavefront aberration correction in a free-space optical communication link using only the fiber-coupled optical power as a feedback," Proc. IEEEI, 2010

[38]   Stotts, L., Andrews, L., et al., "Hybrid Optical RF Airborne Communications," Proc. IEEE, 97, 1109-1127, 2009.

[39]   http://en.wikipedia.org/wiki/Waas

[40]   http://static.garmincdn.com/pumac/GPS18x_TechnicalSpecifications.pdf

[41]   http://www.microstrain.com/inertial/3dm-gx3-45

[42]   http://www.carboceramics.com/attachments/wysiwyg/21/Model_MD900T.pdf

[43]   http://www.magneticsensors.com/magnetometers-compasses.php

[44]   http://www.sbg-systems.com/products/ig-500n

[45]   http://www.moog-crossbow.com/products/inertial-products/products-nav440/

[46]   http://www.xsens.com/en/general/mti-g-100-series

[47]   http://www.canobeam.com

[48]   http://www2.l-3com.com/seo/products/index.htm

[49]   http://gs.flir.com/uploads/file/products/brochures/airborne_brochure.pdf

[50]   http://www.cloudcaptech.com/

[51]   Cap, G., Refai, H., and Sluss Jr., J., "Optical Tracking and Auto-Alignment System," IEEE A&E Systems September, 26-34 (2010)

[52]   Hahn, D., Brown, D., et al., "Fiber optic bundle array wide field-of-view optical receiver for free space optical communications," Optics Letters, Vol. 35, No 21, 2010

[53]   Urabe, H., Haruyama, S., et al., "High data rate ground-to-train free-space optical communication system," Optical Engineering, Vol. 51(3), 2012

[54]   Goetz, P., Rabinovich, W., et al., "Modulating Retro-reflector Lasercom Systems at the Naval Research Laboratory," Proc. IEEE MILCOM, 2010

[55]   Moore, C., Burris, H., et al., "Lasercomm Demonstration during US Navy Trident Warrior 06 Forcenet Exercise," IEEE Antennas and Propagation, 2007

[56]   Cavagnino, A.,Lazzari, M., et al., "A Comparison Between the Axial Flux and the Radial Flux Structures for PM Synchronous Motors," IEEE Trans. On Industry Applications, Vol. 38. No. 6, 2002

[57]   Kaiser, D. "Fundamentals of Servo Motion Control," Parker Compumotor, 2007

[58]   Holzman, E.,"Transreflector Antenna Design for Millimeter-wave Wireless Links,"IEEE Antennas and Propagation, Vol. 47, No. 5, 2005

[59]   http://yaskawa.com/site/Products.nsf/products/Rotary%20Servomotors~SGMCS DirectDrive.html

[60]   http://www.opalkelly.com/products/xem6010/

[61]   Rzasa, J., Milner, S., Davis, C.,"Design and Implementation of Pan-Tilt FSO Transceiver Gimbals for Real-Time Compensation of Platform Disturbances Using a Secondary Control Network," Proc. SPIE, 8162, 2011

[62]   Eslami, M., "Light Field Analysis and its Applications in Adaptive Optics and Surveillance Systems," University of Maryland, 2012

[63]   Eslami M., Rzasa J., Davis, C.," A stereo PTZ tracking and surveillance system with two dynamic cameras operating in a master-slave relationship," Proc. SPIE, 8517, 2012

[64]   http://hompi.sogang.ac.kr/photonics/tech.htm

[65]   http://www.digi.com/products/wireless-modems-peripherals/wireless-range-
extenders-peripherals/xtend#overview

[66]   http://en.wikipedia.org/wiki/Global_Positioning_System

[67]   http://en.wikipedia.org/wiki/Real_Time_Kinematic

[68]   http://www.radusa.com/10/Wireless-Multiplexer/9862/